DISSERTATION

THE ARYL HYDROCARBON RECEPTOR PATHWAY: A MODEL FOR BIOLOGICAL SWITCHING

Submitted by
Carolyn Janelle Broccardo
Department of Environmental and Radiological Health Sciences

In partial fulfillment of the requirements
For the degree of Doctor of Philosophy
Colorado State University
Fort Collins, Colorado
Fall 2004

COLORADO STATE UNIVERSITY

November 3, 2004

WE DO HEREBY RECOMMEND THAT THE DISSERTATION PREPARED UNDER OUR SUPERVISION BY CAROLYN JANELLE BROCCARDO ENTITLED THE ARYL HYDROCARBON RECEPTOR PATHWAY: A MODEL FOR BIOLOGICAL SWITCHING BE ACCEPTED AS FULFILLING IN PART REQUIREMENTS FOR THE DEGREE OF DOCTOR OF PHILOSOPHY.

Committee on Graduate Work

Marie Legare Member

Colin Clay Member

Ruth Billings Member

Michael Fox Outside

John Tessari Member

William Hanneman Advisor

John Zimbrick Department Head/Director

ABSTRACT OF DISSERTATION
THE ARYL HYDROCARBON RECEPTOR PATHWAY: A MODEL FOR BIOLOGICAL SWITCHING

The shape of the dose-response curve may vary depending on whether one examines response at a population or a single cell level. Populations of cells may exhibit a graded response whereas single cell responses may have threshold or switch-like behavior. Studies in vivo and in vitro using primary hepatocyte cultures have shown that induction of CYP1A1 in the liver exhibits switch-like behavior in response to PCB 126 (3,3',4,4',5-pentachlorobiphenyl) (Chubb LS 2002; French *et al.* 2004). The goal of the present study was to determine if two liver cell lines (H4IIE rat hepatoma and Hepa 1c1c7 mouse hepatoma) also show switch-like behavior and develop experimental models for studying mechanisms of these switch-like responses. Both cell lines were analyzed via concentration-response and time-course studies using quantitative real-time PCR, revealing a sigmoid concentration-response curve for CYP1A1 mRNA induction at the population level. To study CYP1A1 protein induction on a single cell level, flow cytometry was employed. In both cell lines the distribution of fluorescence increased with increasing concentrations of PCB 126. The switch behavior was more pronounced in the H4IIE cells than in the Hepa 1c1c7 cells, exhibiting a well-defined shift of induction from the "off" to the "on" state. The concentration-response curve at the single cell level appeared more switch-like with two populations of cells – basal levels and maximally induced. Our data support the hypothesis that PCB 126 induces CYP1A1 in a switch-like fashion in H4IIE rat hepatoma cells. These cells can now be used to study the mechanism of the biological switch.

The AhR pathway is modulated by multiple co-activators and by phosphorylation. Our research reveals a likely role for PKC in this switch response as evidenced by dramatically reduced CYP1A1 induction after inhibition of PKC. We have also demonstrated the regulation of several proteins/phosphoproteins by PCB 126 and that the MAPK pathways ERK and JNK are not activated by PCB 126 in H4IIE cells. This may indicate that the switch-like induction of CYP1A1 by PCB 126 involves the PKC signaling pathway and does not involve the MAPK pathways in this system.

Carolyn Janelle Broccardo
Department of Environmental and Radiological Health Sciences
Colorado State University
Fort Collins, CO 80523
Fall 2004

TABLE OF CONTENTS

CHAPTER 1

Introduction

Environmental Concern of PCBs

Polychlorinated biphenyls (PCBs) are synthetically manufactured, organic chemicals consisting of 209 individual congeners which are generally present in mixtures with various ratios of chlorination. Because of their physical and chemical properties, PCBs have been used widely in industry. They provide thermal stability; resistance to acids, oxidation, hydrolysis and alkalis; low flammability; low solubility in water; low vapor pressure; high electrical resistance and a favorable dielectric constant for such products as capacitors, coolants and lubricants in transformers, hydraulic acid and heat transfer fluids, lubricants, plasticizers, and adhesives (Poland and Knutson 1982).

The manufacturing of PCBs was discontinued in 1977 upon discovery of their toxicity and propensity toward bioaccumulation, but not before their spread into the air, water, soil, fish, wildlife, and human blood, adipose tissue and breast milk (Safe 1989). The "open" applications ceased in the 1970s as well, but the "closed", hermetical uses (dielectric fluids in capacitors and transformers) continued until 1978 (Safe 1989). By this time, the US total production level surpassed 1 billion pounds (Poland and Knutson 1982). Although they are no longer manufactured in the US, PCB mixtures can still be found in old products such as old fluorescent lighting fixtures, certain electrical devices

or appliances containing capacitors manufactured prior to 1977, old microscope oil, and hydraulic fluids.

PCBs within the environment exist as liquid and solid aerosols and vapors. They can be carried long distances via the air and eventually settle back onto the earth due to rain, snow and dust particles. The mixtures range in their composition, volatility and solubility. Within water, PCBs may either remain dissolved or bound to other organic particles. Increased chlorination of the biphenyl rings decreases their solubility in water. They absorb strongly to soil and sediments and may persist in the environment for decades (Safe 1989). They can enter the body via oral, inhalation or dermal exposure (Safe 1989; Safe 1994).

Due to their long half-life, these compounds often bioaccumulate and oral exposure to PCBs occurs through consumption of meat, such as fish and beef, and dairy products. Additionally, physical proximity to contaminated soil, air, and water can result in inhalation or dermal exposure. The major source of ambient exposure is environmental cycling (volatilization and deposition cycles) of PCBs released into the environment years earlier. Workplace exposure may result from maintenance of and accidents involving PCB containing transformers and instruments. Disposal of such material also poses a risk to those involved. Hazardous waste sites represent potential sites of exposure via contact with the soil, or even breathing contaminated air (Safe 1989).

Absorption of PCBs in humans can occur via inhalation, oral and dermal routes. Lipophilic in nature, they passively diffuse through cell membranes and accumulate within lipid-rich tissues, usually within the liver, adipose, skin and breast milk, as

clearance from the blood occurs rapidly (from minutes to hours) (Safe 1994). PCBs are poorly metabolized in the liver to polar metabolites by the microsomal monooxygenase system, which utilizes cytochrome P450 enzymes. Subsequent conjugation with glucuronic acid and glutathione allows for fecal and urinary excretion. Congeners vary in their ADME (absorption, distribution, metabolism, excretion) characteristics and in pharmacokinetics. Metabolism rates vary depending on the degree of chlorination and the pattern of substitution on the biphenyl ring. Congeners with low chlorine content are generally hydroxylated and eliminated in the urine. Those with both higher chlorine content and non-susceptible substitution patterns tend to either be retained by the body for months to years or excreted in the feces or urine (Safe 1984, 1989, 1990; Safe 1994).

Health effects due to PCBs depend on dose and route of exposure. Hence, they vary in nature and severity. Occupational epidemiology studies on human health effects have been greatly supplemented by toxicological studies on laboratory animals. Based on these investigations, health effects include, but are not limited to the following: skin conditions such as chloracne and dermal lesions; irritation of the nose and lungs; lymphoid involution and immunotoxicity; hepatotoxicity; inhibition of body weight gain; reproductive impairment; gastrointestinal lesions; damage to the kidney and thyroid glands; depression and fatigue; and anemia. PCBs are also endocrine active compounds, meaning they demonstrate anti-estrogenic activity and suppress thyroid and testosterone levels and lactation (Safe 1994). PCB treatment in animal studies has resulted in increased cancer incidence in various tissues and they have been labeled by the EPA as probable human carcinogens (Safe 1989). Assays have demonstrated that they are non-

mutagenic and, on the whole, do not form covalent adducts with DNA. Thus they likely serve as promoters of carcinogenesis rather than initiators (Safe 1989; Safe 1994).

The mechanism(s) of toxicity for the coplanar, dioxin-like congeners of PCB is traditionally thought to be mediated by the binding of the aryl hydrocarbon receptor (AhR) and activation of gene expression (Safe 1994). Signal transduction events downstream of ligand binding may lead to most of the non-neural toxic and biochemical effects of PCBs. However, current evidence suggests alternative pathways independent of the AhR account for the toxicities of congeners responsible for estrogenic, carcinogenic, and neurotoxic activity (Hanneman *et al.* 1996).

Congeners are classified based on AhR binding affinity, structural similarity to 2,3,7,8-TCDD (2,3,7,8-tetrachlorodibenzo-*p*-dioxin) and potencies of toxicity and/or enzyme induction. "Dioxin-like" congeners 1) induce P-450 isozymes, 2) have a high binding affinity to the AhR, 3) are coplanar and 4) are chlorine substituted in both para- and at least two meta-, but not in ortho- positions of the rings. These congeners are typically grouped with other halogenated aromatic hydrocarbons due to their similarity in toxic responses and mechanism of action (Poland and Knutson 1982). The dioxin-like congener, 3,3',4,4',5-pentachlorobiphenyl (PCB 126) serves as the AhR agonist for this study. TCDD, TCDF, and the non-ortho-substituted PCBs 77, 81, 126, and 169 all act as full agonists of the AhR and demonstrate high-intrinsic efficacy. Moreover, PCB 126 demonstrates the strongest binding affinity to the AhR among the coplanar congeners (Hestermann *et al.* 2000).

PCBs and The Liver: Physiological Relevance

The physiological link between PCBs and the liver has been firmly established in the literature (Safe 1994). Epidemiology studies on the carcinogenicity of PCBs in humans examined associations between serum or adipose tissue levels of PCBs and occurrence of cancer. Some studies suggest that occupational exposures to PCBs were associated with cancer at several sites, particularly the liver, biliary tract, intestines, and skin (melanoma) (Safe 1994). There is no clear association between occupational exposures to PCBs and cancer in other tissues, including the brain, hematopoietic, and lymphatic systems (Safe 1989; Safe 1994). Overall, the human studies provide some evidence that PCBs are carcinogenic in specific tissues.

In contrast to the studies in humans, there is conclusive evidence that commercial PCB mixtures are carcinogenic in animals based on the promotion of tumors in the liver (Safe 1994). PCB-induced effects that may involve both Ah-receptor dependent and independent mechanisms include liver hypertrophy, and liver cancer through nongenotoxic mechanisms involving promotion of oncogenic cells (Cogliano 1998; Safe 1994) and/or genotoxic mechanisms (Robertson *et al.* 2000). A general working hypothesis for PCB promotion of liver tumors involves indirect stimulation of cell proliferation following cell or tissue injury by reactive metabolites of PCBs (Silberhorn *et al.* 1990). Alternatively, the cell injury could be caused by increased intracellular concentrations of other reactive species (e.g., superoxide anion or other reactive oxygen species) caused by an overall imbalance from PCB-induced perturbations of cellular biochemical processes, including induction of cytochrome P450s and glutathione S-transferases, repression of glutathione peroxidases, and/or disruption of calcium

homeostatic processes and signal transduction pathways (Silberhorn *et al.* 1990). In addition, some PCB congeners are potent inhibitors of in vitro gap junctional cellular communication, an assay that is indicative of tumor promotion capacity (Bager *et al.* 1997). These factors implicate the liver as an important target organ for PCB toxicity and, as such, warrant our study.

Molecular Mechanism of Gene Regulation by AhR Agonists

Gene expression is a tightly regulated process governed by cell type, temporal factors, and endogenous and exogenous stimuli. Genes may be expressed or transcribed on a continuous basis (housekeeping genes) but expression is generally highly ordered or is an adaptive response to stimuli. Transcription factors are regulatory proteins that may be activated by a stimulus/signal transduction pathway or may directly bind a ligand to initiate transcription of a specific gene.

My model system is one of the most extensively studied transcription factor pathways: the arylhydrocarbon receptor or AhR pathway. The AhR is a cytosolic receptor that binds to a variety of endogenous and exogenous compounds and is an inducer of several enzymes, most notably the cytochrome P450 proteins. My study ligand is PCB 126 (3,3',4,4',5-pentachlorobiphenyl) which is the most potent polychlorinated biphenyl AhR ligand.

The AhR is a ligand-activated transcription factor belonging to the basic helix-loop-helix (bHLH) PER-ARNT-SIM (PAS) family (Carlson and Perdew 2002). PAS proteins serve as "biological sensors," responding to endogenous and exogenous stimuli. As such, the AhR may be involved in cell cycle regulation, cell-cycle arrest, and

apoptosis (Carlson and Perdew 2002; Nebert *et al.* 2000; Puga *et al.* 2002; Santini *et al.* 2001). The AhR is a cytosolic receptor bound to two 90 kDa heat shock proteins (Hsp90), an immunophilin-related AIP/XAP/ARA9 protein, and to a p23 chaperone protein. Upon ligand binding, the AhR complex translocates into the nucleus via importins on the nuclear membrane. Importin α recognizes the nuclear localization signal (NLS) on the AhR, and this complex is then recognized by importin β, which mediates the docking of the complex to the cytoplasmic face of the nuclear pore complex (Petrulis *et al.* 2003). Upon nuclear entry, the AhR dissociates from its chaperone proteins and dimerizes with ARNT (**ar**ylhydrocarbon **r**eceptor **n**uclear **t**ranslocator). Of note, the current notion is that the chaperone proteins assist in the nuclear entry of the AhR, as it was once thought that they dissociated from the complex in the cytoplasm. (McGuire *et al.* 1994; Petrulis and Perdew 2002). The ligand-bound AhR-ARNT complex acts as a transcription factor complex and binds to specific dioxin response elements (DREs) located in the enhancer/promoter region of dioxin responsive genes such as cytochrome P450 1A1 or CYP1A1 (Ma 2001; Whitlock 1999). The sequence for the DRE is 5'-GCGTG-3' and is highly conserved across species (Fujisawa-Sehara *et al.* 1987; Nebert *et al.* 2000).

A multitude of structurally dissimilar endogenous and exogenous compounds have been shown to bind the AhR with varying affinity. Most notable of the exogenous compounds are the polyhalogenated dibenzo-*p*-dioxins, polyhalogenated dibenzofurans, some polycyclic aromatic hydrocarbons, a variety of flavone derivatives, and coplanar members of the polyhalogenated biphenyl family. Compounds with the highest affinity

tend to be hydrophobic, planar, and of a defined size that is thought to fit within the ligand binding pocket (Petrulis and Perdew 2002).

The precise nature and physiologic role of endogenous ligand/s for AhR remain elusive, placing the AhR into an emerging group of orphan receptors (Santiago-Josefat and Fernandez-Salguero 2003). Nonetheless, several physiologic compounds have been shown to interact with the AhR and activate or inhibit signal transduction. These include tryptophan and other indole-containing compounds (Chen *et al.* 1995; Miller 1997; Wei *et al.* 1998), bilirubin (Sinal and Bend 1997), 7-ketocholesterol (Savouret *et al.* 2001), lipoxin A4 (Schaldach *et al.* 1999), indigoids (Adachi *et al.* 2001; Peter Guengerich *et al.* 2004) and flavones and related compounds (Reiners *et al.* 1999). Overall, the low levels, lack of potency, and restricted distribution of these compounds do not implicate them as major endogenous regulators of AhR signaling in most tissues.

Despite the lack of a confirmed endogenous ligand, much is known about the nature of gene activation via the AhR. A "gene battery" is defined as a "group of (generally, nonlinked) genes that exhibit cross-talk, having an intricate interrelationship with regard to up- and down-regulation, in response to a particular endogenous or exogenous signal; the battery's response is mediated by certain regulatory proteins whose effects may be combinatorial in nature" (Britten and Davidson 1969; McKnight and Tjian 1986). The AhR gene battery is one of the best characterized examples in eukaryotes (Nebert *et al.* 2000). The most notable of the inducible genes are detoxifying enzymes such as cytochrome P450 1A1 and 1A2 (CYP1A1/1A2), NAD(P)H:quinone oxidoreductase (NQO1), aldehyde dehydrogenase 3 (ALDH3A1), UDP glucuronosyltransferase (UGT1A6), and glutathione transferase (GSTa1,Ya) (Nebert *et*

al. 2000). Many other genes are now known to be regulated by AhR ligands (Frueh *et al.* 2001; Zeytun *et al.* 2002), but CYP1A1 is the classical biomarker for AhR activation (Whitlock 1999).

Switching Concept

The purpose of this research is to study the nature of gene expression at the single cell level. Gene expression may exhibit either a graded or a "switch-like" response to a stimulus (see figures 1.1, 1.2, 1.3) (Louis and Becskei 2002). Single cell studies have further revealed that many enhancer linked genes are generally "on" or "off" in individual cells; the active enhancer increases the probability that the gene will be active in a given cell (Fiering *et al.* 2000). However, given identical stimuli, some cells will still remain in the "off" state in such a stochastic model of enhancer-gene interaction. Other factors that may contribute to this switch-like, binary response include protein kinase cascades (Ferrell 1996; Ferrell and Machleder 1998), transcriptional synergy between transcription factors and promoter elements (Carey 1998), the interactions of repressors, activators, and coactivators (Blankenship and Matsumura 1997; Gradin *et al.* 1999; Mimura *et al.* 1999), and chromatin remodeling (Okino and Whitlock 1995). Switch-like behavior of gene induction could explain the observed threshold response of a cell to a particular chemical, and perhaps the phenomenon that some cells appear to be non-responders, even at the highest concentration tested (French *et al.* 2004).

The shape of the dose-response curve may vary depending on whether one examines response for a population of cells or for individual cells. A population of cells may exhibit a graded response whereas on a single cell basis the response appears

threshold or switch-like (Ferrell and Machleder, 1998). Studies of gene induction at the level of individual cells and of the processes that lead to different sensitivities of cells to induction are required to develop improved low dose extrapolations for switch-like or so-called binary responses of cells.

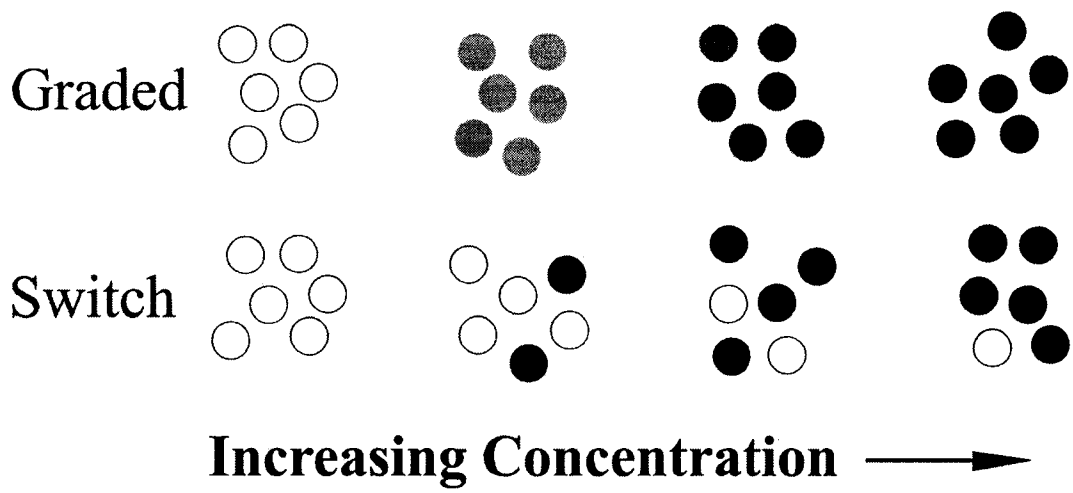

Figure 1.1. Two gene induction models presented on a diagrammatic, cellular level. The graded model has uniform gene induction within one concentration, with all cells eventually responding. The switch model displays more and more cells responding in a binary fashion with increasing concentration, with some non-responders even at the highest dose.

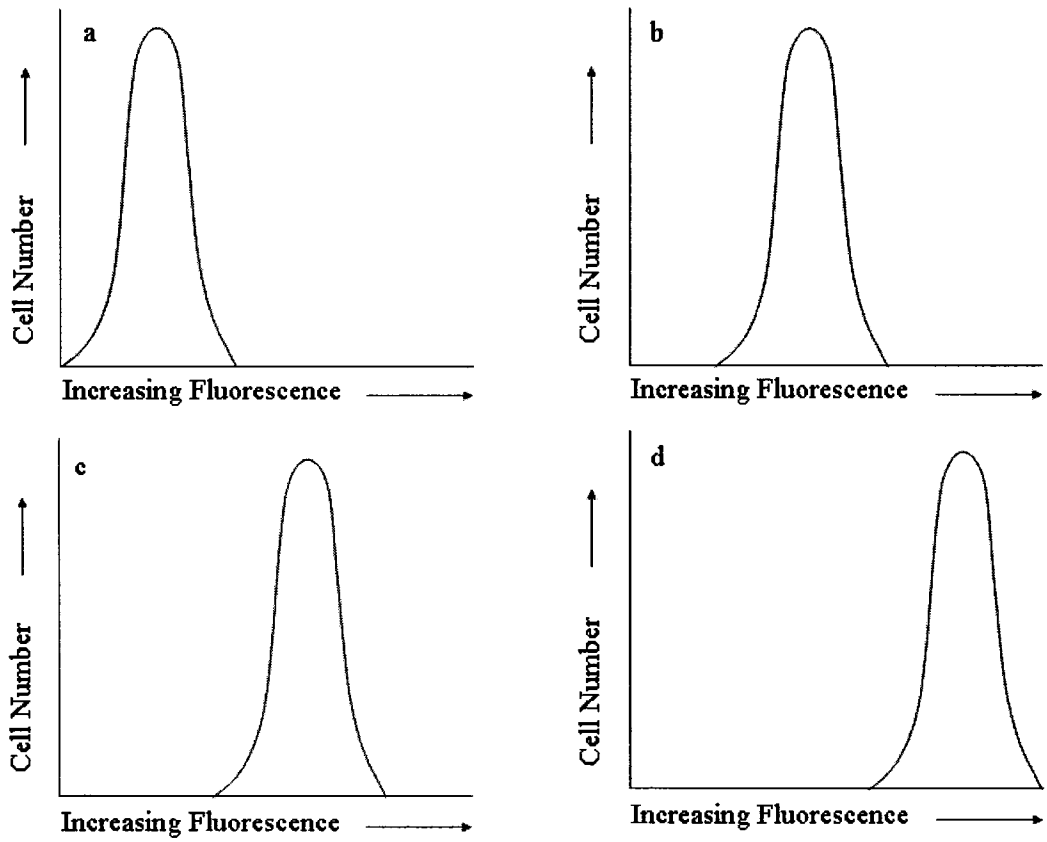

Figure 1.2. Population Level Movement with a Graded Response. This diagram is similar to a flow cytometry histogram representing the response of cells to increasing concentration of a chemical. Panel a represents no chemical, and panels b, c, and d each represent successively increasing concentrations of a chemical. The y-axis is cell number. With a graded response, the entire population of cells moves in unison, expressing more fluorescence with increasing concentrations as a group.

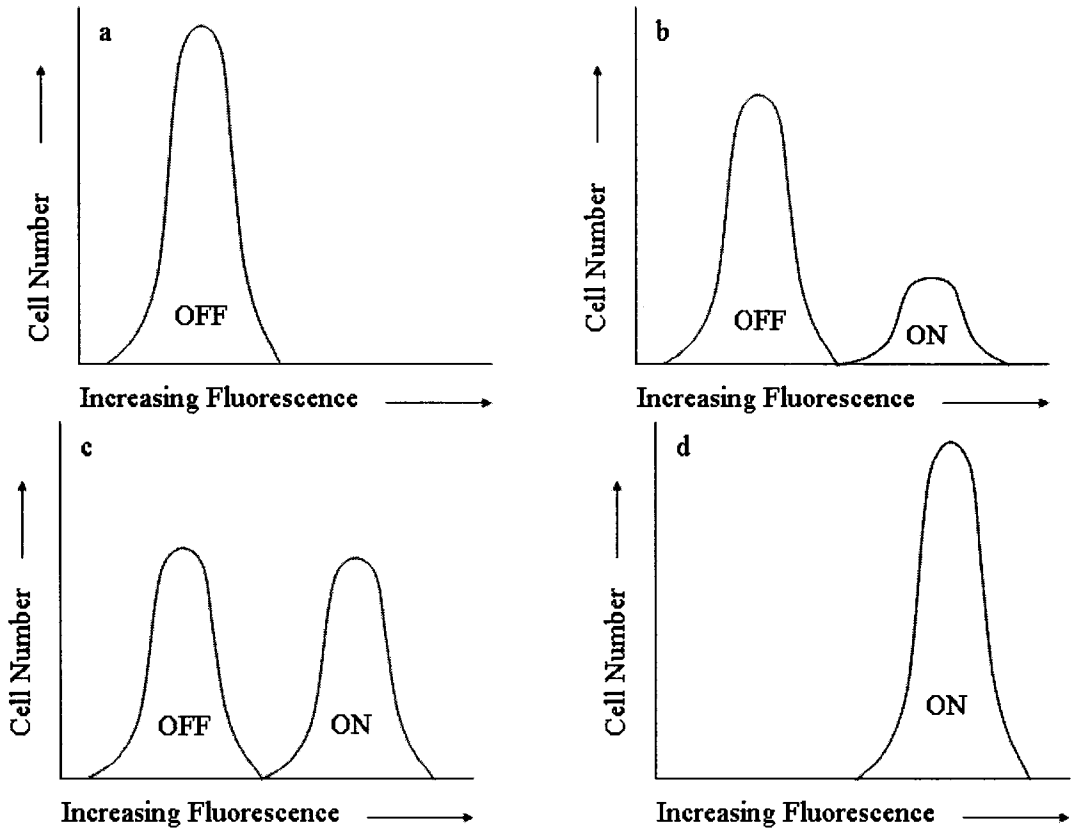

Figure 1.3. Population Level Movement with a Switch Response. This diagram is similar to a flow cytometry histogram representing the response of cells to increasing concentration of a chemical. Panel a represents no chemical, and panels b, c, and d each represent successively increasing concentrations of a chemical. The y-axis is cell number. With a switch response, individual cells move from off to on, with increasing concentrations of chemical. Note how the pool of off cells decreases while the pool of on cells increases with increasing concentration. Once a cell is on, a similar range in fluorescence over the population is observed. The levels of fluorescence do not increase with increasing concentration.

CHAPTER 2

Single Cell Analysis of Switch-Like Induction of CYP1A1 in Liver Cell Lines

Note: The following chapter is reformatted from the publication (Broccardo *et al.* 2004).

Introduction

Gene expression may exhibit either a graded or a "switch-like" response to a stimulus (Louis and Becskei 2002). Single cell studies have further revealed that many enhancer linked genes are generally "on" or "off" in individual cells; the active enhancer increases the probability that the gene will be active in a given cell (Fiering *et al.* 2000). However, given identical stimuli, some cells will still remain in the "off" state in such a stochastic model of enhancer-gene interaction. Other factors that may contribute to this switch-like, binary response include protein kinase cascades (Ferrell 1996; Ferrell and Machleder 1998), transcriptional synergy between transcription factors and promoter elements (Carey 1998), the interactions of repressors, activators, and coactivatorss (Blankenship and Matsumura 1997; Gradin *et al.* 1999; Mimura *et al.* 1999), and chromatin remodeling (Okino and Whitlock 1995). Switch-like behavior of gene induction could explain the observed threshold response of a cell to a particular chemical, and perhaps the phenomenon that some cells appear to be non-responders, even at the highest concentration.

The shape of the dose-response curve may vary depending on whether one examines response for a population of cells or for individual cells. A population of cells may exhibit a graded response whereas on a single cell basis the response appears threshold or switch-like (Ferrell and Machleder, 1998). Studies of gene induction at the level of individual cells and of the processes that lead to different sensitivities of cells to induction are required to develop improved low dose extrapolations for switch-like or so-called binary responses of cells.

Cytochrome P450 proteins are a superfamily of enzymes involved in the biotransformation of various drugs, carcinogens and steroid hormones (Estabrook 1996). CYP1A1 is the classic biomarker of exposure to halogenated aromatic hydrocarbons (HAHs), including 2,3,7,8-tetrachlorodibenzo-*p*-dioxin (TCDD), and the most potent polychlorinated biphenyl agonist, PCB 126 (Hestermann *et al.* 2000). CYP1A1 is part of the **a**ryl **h**ydrocarbon **r**eceptor (AhR) gene battery (Nebert *et al.* 2000). AhR is a cytosolic receptor that, upon ligand binding, translocates into the nucleus and dimerizes with the **a**ryl **h**ydrocarbon **n**uclear **t**ranslocator (ARNT) (Ma 2001). The ligand-bound AhR-ARNT complex binds to dioxin response elements (DREs) located in the enhancer/promoter region of TCDD responsive genes such as CYP1A1. CYP1A1 displays minimal to no constitutive expression and is highly inducible by PCB 126 and TCDD (Whitlock 1999).

Previous research has demonstrated a distinctly heterogeneous pattern of CYP1A1 enzyme induction within the rat liver (Andersen *et al.* 1995; Bars and Elcombe 1991; Tritscher *et al.* 1992). Immunohistochemical staining following in vivo treatment with TCDD demonstrate that low doses induce CYP1A1 solely within the centrilobular

region and as the dose increases the proportion of induced cells increases and staining spreads out toward periportal areas. Within the induced liver, there is a clear boundary between responsive regions (Bars and Elcombe 1991; Bars *et al.* 1989). Hence individual hepatocytes appear as either uninduced or fully induced at any specific concentration of TCDD. In our laboratory, primary rat hepatocyte cultures display similar behavior (French *et al.* 2004). On a single cell basis, adjacent cells appear induced/uninduced for CYP1A1 protein and mRNA after in vitro PCB 126 treatment as seen by in situ hybridization and immunocytochemistry. The concentration-dependent switching response was accompanied by an increase in the proportion of cells within the induced pool; however a single, maximal induction peak did not result. Instead, groups of induced cells exhibited varying degrees of induction intensity. Overall, the resulting distributions appear to support a hybrid switch response, where a switch works in concert with a rheostat, much like a dimmer on a light switch in a home.

The research described here extends the primary rat hepatocyte model focusing on two liver cell lines, the H4IIE rat hepatoma, and the Hepa 1c1c7 mouse hepatoma cells. The H4IIE cells display switch-like behavior, as previously noted in the in vivo and in vitro liver cell models. Using flow cytometry to study single cell CYP1A1 protein induction, cells appear either "on" or "off." Studies using small concentration increments to better elucidate the shape of the concentration-response curve and the apparent switch support this hypothesis. As concentration increases, the number of cells expressing CYP1A1 protein increases to the same maximal level of induction, with some cells still not responding, even at the highest concentrations.

Materials and Methods

Culture of Cell Lines: All cell culture products were obtained from Gibco unless otherwise noted. Rat hepatoma H4IIE cells (ATCC) were cultured in DMEM supplemented with 10% FBS (Hyclone) and 100 units/ml penicillin/100 μg/ml streptomycin and maintained at 37°C and 5% CO_2. Mouse hepatoma Hepa 1c1c7 cells (ATCC) were cultured in α-MEM without nucleosides supplemented with 10% FBS, 100 units/ml penicillin/100 μg/ml streptomycin and maintained at 37°C and 5% CO_2. For PCR and flow cytometry both cell lines were seeded at 1 x 10^6 cells in 60 mm culture dishes (Falcon).

PCB 126 Treatment: PCB 126 (3,3',4,4',5-pentachlorobiphenyl) was obtained from Accustandard and confirmed by GCMS to be pure and free of other congeners. For treatment, PCB 126 was dissolved in DMSO; treatments contained less than 0.25% DMSO. No changes in growth rate or morphology were observed after treatment with DMSO or PCB as compared to naïve cells.

RNA Isolation and cDNA Synthesis: RNA was isolated using the RNeasy mini kit (Qiagen). Briefly, lysis buffer was added to each 60 mm dish and cells were removed using a rubber policeman. The lysate was then homogenized in a QIAshredder spin column and then applied to the RNeasy mini column. The membrane bound RNA was then put through a series of washes and eluted in DEPC water. RNA was quantified on a spectrophotometer and purity was verified on a 1% agarose gel. One μg of total RNA was reverse transcribed using the Promega Reverse Transcription system containing oligo

$d(T)_{15}$ primers (0.5μg), AMV reverse transcriptase (15 units), dNTP mix (1 mM each), first strand buffer (10 mM Tris-HCl, 50 mM KCl, 0.1% Triton X-100), $MgCl_2$ (5 mM) and recombinant Rnasin ribonuclease inhibitor (0.5 units) in a final reaction volume of 20 μl. The reaction was performed at 42°C for 15 minutes and then incubated at 99°C for 5 minutes to inactivate the reverse transcriptase.

Real-time Quantitative RT-PCR: Quantitative PCR was performed in the Bio RAD iCycler iQ Real-Time Detection System. Dr. Nigel Walker (NIEHS) kindly provided the primer and Taqman probe sequences in Table 2.1. All primer sequences have homology to both the rat and mouse as determined by a BLAST search. The cDNA (50 ng) was amplified in a mixture of 1 mM dNTPs (Invitrogen), 0.5 μM each of forward and reverse primers, (Invitrogen), 0.2 μM Taqman probe primers, 1X PCR buffer F (Invitrogen) and 1 unit Platinum Taq polymerase (Invitrogen) in a 50 μl total reaction. The fluorescent moieties of the Taqman probe primers were 5' 6-FAM and 3' Black Hole Quencher-1 (Integrated DNA Technologies Inc.) Conditions of the PCR were 3 minutes at 95°C followed by 50 cycles of 2-step PCR for 15 seconds at 95°C and one minute at 55°C. Each sample was performed in duplicate. The data were normalized by subtracting the difference of the C_T values between the CYP1A1 gene of interest and the β-actin housekeeping gene. This calculation of (CYP1A1 C_T)-(β-actin C_T) is ΔC_T. Fold induction (relative expression) was calculated as $2^{-(S\Delta C_T - C\Delta C_T)}$ where $S\Delta C_T$-$C\Delta C_T$ is the difference between the sample ΔC_T (PCB 126 treated) and the control ΔC_T (DMSO, untreated). Both the CYP1A1 and β-actin reactions approached 100% efficiency as

determined by standard curves. The PCR products were analyzed on agarose gels and found to produce single products.

Table 2.1 Primer Sequences Used in Real Time RT-PCR[a]

Gene	Forward Primer	Reverse Primer	Taqman Probe
CYP1A1	5'-tcaaagagcactacaggacatttg	5'-gggttggttaccaggtacatgag	5'-aagggccacatccgggacatca
β-actin	5'-gacaggatgcagaaggagattactg	5'-gctgatccacatctgctggaa	5'-atcaagatcattgctcctcctgag

[a] Primer sequences kindly provided by Dr. Nigel Walker (NIEHS)

Flow Cytometry: After treatment, cells were trypsinized and washed once in PBS. Cells were resuspended in 2% formaldehyde, EM grade, without methanol (Polysciences) and fixed on ice for 30 minutes. Cells were washed twice in PBS/1% BSA and then permeabilized for 10 minutes in 0.8% saponin (Sigma) in PBS/1% BSA. Cells were washed once in PBS/1% BSA and blocked for 15 minutes in 5% goat serum (Sigma) in PBS/1% BSA. Cells were washed once in PBS/1% BSA and incubated with rabbit anti-rat CYP1A1 polyclonal antibody (1:500 dilution, Chemicon) in PBS/1% BSA, 0.8% saponin for 60 minutes. Cells were washed 3 times in PBS/1% BSA and incubated with Alexa Fluor 488 goat anti-rabbit IgG (1:200 dilution, Molecular Probes) in PBS/1% BSA, 0.8% saponin for 30 minutes in the dark. Cells were washed 3 times in PBS/1% BSA and resuspended in 1 ml PBS and analyzed on the Beckman Coulter EPICS 5 Flow Cytometer. Alexa Fluor 488 was excited by the 488 nm line of an argon ion laser operating at 200 mW of power. Fluorescence was detected by a photomultiplier equipped with a 525 band pass filter. Light scatter was collected in both the forward and right angle directions. Data were processed and displayed on the Cyclops software (Dako

Cytomation). To assess nonspecific binding of the antibodies, DMSO and PCB 126 treated samples were incubated with rabbit IgG (Sigma) instead of the rabbit anti-rat CYP1A1 primary antibody. A PCB 126 sample was also incubated with no primary antibody (vehicle only) and then with Alexa 488 to assess any nonspecific binding of the secondary antibody.

Immunocytochemistry (ICC): Cells were seeded on permanox 2-well chamber slides (Nunc) at 140,000 cells/well. Cells fixed on slides were stained through immunocytochemistry to visualize CYP1A1 protein levels in individual cells. ICC was performed on duplicate slides for each treatment group. On the day of staining, slides were rehydrated and incubated in 0.3% hydrogen peroxide to quench exogenous peroxidase activity. Slides were immersed in Citra Antigen Retrieval Solution (Biogenex) and microwaved until boiling (approximately 3 minutes). They were then microwaved another 10 minutes at low power and allowed to cool. After a 5 minute wash in running deionized water, the slides were incubated in PBS with Avidin blocking solution (Vector Labs) at 37°C for 15 minutes followed by a rinsing off with PBS and incubation with Biotin blocking solution (Vector Labs) for 15 minutes at 37°C. After another quick wash, slides were incubated for 10 minutes with normal goat serum from Vectastain Avidin-Biotin Complex (ABC) kit (Vector Labs). Without washing, rabbit anti-rat CYP1A1 antibody (Chemicon) was added at 1:500 dilution for 15 minutes at 37°C. After a 5-minute wash in PBS, biotinylated anti-rabbit IgG antibody was added (Vectastain kit) for 25 minutes. Slides were washed for 5 minutes in PBS and ABC reagent (Vectastain kit) was added for 30 minutes. Following another 5 minute wash in

PBS, 3-amino-9-ethylcarbazole (AEC, Biomeda) was prepared and added for approximately 5 minutes at 37°C, then washed off with deionized water. The slides were then counterstained for 30 s with Gill's hematoxylin and washed in running tap water for 10 minutes. Slides were cover-slipped using water based (Kaiser's) mounting media.

Statistical Methods: Real Time PCR. Fold induction of the real-time PCR data were calculated using the $2^{-\Delta\Delta C}{}_T$ method (Livak and Schmittgen 2001). This method normalizes using the housekeeping gene of choice and determines fold induction of a gene due to a chemical treatment. Concentration-response and time-course curves were generated using Graph Pad Prism® 3.0. These data were fit based on the Hill relationship:

$$Induction = Induction_{max} * Concentration^n / (Concentration^n + K_d^n)$$

Where n is the Hill coefficient and K_d is ligand receptor binding affinity.

The actual transformed equation applied was:

$$R(d,t) = R_0 + (R_{max,t} - R_0)/(1+10\text{^}(LogEC_{50}\text{-}LogDose)*n^H))$$

Where R(d,t)=response at a given time t after dosing; R_0=initial response; $R_{max,t}$=maximal response at a given time t after dosing; $LogEC_{50}$= log dose at 50 percent maximal response; n^H = Hill slope.

This is a sigmoidal dose-response (variable slope) equation that generates a n^H (Hill slope), EC_{50} and r^2 for the concentration-response studies. Each point on the curve represents duplicate experiments. For the time course study, a nonlinear regression (sigmoidal dose-response, identical to the formula above minus the Hill coefficient) was used for the H4IIE cells. R_0, R_{max}, and Log EC_{50} were held constant. Linear regression was used for the Hepa 1c1c7 cells for the time course study.

Flow Cytometry. The histograms directly from the flow cytometer were generated in Cyclops (Dako Cytomation). Statistical analyses were performed using GraphPad® Prism 3.0 and curves were fit using the same sigmoidal dose-response (variable slope) curve fit algorithm as for PCR. Differences between treatments were evaluated using ANOVA and Tukey's Multiple Comparison test ($p<0.05$).

Results

Real Time RT-PCR: Real time RT-PCR was performed in order to compare previously determined CYP1A1 induction levels in primary rat hepatocytes to the H4IIE rat hepatoma and Hepa 1c1c7 mouse hepatoma cell lines. Both concentration-response and time-course analyses were performed on the two cell lines. H4IIE cells display approximately 1000 fold induction of CYP1A1 at 24 h (Figure 2.1a). Induction shifted to maximal between 2.5×10^{-11} to 2.5×10^{-9} M PCB 126 ($EC_{50}=1.6 \times 10^{-10}$ M, $r^2=.99$) on this semi-log plot. The time course analysis, at a concentration of 2.5×10^{-8} M, revealed that induction was maximal by 16 h, rising to 2000 fold induction, and down to 1000 fold induction by 48 h (Figure 2.1b). The Hepa 1c1c7 cells displayed approximately 30 fold

Figure. 2.1a

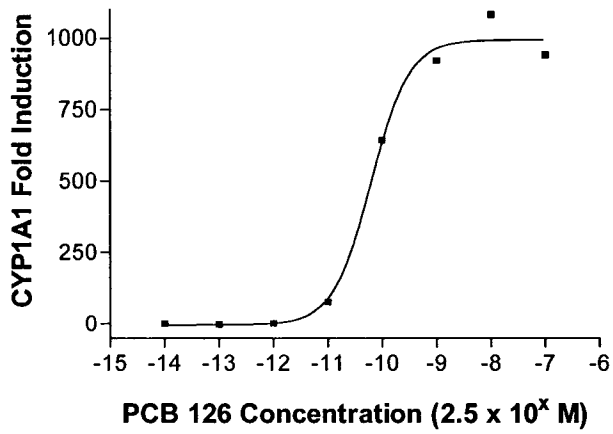

Figure 2.1b

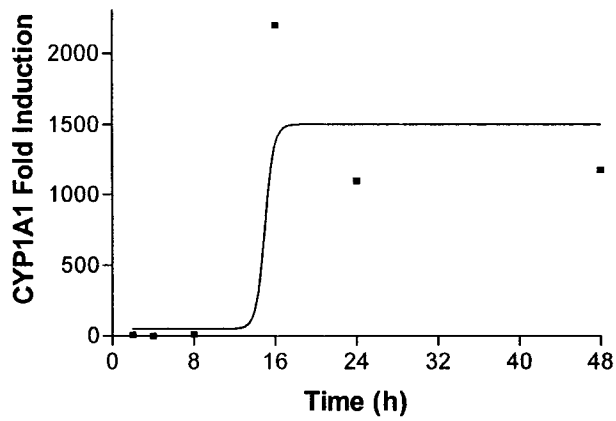

Figure 2.1. CYP1A1 mRNA fold induction levels in H4IIE cells. Relative quantification of the mRNA induction levels was accomplished by real time RT-PCR using primers specific for the gene of interest, CYP1A1, and a housekeeping gene, β-actin. (a) 24 h treatment with PCB 126 with concentrations ranged 10-fold from 2.5×10^{-14} to 2.5×10^{-7} M (b) treatment with 2.5×10^{-8} M PCB 126 for 2, 4, 8, 16, 24, 48 h.

Figure 2.2a

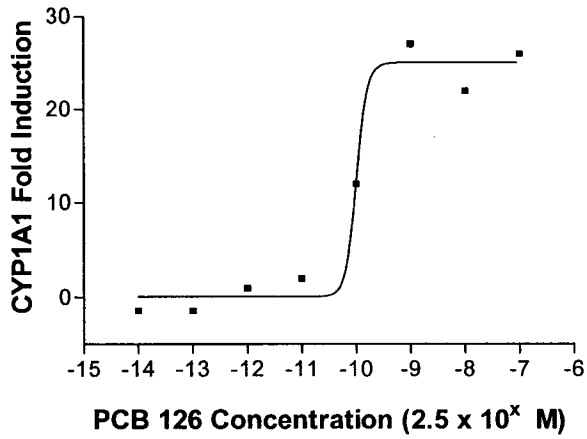

Figure 2.2b

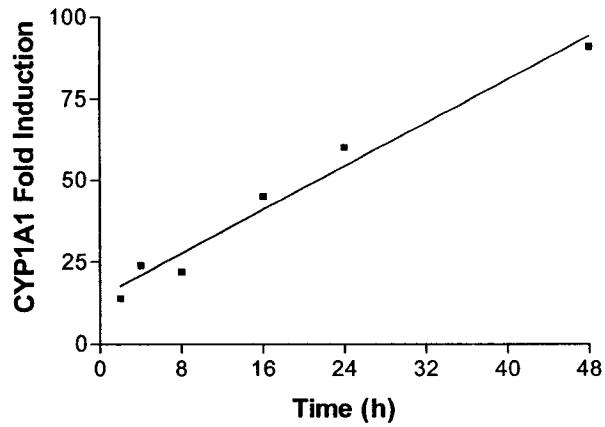

Figure 2.2. CYP1A1 mRNA fold induction levels in Hepa 1c1c7 cells. Relative quantification of the mRNA induction levels was accomplished by real time RT-PCR using primers specific for the gene of interest, CYP1A1, and a housekeeping gene, β-actin. (a) 24 h treatment with PCB 126 with concentrations ranged 10-fold from 2.5 x 10^{-14} to 2.5 x 10^{-7} M (b) treatment with 2.5 x 10^{-8} M PCB 126 for 2, 4, 8, 16, 24, 48 h.

induction of CYP1A1 by 24 h with induction shifting to maximal between 2.5 x 10^{-11} to 2.5 x 10^{-9} M PCB 126 (EC_{50}=2.5 x 10^{-10} M, r^2=.98) (Figure 2.2a). The time-course analysis, at a concentration of 2.5 x 10^{-8} M, revealed approximately 100 fold induction of CYP1A1 by 48 h (Figure 2.2b) and the level of induction was still increasing. It was determined that the Hill slope for these curves were not reliable due to minimal data points around the midpoint of the curve.

Immunocytochemistry: Immunocytochemistry was performed in order to visually localize CYP1A1 protein on an individual cell basis. The pattern of CYP1A1 staining in H4IIE cells reveal, at a representative maximal concentration of 2.5 x 10^{-9} M PCB 126 for 24 h, some cells intensely stained for CYP1A1 adjacent to cells that display little to no CYP1A1 staining (Figure 2.3b) as compared to DMSO vehicle control (Figure 2.3a) which is negative for CYP1A1. A similar pattern can be observed in the Hepa 1c1c7 cells at the same concentration 2.5 x 10^{-9} M for 24 h (Figure 2.3d) as compared to DMSO (Figure 2.3c). Deciphering a clear pattern of CYP1A1 expression across the population is not entirely possible. Once a cell is on there are several patterns seen. Many neighboring cells may be on, but there are also neighboring cells with far less expression or cells that are off. Further, completely isolated cells, i.e. cells with no direct contact with other cells, may be on or off. As such, it is not possible to say that CYP1A1 expression occurs in definitive "clusters."

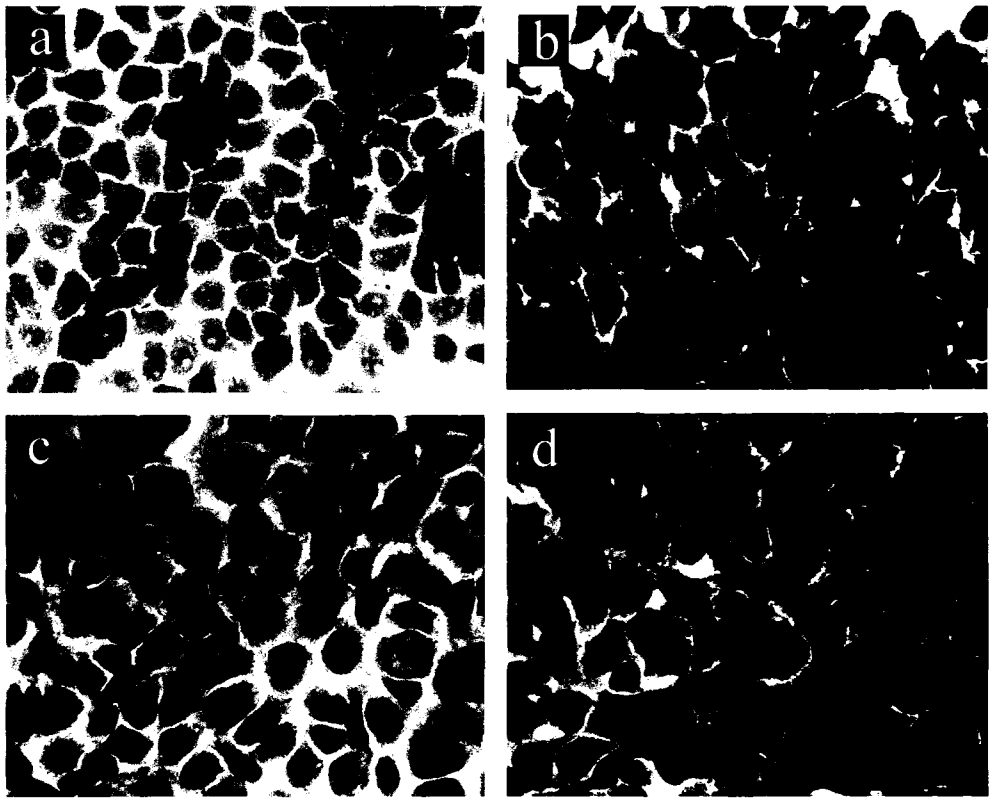

Figure 2.3. Immunocytochemistry stained slides reflecting the distribution of induced CYP1A1 protein within cells after 24 h. The Gill's hematoxylin counterstained photomicrographs are under 40X magnification. (a) H4IIE cells, DMSO (b) H4IIE cells, 2.5 x 10^{-9} M (c) Hepa 1c1c7 cells, DMSO (d) Hepa 1c1c7 cells, 2.5 x 10^{-9} M

Flow Cytometry: Flow cytometry was used to measure CYP1A1 protein levels after PCB 126 treatments in H4IIE and Hepa 1c1c7 cell lines. Within the histograms (Figures 2.4, 2.5) region 1 is gated to include the background fluorescence of the DMSO vehicle control; cells within region 2 show an increase in green fluorescence representing CYP1A1 expression. There is a concomitant increase in cells in region 2 as concentration increases, representing more cells expressing CYP1A1 on a single cell basis. The increase in the number of cells expressing CYP1A1 is marked between 1.6×10^{-10} to 2.5×10^{-9} M in the H4IIE cells (Figure 2.4), and between 2.5×10^{-10} to 2.5×10^{-9} M in the Hepa 1c1c7 cells (Figure 2.5) with the population of induced cells expressing similar levels of CYP1A1 as seen by the overlap of the curves. The concentration 2.5×10^{-13} M has a nearly identical curve to that of the DMSO control in both cell lines. Rabbit IgG isotype controls and secondary antibody only controls had minimal to no fluorescence, as compared to the DMSO curves in all experiments. Single cell flow cytometry concentration-response analysis of H4IIE cells is shown in figure 2.6. A concentration-response ranging from 2.5×10^{-13} M to 2.5×10^{-5} M revealed maximal induction of CYP1A1 by 2.5×10^{-10} M with approximately 80% of the cell population responding. The concentrations of 2.5×10^{-13} to 2.5×10^{-11} are not statistically significant from DMSO ($p < 0.05$). To better define the shape of the H4IIE concentration-response curve smaller concentration increments were used as seen in figure 2.7. The incremental doses used were: 1.6×10^{-9}, 10×10^{-10}, 6.3×10^{-10}, 4×10^{-10}, 2.5×10^{-10}, 1.6×10^{-10}, 10×10^{-11}, 6.3×10^{-11}, and 4×10^{-11} M PCB 126. These are equally spaced doses between 2.5×10^{-9} and 2.5×10^{-11} M on a log scale. Triplicate experiments were performed using the dose increments, and these data were combined with the original dose response curve (figure

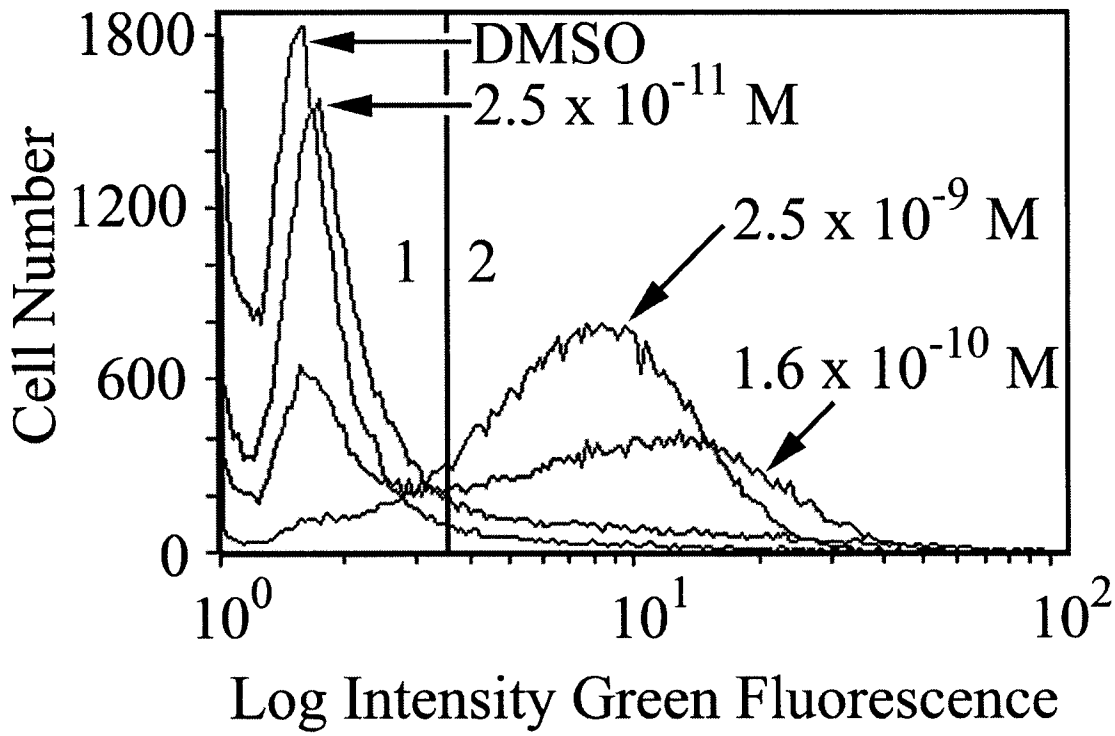

Figure 2.4. CYP1A1 protein induction in H4IIE cells. This histogram overlay of several concentrations from figure 2.7 shows the pattern of induction on a single cell basis within a concentration, and between concentrations of PCB 126. The populations of induced cells express similar levels of CYP1A1 as seen by the overlap of the curves, with the number of induced cells increasing with concentration of PCB 126.

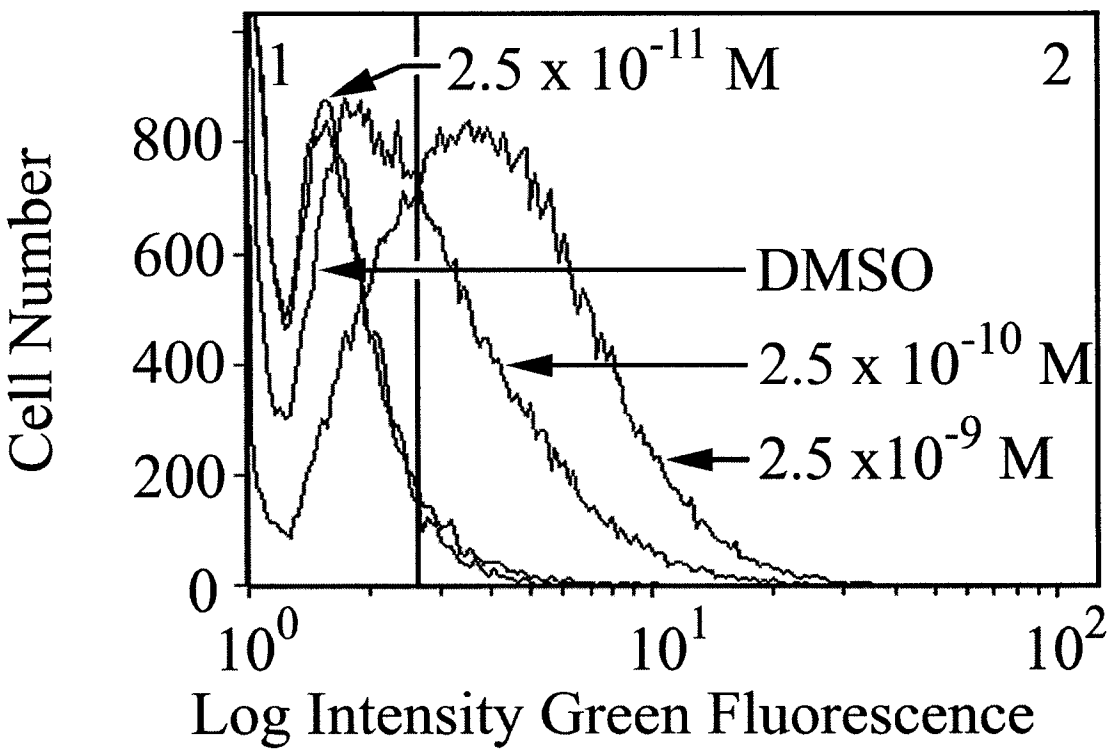

Figure 2.5. CYP1A1 protein induction in Hepa 1c1c7 cells. This histogram overlay of several concentrations from figure 2.9 shows the pattern of induction on a single cell basis within a concentration, and between concentrations of PCB 126. The populations of induced cells express similar levels of CYP1A1 as seen by the overlap of the curves, with the number of induced cells increasing with concentration of PCB 126.

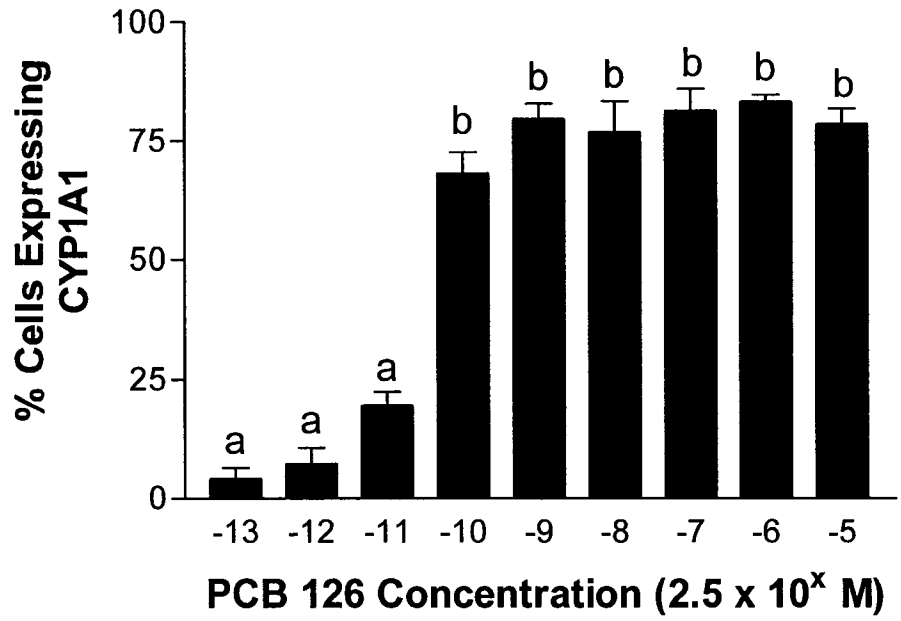

Figure 2.6. CYP1A1 protein induction in H4IIE cells following a 24 h PCB 126 treatment using concentrations ranging 10-fold from 2.5 x 10^{-13} to 2.5 x 10^{-5} M as measured with flow cytometry. The concentrations 2.5 x $10^{-13\ to\ -11}$ are not statistically significant from DMSO ($p<0.05$). Bars represent the $\pm$ SEM of at least three independent experiments. Different letters above bars represent significant difference between treatments ($a \neq b$) $p<0.05$.

2.6) to create figure 2.7. The r^2=.93, EC_{50}=7.2 x 10^{-11} M, and n^H=1.3. Identical experiments were performed with the Hepa 1c1c7 cells, as seen in figures 2.8 and 2.9. Maximal induction of CYP1A1 was obtained by 2.5 x 10^{-9} M, with approximately 70% of the cell population responding (Figure 2.8). The concentrations of 2.5 x 10^{-13} to 2.5 x 10^{-11} were not statistically significant from DMSO ($p < 0.05$). Incremental concentrations yielded an r^2=.96, EC_{50}=2.13 x 10^{-10} M, and n^H =1.8 (Figure 2.9).

Discussion

This research demonstrates that the H4IIE rat hepatoma cell line also demonstrates a threshold, switch-like response at the single cell level to the CYP1A1 inducer, PCB 126. This behavior agrees with previous research from our laboratory, supporting a switch model of CYP1A1 induction in primary rat hepatocytes as seen using in situ hybridization (French *et al.* 2004). Studies in vivo also indicated that hepatic CYP1A1 induction was switch-like with characteristics of a hybrid-model (Bars and Elcombe 1991; Bars *et al.* 1989). Such a hybrid switch model is comparable to a dimmer on a light switch in a home, where a switch works in concert with a rheostat. Experimentally, such a hybrid switch model on the single cell level represents an initial induction threshold then a graded response thereafter. In the present study, flow cytometry was used to quantify the level of CYP1A1 protein in single cells. It is assumed that CYP1A1 protein levels reflect PCB 126's effects on CYP1A1 gene expression since the correlation of CYP1A1 protein and mRNA is well documented. The correspondence between protein induction and mRNA induction was also examined in the studies with primary hepatocytes (French *et al.* 2004).

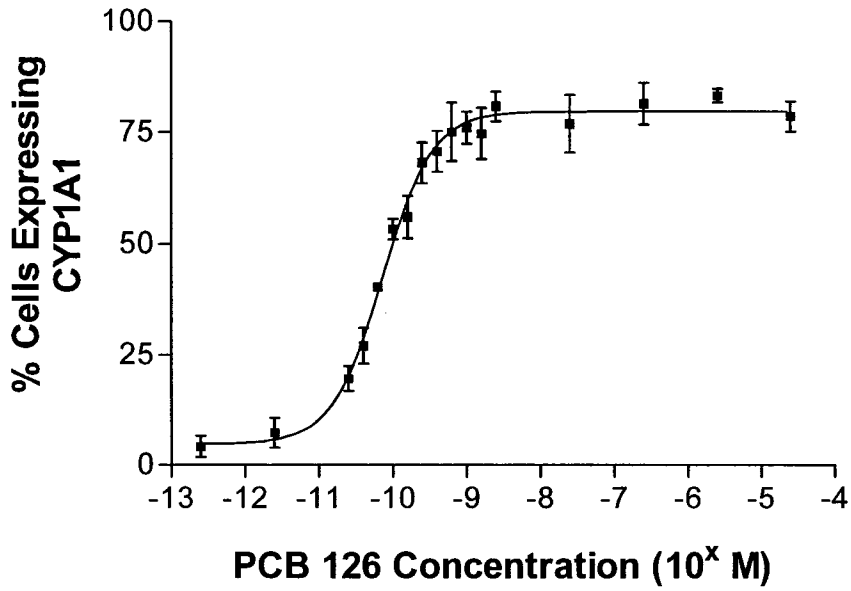

Figure 2.7. CYP1A1 protein induction in H4IIE cells following a 24 h PCB 126 treatment. This figure is a combination of the triplicate data from fig. 2.4 and the addition of 8 small dose increments between 2.5 x 10^{-11} to 2.5 x 10^{-9} M, performed in triplicate, as measured with flow cytometry. Bars represent the $\pm$ SEM of at least three independent experiments.

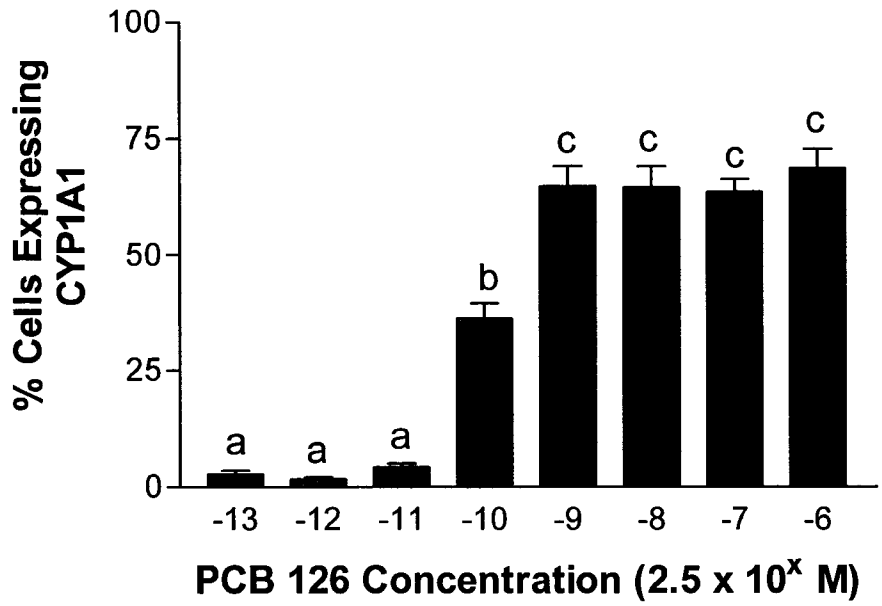

Figure 2.8. CYP1A1 protein induction in Hepa 1c1c7 cells following a 24 h PCB 126 treatment using concentrations ranging 10-fold from 2.5 x 10^{-13} to 2.5 x 10^{-6} M as measured with flow cytometry. The concentrations 2.5 x $10^{-13\ to\ -11}$ are not statistically significant from DMSO ($p<0.05$). Bars represent the $\pm$ SEM of at least three independent experiments. Different letters above bars represent significant difference between treatments ($a \neq b \neq c$) $p<0.05$.

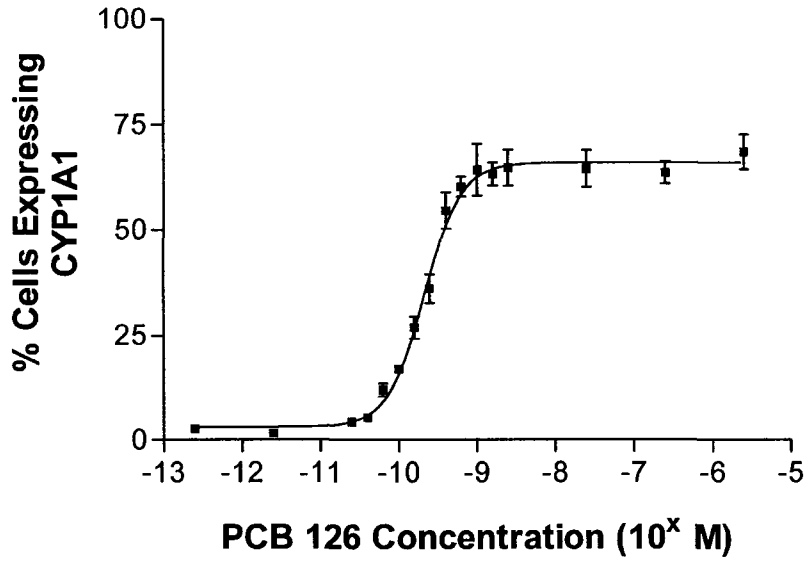

Figure 2.9. CYP1A1 protein induction in Hepa 1c1c7 cells following a 24 h PCB 126 treatment. This figure is a combination of the triplicate data from fig. 2.6 and the addition of 8 small dose increments between 2.5 x 10^{-11} to 2.5 x 10^{-9} M, performed in triplicate, as measured with flow cytometry. Bars represent the $\pm$ SEM of at least three independent experiments.

Gene induction at the single cell level may display two types of responses: graded (linear) or threshold/switch (binary). The linear curve implies that there is a uniform, cellular response at every concentration; therefore all cells will display the same level of CYP1A1 induction. With a binary switch, there are some concentrations where there is no response, and then a sharp rise in induction occurs with increasing concentration. As a result, a cell exists in two stable states: uninduced or induced. In reality, however, cellular response may not be as clear cut as the graded or switch theoretical models would define. Cells may, in fact, respond in an intermediate, hybrid fashion. Such a response could be defined as a hybrid switch, whereby cells must pass an initial concentration-threshold, then exhibit a graded response thereafter (Figure 2.10).

The H4IIE flow cytometry data presented here support a switch response. In this case, the induced population has a distribution of staining characteristics, but populations still move from a basal state to an induced state in a binary manner. Within one concentration, once a cell is induced it may express varying amounts of CYP1A1 (Figure 2.4, 2.5). Further, with increasing concentration, the number of CYP1A1 expressing cells increases, with all activated cells displaying the same range in induction as seen by the overlapping curves (in region 2). If the response were graded at the single cell level, a concentration-dependent horizontal shift in curves would be seen, representing a simultaneous shift in all cells with increasing concentration. The data with the Hepa 1c1c7 cells show an increase in CYP1A1 expression with dose, however, provide less resolution between induced and uninduced curves which results in a less definitive conclusion regarding the switch-like nature of this cell line.

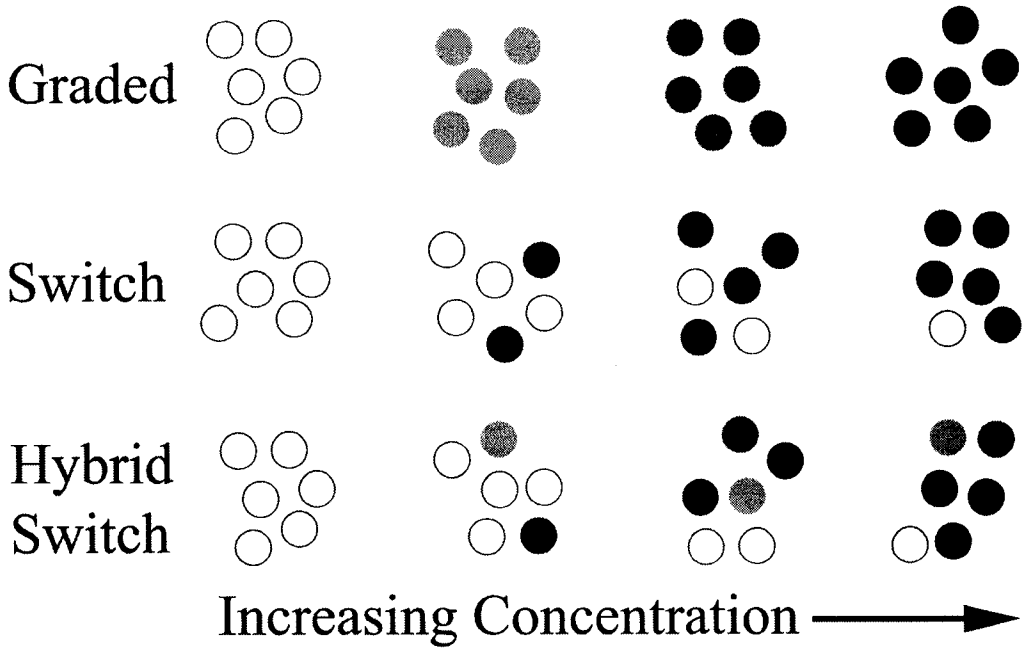

Figure 2.10. Three induction models presented on a diagrammatic, cellular level. The graded model has uniform gene induction within one dose, with all cells eventually responding. The switch model displays more and more cells responding in a binary fashion with dose, with some non-responders even at the highest dose. The hybrid switch model is a combination of the graded and switch models. Once a cell is induced it may display a range of induction levels. There are still non-responders even at the highest dose.

The goal of the ICC was to qualitatively show the phenomenon of on and off cells within one dose, and as such was consistent with the flow cytometry data. Cells exposed to a single concentration of PCB 126 displayed a range of induction once they are "on" and can be seen adjacent to uninduced cells (Figure 2.3). If the cells responded in a graded, linear fashion, one would expect all of the cells to have a similar level of induction within one concentration.

Further, cell cycle does not appear to affect the CYP1A1 protein expression pattern. Cells were serum starved for 48 h, treated with 2.5×10^{-7} M PCB 126, 2.5×10^{-10} M PCB 126, or DMSO for 24 h. The pattern of CYP1A1 protein expression did not change as seen in ICC (data not shown). Both the immunocytochemistry and flow cytometry experiments show that there are some cells in which CYP1A1 is not induced, even at high concentrations of PCB 126. Interestingly, flow cytometry using murine epidermal cells also showed a population of cells which did not respond to β–naphthoflavone in the induction of CYP1A1 (Stauber *et al.* 1995).

On a population level, the H4IIE and Hepa 1c1c7 cells display a continuous concentration-response curve for CYP1A1 mRNA induction as seen in primary rat hepatocytes (French *et al.* 2004) using quantitative real-time PCR (Figure 2.1, 2.2). Of note, there appears to be low-level constitutive expression of CYP1A1 mRNA in the Hepa 1c1c7 cells as seen in figure 2.2b at time zero. This is not without precedence; Santini *et. al.* (Santini *et al.* 2001) also found low-level constitutive expression of CYP1A1 mRNA in DMSO treated Hepa 1c1c7 cells. This might explain the comparatively lesser fold-induction of CYP1A1 mRNA as compared to the H4IIE cells.

This low-level constitutive expression is not detectable using ICC or flow cytometry methods which measure protein, perhaps due to the higher sensitivity of quantitative real-time PCR.

How might such a hybrid switch response fit in with the accepted CYP1A1 induction model? AhR is a cytosolic receptor bound to two 90 kDa heat shock protein (Hsp90) molecules, an immunophilin-related AIP/XAP/ARA9 protein, and to a p23 chaperone protein. After ligand binding, AhR dissociates from this complex, translocates into the nucleus and dimerizes with the ARNT. The ligand-bound AhR-ARNT complex acts as a transcription factor complex and binds to specific dioxin response elements (DREs) located in the enhancer/promoter region of dioxin responsive genes such as CYP1A1 (Ma 2001; Whitlock 1999). However, there are additional modulators in this process that may contribute to the switch response. For example, it is known that the MAPKs (mitogen activated protein kinases) ERK (extracellular regulated kinase) and JNK (c-Jun N-terminal kinase) are activated independently of the AhR (i.e. AhR is not required for their activation), yet are essential for AhR mediated CYP1A1 induction (Tan *et al.* 2002). Further, the MAPK cascade has the potential to convert a graded stimulus into a switch-like response, through a phenomenon termed ultrasensitivity, whereby multiple events working in concert allow for a rapid activation of a signal transduction cascade (Ferrell 1996; Goldbeter and Koshland 1984; Huang and Ferrell 1996). The concept of ultrasensitivity emphasizes the fact that the slope of the stimulus/response curve is steeper than that of a hyperbolic Michaelis-Menten enzyme. The necessity of the MAPK cascade for CYP1A1 induction introduces the possibility of a MAPK mediated switch acting through a form of ultrasensitivity. In addition, a variety of serine/threonine

and/or tyrosine phosphorylation events are now recognized to be crucial to the regulation and activity of the AhR pathway. For example, phosphorylation of AhR positively regulates the DNA binding activity of AhR, and phosphorylation on ARNT is necessary for dimerization between AhR and ARNT (Park *et al.* 2000). Protein kinase C (PKC) has also been shown to cause a synergistic increase in ligand-induced CYP1A1 gene induction (Chen and Tukey 1996) and has also been shown to be activated by AhR ligand (Hanneman *et al.* 1996), perhaps by AhR-dependent sustained elevation of intracellular free calcium (Puga *et al.* 1997). These nongenomic, enzymatic events are additional processes that may contribute to the observed threshold response.

In addition to nongenomic, enzymatic cell-signaling events, the genomic interactions of the AhR-ARNT heterodimer with the DREs may also generate a switch. Conversion of the CYP1A1 gene from a silent phenotype to an accessible target for activation by the heterodimeric transcription complex may require histone modification that could also regulate a switch (Okino and Whitlock 1995). Whether the switch is genomic or non-genomic, the result would be the same: transcription cannot begin until some critical event occurs in the AhR pathway.

In conclusion, these studies support the hybrid switch model for CYP1A1 induction by PCB 126 in the H4IIE rat hepatoma cells. More critically, even at high concentrations, there are non-responding cells, indicating some critical event has not transpired in these cells: the so-called switch. Studies to further elucidate the mechanism of the hybrid switch response are currently underway in our laboratory.

CHAPTER 3

Modulation of the PCB 126 Mediated Switch Response by Phosphorylation Pathways

Introduction

Gene expression may exhibit either a graded or a "switch-like" response to a stimulus (Louis and Becskei 2002). Single cell studies have further revealed that many enhancer linked genes are generally "on" or "off" in individual cells; with an active enhancer increasing the probability that the associated gene will be transcriptionally active in a given cell (Fiering *et al.* 2000). However, given identical stimuli, some cells will still remain in the "off" state in a stochastic model of enhancer-gene interaction. Other factors that may contribute to this switch-like, binary response include protein kinase cascades (Ferrell 1996; Ferrell and Machleder 1998), transcriptional synergy between transcription factors and promoter elements (Carey 1998), the interactions of repressors, activators, and co-activators (Blankenship and Matsumura 1997; Gradin *et al.* 1999; Mimura *et al.* 1999), and chromatin remodeling (Okino and Whitlock 1995). Switch-like behavior of gene induction could explain the observed threshold response of a cell to a particular chemical (French *et al.* 2004), and perhaps the phenomenon that some cells appear to be non-responders, even at the highest concentration tested.

Cytochrome P450 proteins are a superfamily of enzymes involved in the biotransformation of various drugs, carcinogens and steroid hormones (Estabrook 1996).

CYP1A1 is the classic biomarker of exposure to halogenated aromatic hydrocarbons (HAHs), including 2,3,7,8-tetrachlorodibenzo-*p*-dioxin (TCDD), and the most potent polychlorinated biphenyl agonist, PCB 126 (Hestermann *et al.* 2000). CYP1A1 is part of the **a**ryl **h**ydrocarbon **r**eceptor (AhR) gene battery (Nebert *et al.* 2000). AhR is a cytosolic receptor that, upon ligand binding, translocates into the nucleus and dimerizes with the **a**ryl hydrocarbon **r**eceptor **n**uclear **t**ranslocator (Arnt) (Ma 2001). The ligand-bound AhR-Arnt complex binds to dioxin response elements (DREs) located in the enhancer/promoter region of TCDD responsive genes such as CYP1A1. CYP1A1 displays minimal to no constitutive expression and is highly inducible by PCB 126 and TCDD (Whitlock 1999).

Previous research has demonstrated a distinctly heterogeneous zonal pattern of CYP1A1 enzyme induction within the rat liver (Andersen *et al.* 1995; Bars and Elcombe 1991; Tritscher *et al.* 1992). Within the induced liver, there is a clear boundary between responsive and nonresponsive regions (Bars and Elcombe 1991; Bars *et al.* 1989). Hence individual hepatocytes appear as either uninduced or fully induced at any given concentration of TCDD. In our laboratory, primary rat hepatocyte cultures display similar behavior (French *et al.* 2004). On a single cell basis, adjacent cells appear induced/uninduced for CYP1A1 protein and mRNA after in vitro PCB 126 treatment as seen by in situ hybridization and immunocytochemistry. This research was further extended to two rodent liver cell lines, H4IIE rat hepatoma and Hepa 1c1c7 mouse hepatoma cells. The H4IIE cells displayed a robust switch response to PCB 126 treatment as seen using flow cytometry and immunocytochemistry for CYP1A1 protein (Broccardo *et al.* 2004). The concentration-dependent switching response was

accompanied by an increase in the proportion of cells within the induced pool; however a single, maximal induction peak did not result. Instead, groups of induced cells exhibited varying degrees of induction intensity. Overall, the resulting distributions appear to support a hybrid switch response, where a switch works in concert with a rheostat, much like a dimmer on a light switch in a home.

Such a switch response might be explained by nongenomic factors modulating the AhR pathway, such as MAPKs, PKC, co-activators, or other associated proteins that are activated by PCB 126 or other AhR ligands (Ferrell and Machleder 1998; Long *et al.* 1999; Long *et al.* 1998; Minsavage *et al.* 2004; Tan *et al.* 2002; Tan *et al.* 2004; Tian *et al.* 2003; Torchia *et al.* 1998; Yim *et al.* 2004). The effects of such mediators appear to be highly cell specific and not all mediators appear to be crucial for CYP1A1 induction in all tissues. Such variability may account for the distinct tissue-specific responses to AhR ligands.

This research is intended to further study the nature of this documented switch-like response and begin to explain the molecular mechanism of such a response in H4IIE cells. The primary goal of this paper is to identify crucial signal transduction pathways that may be key modulators in the switch response. These results confirm that such a switch cannot be explained by a lack of the AhR on a single cell basis. PKC inhibition, instead, dramatically reduced PCB 126 mediated CYP1A1 induction from 62% to 18% of the cells as seen using flow cytometry. However, PCB 126 treatment did not induce membrane translocation of PKC α, δ, ε, or λ as seen after subcellular fractionation and Western blotting and PKC kinase activity did not increase after PCB 126 treatments.

Materials and Methods

Cell Culture: All cell culture products were obtained from Gibco (Carlsbad, CA) unless otherwise noted. Rat hepatoma H4IIE cells (ATCC) were cultured in DMEM supplemented with 10% FBS (Hyclone, Logan, UT) and 100 units/ml penicillin/100 μg/ml streptomycin and maintained at 37°C and 5% CO_2. Cells were seeded at 2.5 x 10^6 or 6.5 x 10^6 cells in 60-mm or 100-mm culture dishes, respectively (Falcon).

Cell Treatments: PCB 126 (3,3',4,4',5-pentachlorobiphenyl) was obtained from Accustandard (New Haven, CT) and confirmed by GC/MS to be 100% pure and free of other congeners. For treatment, PCB 126 was dissolved in DMSO; treatments contained less than 0.2% DMSO. H-7 and HA-1004 (Biomol, Plymouth Meeting, PA) were dissolved in PBS. PMA (phorbol-12-myristate-13-acetate) was dissolved in DMSO (Cell Signaling, Beverly, MA). U0126 (Biomol) was dissolved in DMSO. No changes in growth rate or morphology were observed after treatment with DMSO or PCB 126 as compared to naïve cells.

CYP1A1 Flow Cytometry: 2.5 x 10^6 cells were plated on 60-mm dishes for 24 h, serum starved for 24 h, then treated with DMSO or 2.5 x 10^{-8} M PCB 126 for the indicated time points. The inhibitors H-7 (50 μM), HA-1004 (10, 20, 50 μM), and U0126 (10 μM) were applied 30 min prior to the addition of PCB 126. PMA (10, 40, 80, 120 nM) was applied with PCB treatment. After treatment, cells were trypsinized and washed once in PBS. Cells were resuspended in 2% formaldehyde, EM grade, without methanol (Polysciences, Warrington, PA) and fixed on ice for 30 minutes. Cells were washed twice in PBS/1%

BSA and then permeabilized for 10 minutes in 0.8% saponin (Sigma, St Louis, MO) in PBS/1% BSA. Cells were washed once in PBS/1% BSA and blocked for 15 minutes in 5% goat serum (Sigma) in PBS/1% BSA. Cells were washed once in PBS/1% BSA and incubated with rabbit anti-rat CYP1A1 polyclonal antibody (Chemicon, Temecula, CA; 1:500) in PBS/1% BSA, 0.8% saponin for 60 minutes. Cells were washed 3 times in PBS/1% BSA and incubated with Alexa Fluor 488 goat anti-rabbit IgG (Molecular Probes, Eugene, OR; 1:200) in PBS/1% BSA, 0.8% saponin for 30 minutes in the dark. Cells were washed 3 times in PBS/1% BSA and resuspended in 0.5 ml PBS and analyzed on the Beckman Coulter EPICS 5 Flow Cytometer. Alexa Fluor 488 was excited by the 488 nm line of an argon ion laser operating at 200 mW of power. Fluorescence was detected by a photomultiplier equipped with a 525 band pass filter. Light scatter was collected in both the forward and right angle directions. Data were processed and displayed on the Cyclops software (DakoCytomation, Ft Collins, CO). To assess nonspecific binding of the antibodies, DMSO and PCB 126 treated samples were incubated with rabbit IgG (Sigma) instead of the rabbit anti-rat CYP1A1 primary antibody. A PCB 126 sample was also incubated with no primary antibody (vehicle only) and then with Alexa 488 to assess any nonspecific binding of the secondary antibody.

Arylhydrocarbon Receptor Flow Cytometry: 2.5×10^6 cells were plated on 60-mm dishes for 24 h, and then treated with DMSO or 2.5×10^{-8} M PCB 126 for 16 h. The same protocol as for CYP1A1 was employed, except for the use of the rabbit anti-rat AhR polyclonal antibody (Biomol; 8 μg/mL). Rabbit IgG (Sigma; 8 μg/mL) was used for

gating purposes. Samples were analyzed on the CyAn™ LX (DakoCytomation). Alexa Fluor 488 was excited by a 488 nm (20 mW) solid state laser. Fluorescence was detected by a photomultiplier tube equipped with a 530/40 bandpass filter. Light scatter was collected in both the forward and right angle directions. Data were analyzed using the Summit™ software (DakoCytomation).

Custom Protein Array: Cells were seeded at 6.5 x 10^6 cells in 100-mm dishes, allowed to plate down for 24 h, then serum starved for 24 h. Cells were exposed to 2.5 x 10^{-7} M PCB 126 or DMSO for 30 min or 6 h. Cells were rinsed with ice cold PBS and 1 ml of boiling lysis buffer was added (10 mM Tris HCl, pH 7.4, 1 mM sodium ortho-vanadate, 1% SDS). Lysate was removed with a cell scraper, and 3 100-mm dishes per treatment were combined into a 50 ml conical tube, microwaved for 5-10 seconds, and sonicated for 30 seconds. Protein concentration was determined using a BCA protein assay using bovine serum albumin as a standard (Pierce, Rockford, IL). We contracted with BD Biosciences Pharmingen (San Diego, CA) to perform a custom "PowerBlot" 40-antibody miniscreen via large scale western blotting. 200 μg protein was loaded across the entire width of a 13 x 10 cm, 4-15% gradient SDS-polyacrylamide, 0.5 mm thick gel. A Bio-Rad Criterion IPG well comb was used (Hercules, CA). The gel was run for 1.5 h at 150 volts then transferred to Immobilon-P membrane (Millipore, Billerica, MA) for 2 h at 200 mAmp using a wet electrophoretic transfer apparatus TE Series (Hoefer, San Fransisco, CA). After transfer the membrane was dried and soaked in methanol. The membrane was blocked for 1 h with blocking buffer (LI-COR, Lincoln, NE). The membrane was then clamped with a western blotting manifold that isolates 41 channels across the

membrane. In each channel a complex antibody cocktail was added and allowed to hybridize for 1 h at 37°C. Two different molecular weight standard cocktails were loaded in lanes 5 and 39 of each blot. The blot was then removed from the manifold, washed and hybridized for 30 min at 37°C with goat anti-mouse Alexa 680 (Molecular Probes) and goat anti-rabbit IR Dye 800 (Rockland, Gilbertsville, PA). The membrane was then washed, dried, and scanned at 700 nm (for monoclonal antibody target detection) and 800 nm (for polyclonal antibody target detection) using the Odyssey Infrared Imaging System (LI-COR). Blots were performed in triplicate for each treatment.

Data Analysis of Custom Protein Array: Fluorescent intensities of the spots on the membrane were normalized to the sum intensity of all valid spots on a blot and then multiplied by 1,000,000. The normalized quantity for experimental spots (PCB 126) was expressed as a ratio of the normalized quantity for the corresponding control spots (DMSO). This ratio was used to determine changes in protein expression. Triplicate blots were analyzed using a 3 x 3 matrix comparison method. For example, runs 1, 2, 3 of the control were compared independently to runs 1, 2, 3 of the experimental samples. Results are finally expressed as a fold change, a semi-quantitative value that represents the general trend of protein changes, either increasing or decreasing, for the experimental sample relative to control.

P-ERK, ERK, P-JNK, JNK Western Blotting: Cells were allowed to plate down with serum at 6.5 x 10^6 cells per 100-mm dish for 24 h and then serum starved for 24 h. Cells were treated with 120 nM PMA, 2.5 x 10^{-7} M PCB 126 or DMSO for 5 min, 15 min, 30

min, and 60 minutes. Cells were rinsed with ice cold PBS and 0.6 ml of ice cold RIPA buffer (1% NP-40, 0.1% SDS, 0.5% sodium deoxycholate, 1 mM sodium orthovanadate, protease inhibitor cocktail tablet (Complete Mini, Roche, Indianapolis, IN) in phosphate buffered saline) was added. Cells were incubated on ice for 5 min, removed with a cell scraper, and transferred to a microcentrifuge tube. Plates were rinsed with 0.3 ml cold RIPA buffer, combined with the first lysate, and cells/DNA were sheared using a 21- and 24-gauge needle, successively and then incubated for 30-60 min on ice. Lysates were centrifuged at 10,000 x g for 10 min at 4°C and the supernatant was removed and frozen at -80°C. A BCA protein assay was performed (Pierce) using albumin standards in RIPA buffer. 10 μg protein (P-ERK), 30 μg protein (P-JNK), and positive control PC12 cell extracts treated with NGF (for P-ERK) or sorbitol (for P-JNK) (Promega, Madison, WI) were diluted with 2x Laemmli buffer (Bio-Rad) and boiled for 3 minutes. An unstained Precision Plus Protein standard (Bio-Rad, 1:60), and a prestained Precision Plus Protein Kaleidescope standard were loaded (Bio-Rad) for chemiluminescent detection of band size, and to monitor transfer, respectively. Samples were subjected to sodium dodecyl sulfate-polyacrylamide gel electrophoresis using 10% Tris-HCl polyacrylamide gels, 50 μl/well, 10 wells (Bio-Rad) in a Mini-Protean II Electrophoresis Cell (Bio-Rad). The gel was run for 1.5-2 h at 80 V, and then proteins were transferred to a nitrocellulose membrane of 0.45 μm pore size (Bio-Rad). Membranes were blocked for 60 min in Tris-buffered saline pH 7.6 with 1% Tween 20 (TBS-T) containing 5% nonfat dried milk. Thereafter, polyclonal rabbit P-ERK or monoclonal mouse P-JNK (Cell Signaling; 1:2000) antibodies were incubated in TBS-T containing 5% bovine serum albumin (BSA) overnight on a shaker at 4°C. Membranes were then washed 6 times for 10 min on a

shaker in TBS-T. Horseradish peroxidase-conjugated secondary antibodies (goat anti-mouse for P-JNK, Bio-Rad; goat anti-rabbit for P-ERK, Santa Cruz; 1:2000) were incubated on a shaker for 60 min in TBS-T containing 5% nonfat dried milk. The Precision StrepTactin-HRP conjugate (Bio-Rad) secondary antibody against the unstained Precision Plus Protein standard was simultaneously added at 1:15,000. Membranes were then washed 6 times for 10 min on a shaker in TBS-T. Bands were visualized after a 3 min incubation in Immun-Star HRP (Bio-Rad) and viewed using the UVP BioImaging Systems Epi Chemi II Darkroom. Membranes were then stripped in boiling buffer (62.5 mM Tris pH 6.7, 2% SDS, 100 mM β-mercaptoethanol) twice for 30-45 s, rinsed in copious volumes of TBS-T, and blocked in 5% nonfat dried milk in TBS-T for 60 min on shaker. Polyclonal rabbit ERK and JNK antibodies (Cell Signaling, 1:2000) were incubated in 5% BSA in TBS-T overnight at 4°C on a shaker. Membranes were washed and a secondary goat anti-rabbit HRP conjugate (Santa Cruz, 1:2000) and the Precision StrepTactin-HRP conjugate were added as above. Membranes were washed and visualize as with P-ERK and P-JNK.

Protein Kinase C Subcellular Fractionation: H4IIE cells were plated onto 100 mm dishes at a density of 6.5×10^6 cells. Cells were allowed to adhere for 24 h then serum was removed for 24 h. 6 100-mm dishes per treatment were exposed to 2.5×10^{-8} M PCB 126 or equivolume DMSO equivalent to 0.2% for 10 min, 30 min, 2 h, 6 h, or 16 h. 120 nM PMA (Phorbol-12-Myristate-13-Acetate; Cell Signaling) in DMSO was applied for 10 minutes. After treatment, the media was removed and the plates were rinsed twice in ice cold PBS and plates were kept on ice. 350 μl of ice cold homogenization buffer (20

mM Tris-HCl pH 7.5, 0.25 M sucrose, 5 mM EGTA pH 8.0, 20 mM β-mercaptoethanol, 1 mM sodium orthovanadate, protease inhibitor cocktail tablet in phosphate buffered saline) was added to each dish and cells were scraped into a tube and kept on ice. The 6 100-mm dishes per treatment were combined into one tube. Cells were sonicated for three 10 s pulses at 25 Hz with intervals of 15 s on ice. Cells were centrifuged at 100,000 x g at 4°C for 45 min to separate the soluble (cytosolic) fraction from the particulate (membrane) fraction. The supernatant was then removed and saved as the cytosolic fraction at -80°C. The pellet was resuspended in homogenization buffer containing 1% Triton X-100 and 2 mM EDTA, pH 8.0 and incubated on ice for 10 min. The pellets were then sonicated for 3 10 s pulses at 25 Hz with intervals of 15 s on ice. The samples were then centrifuged at 100,000 x g at 4°C for 45 minutes. The supernatant was saved as the soluble membrane fraction and frozen at -80°C and the pellet of insoluble protein was discarded. A BCA protein assay was performed (Pierce) using albumin standards in homogenization buffer.

Protein Kinase C Western Blotting: 25 μg protein was diluted with 2x Laemmli buffer (Bio-Rad) and boiled for 3 minutes. An unstained Precision Plus Protein standard (Bio-Rad, 1:60), and a prestained Precision Plus Protein Kaleidescope standard were loaded (Bio-Rad) for chemiluminescent detection of band size, and to monitor transfer, respectively. 10 μg rat cerebrum lysate (BD Transduction Laboratiries) was loaded as a positive control to confirm band localization. Samples were subjected to sodium dodecyl sulfate-polyacrylamide gel electrophoresis using 7.5% Tris-HCl polyacrylamide gels, 50 μl/well, 10 wells (Bio-Rad) in a Mini-Protean II Electrophoresis Cell (Bio-Rad). The gel

was run for 1.5 at 80 V, and then proteins were transferred to a nitrocellulose membrane of 0.45 μm pore size (Bio-Rad). Membranes were blocked for 60 min in Tris-buffered saline pH 7.6 with 1% Tween 20 (TBS-T) containing 5% BSA. Thereafter, the PKC delta, epsilon, and lambda mouse monoclonal antibodies (1:1000, BD Transduction Laboratories) and mouse monoclonal PKC alpha (1:100, Santa Cruz) were incubated in TBS-T containing 5% bovine serum albumin (BSA) overnight on a shaker at 4°C. Membranes were then washed 5 times for 10 min on a shaker in TBS-T. Horseradish peroxidase-conjugated goat anti-mouse secondary antibody (1: 5000, Bio-Rad) was incubated on a shaker for 60 min in TBS-T containing 5% nonfat dried milk. The Precision StrepTactin-HRP conjugate (Bio-Rad) secondary antibody against the unstained Precision Plus Protein standard was simultaneously added at 1:15,000. Membranes were then washed 5 times for 10 min on a shaker in TBS-T. Bands were visualized after a 3 min incubation in Immun-Star HRP (Bio-Rad) and viewed using the UVP BioImaging Systems Epi Chemi II Darkroom.

PKC Kinase Activity Assay: H4IIE cells were plated onto 100 mm dishes at a density of 6.5×10^6 cells. Cells were allowed to adhere for 24 h then serum was removed for 24 h. One 100 mm dish per treatment was exposed to 2.5×10^{-8} M PCB 126 or equivolume DMSO equivalent to 0.2% for 5 min, 10 min, 30 min, and 1 h. A media only control was also used. After treatments media was removed and cells were rinsed with ice cold PBS. 1 ml of lysis buffer (20 mM MOPS, 50 mM β–glycerolphosphate, 50 mM sodium fluoride, 1 mM sodium orthovanadate, 5 mM EGTA, 2 mM EDTA, 1% NP40, 1 mM dithiothreitol (DTT), 1 mM benzamidine, and protease inhibitor cocktail tablet (Roche))

was then added per 100 mm dish and allowed to stand for 10 m on ice. Cells were then removed with a cell scraper and the lysate was collected in a pre-chilled microcentrifuge tube. Samples were then centrifuged at 13,000 rpm for 15 min at 4°C. The supernatants were then transferred to new microcentrifuge tubes, aliquoted into 100 µl samples, and frozen at -80°C. Protein was measured using the RC-DC Protein Assay kit and the protocol was modified to be read on a plate reader set to 750 nm (BioRad). PKC kinase activity was measured using the ELISA-based PKC kinase activity assay kit (Stressgen, Victoria, BC, Canada) according to company directions. Each treatment was run on triplicate wells. Briefly, 0.1 µg protein was used per well, the reaction was initiated by the addition of ATP, and then a phosphospecfic antibody against the substrate CREB was added. Anti-rabbit IgG:HRP conjugate was then applied to each well, followed by the addition of the TMB (tetramethylbenzidine) substrate. Acid stop solution was added and absorbances were read on a plate reader set to 450 nm. Active PKC was used as a positive control and a blank well without antibodies was used to measure the background fluorescence of the buffers. For data analysis, the triplicate wells for each treatment were averaged, the background fluorescence of the blank well was subtracted, and the PCB treatment value was divided by the respective control value to determine a relative percent kinase activity. ANOVA analysis was used to determine significant difference between the PCB treatment at each time point and the DMSO control at each time point.

Results

PMA Treatment, PKC, PKA, and MEK Inhibitors and CYP1A1 Flow Cytometry: The PKC inhibitor H-7 and PKA inhibitor HA-1004 were used to assess the roles of PKC

and/or PKA in PCB 126 mediated induction of CYP1A1 in H4IIE cells. Cells were pretreated for 30 min with 50 μM H-7 or 10 μM, 20 μM, or 50 μM HA-1004 then treated for 16 h with 2.5 x 10^{-8} M PCB 126. CYP1A1 protein levels decreased significantly ($p<0.05$) from 62% of the cells to 18% after the use of the PKC inhibitor H-7 (Figure 3.1a). 50 μM H-7 plus DMSO treatment resulted in no significant difference between DMSO treatment alone ($p>0.05$). The histogram overlay distinctly shows the decrease in CYP1A1 protein levels due to H-7 treatment (Figure 3.1b). Cells within region 1 represent the "off" cells for CYP1A1 expression and general background fluorescence, and cells showing an increase in log intensity green fluorescence in region 2 are positive for CYP1A1 expression. The shift of the curve from region 2 to region 1 for the PCB 126 plus H-7 treatment highlights the movement of cells from "on" to "off." In contrast, only at the highest dose of the PKA inhibitor HA-1004 (50 μM) was there a significant decrease in CYP1A1 expression from 57% to 43% of the cells ($p<0.05$) (Figure 3.2a). As seen in the histogram overlay, there is a subtle decrease in the percent of cells expressing CYP1A1 due to HA-1004 treatment as compared to PCB 126 treatment alone (Figure 3.2b). PMA, which can increase or decrease CYP1A1 induction in a time dependent fashion, was used to further study the role of PKC in CYP1A1 induction. PMA (10, 40, 80, 120 nM) was applied in conjunction with 2.5 x 10^{-8} M PCB 126 for 4, 8, and 16 h and compared to PCB alone, DMSO alone, and 120 nM PMA alone (Figure 3.3). Only at the 4 h time points did all concentrations of PMA appear to decrease CYP1A1 induction. The MEK inhibitor U0126 appeared to subtly, but significantly increase the % cells expressing CYP1A1 (Figure 3.4). This is not without precedence; U0126 has been shown to be an AhR ligand (Andrieux *et al.* 2004).

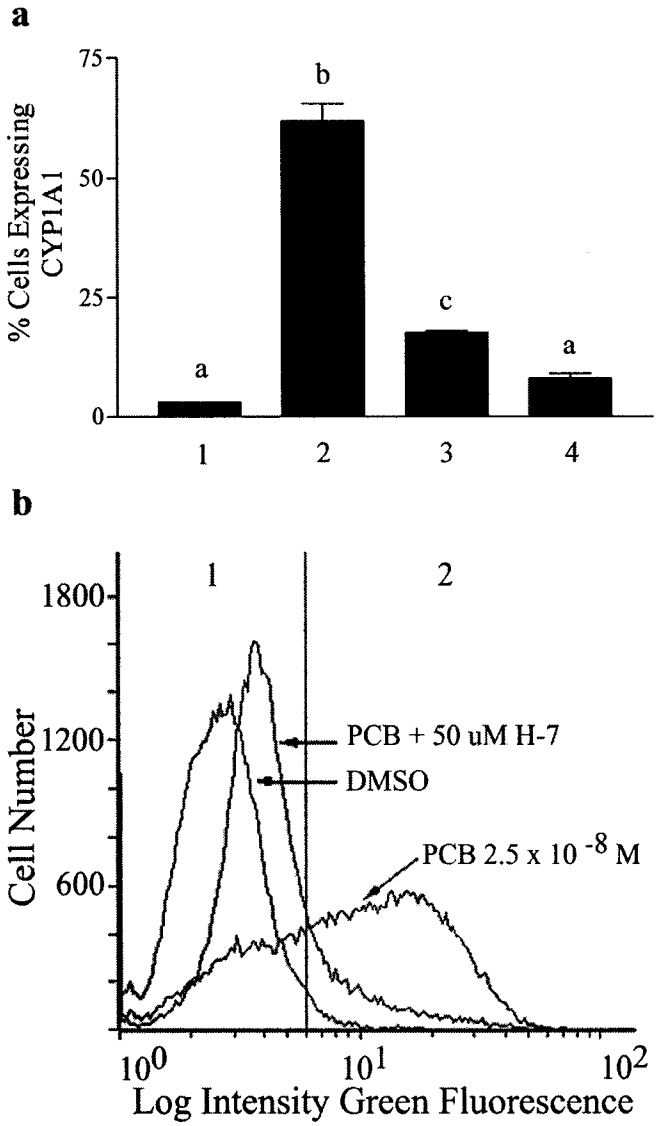

Figure 3.1. a) PKC Inhibitor and CYP1A1 Flow Cytometry. (1) DMSO **(2)** PCB **(3)** PCB + H-7 **(4)** DMSO + H-7. Cells were pretreated for 30 min with 50 μM H-7 then treated with 2.5 x 10^{-8} M PCB 126 for 16 h. The percent of cells expressing CYP1A1 protein decreased from 62% to 18% after H-7 treatment ($p<0.05$). Bars with different letters are significantly different ($p<0.05$). **b)** Histogram overlay showing the decline in CYP1A1 protein due to H-7 treatment. Cells within region 1 are negative for CYP1A1 protein; cells in region 2 are positive for CYP1A1.

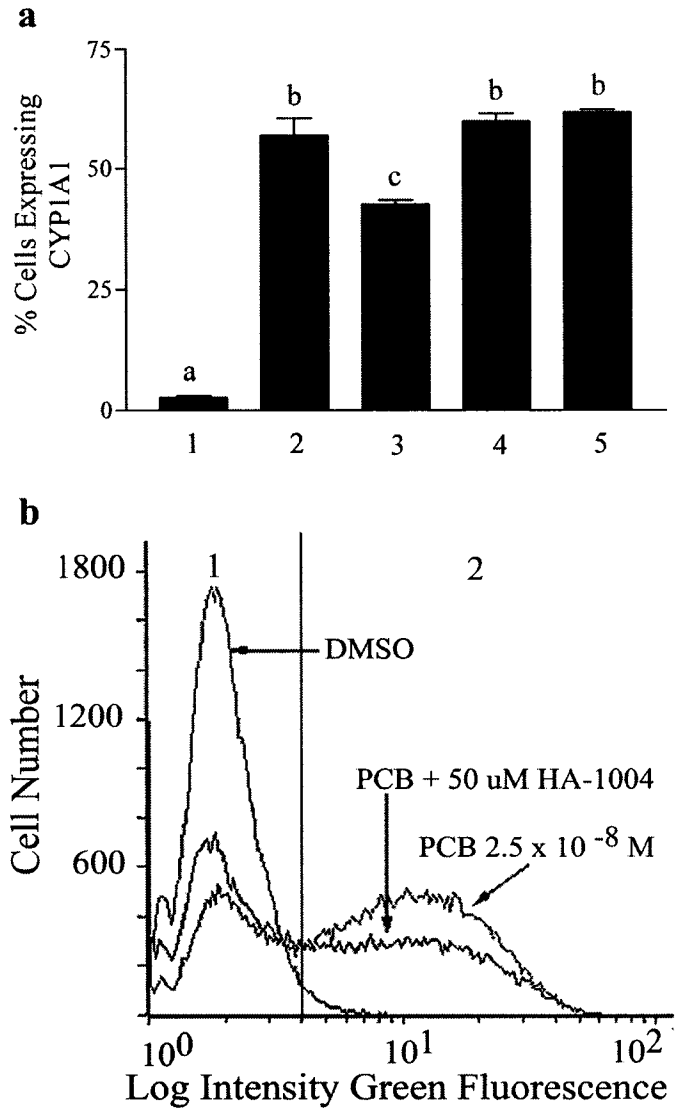

Figure 3.2. a) PKA Inhibitor and CYP1A1 Flow Cytometry. (1) DMSO **(2)** PCB **(3)** PCB + 50 μM HA-1004 **(4)** PCB + 20 μM HA-1004 **(5)** PCB + 10 μM HA-1004. Cells were pretreated for 30 min with 50, 20, or 10 μM HA-1004 then treated with 2.5 x 10^{-8} M PCB 126 for 16 h. The percent of cells expressing CYP1A1 protein decreased from 57% to 43% only after the 50 μM treatment ($p<0.05$). Bars with different letters are significantly different ($p<0.05$). **b)** Histogram overlay showing the subtle decline in CYP1A1 protein due to HA-1004 treatment. Cells within region 1 are negative for CYP1A1 protein; cells in region 2 are positive for CYP1A1.

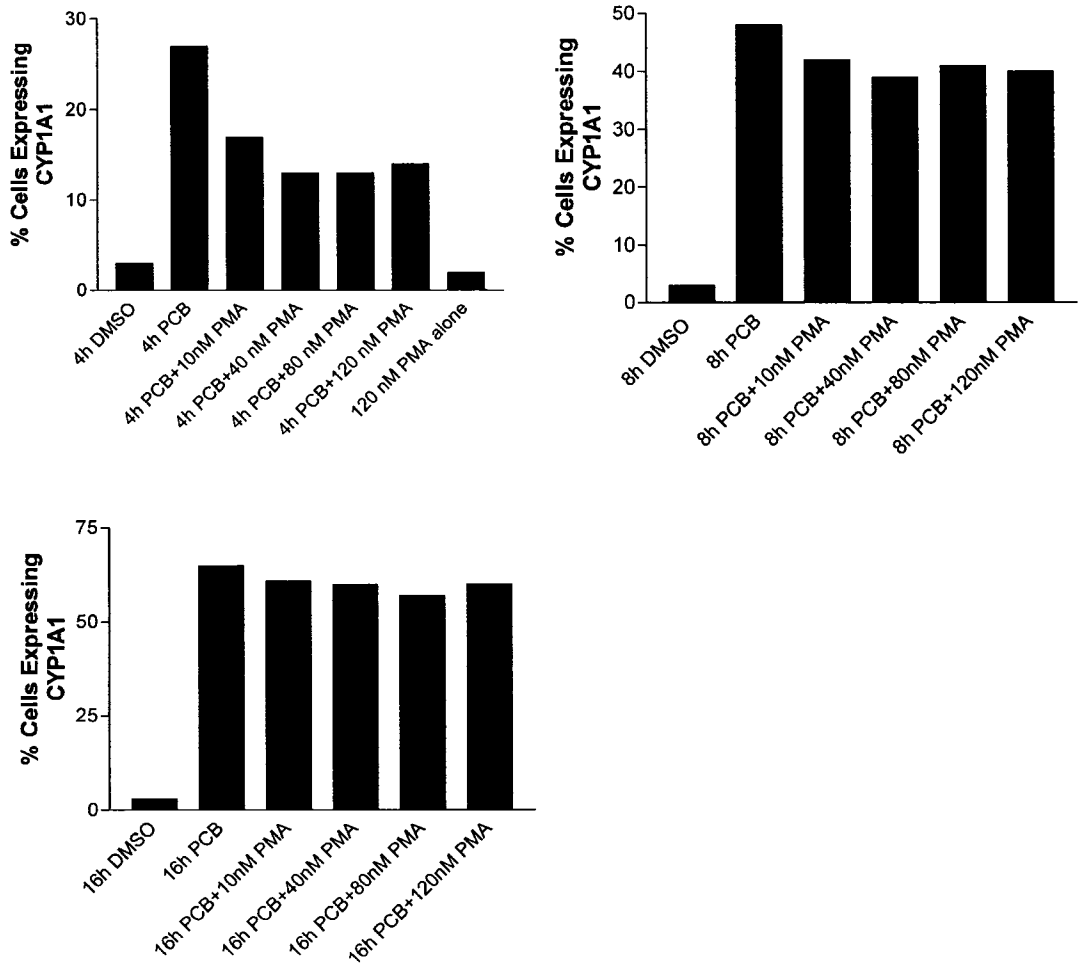

Figure 3.3. PMA + PCB Treatment and CYP1A1 Flow Cytometry. H4IIE cells were treated with DMSO, 2.5 x 10^{-8} M PCB or PCB plus 10, 40, 80, or 120 nM PMA for 4, 8, or 16 h. Only at the 4 h time point did PMA treatment appear to decrease the % of cells expressing CYP1A1. All PMA concentrations appeared to have an effect, and PMA treatment alone did not induce CYP1A1 markedly more than DMSO.

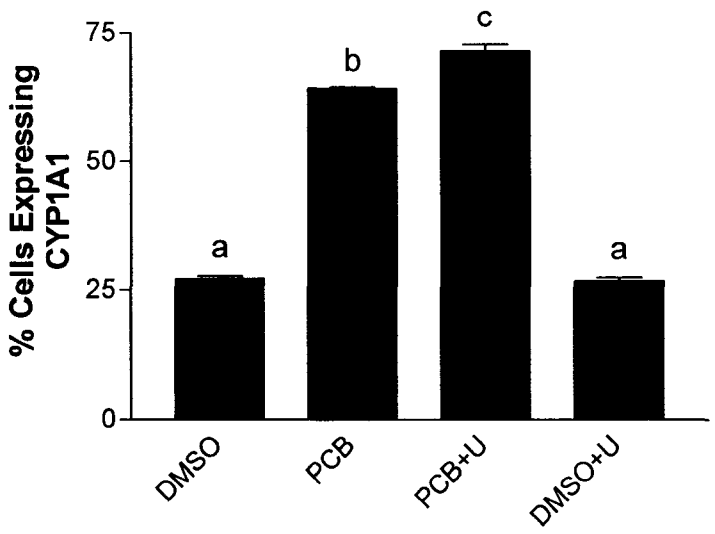

Figure 3.4. MEK Inhibitor U0126 and CYP1A1 Flow Cytometry. U=U0126. H4IIE cells were treated with DMSO, PCB, PCB + U0126, or DMSO + U0126 for 16 h. U0126 was applied 30 min before PCB or DMSO. Columns with different letters are significantly different ($p<0.001$).

Further, potential contamination issues with the DMSO used as the vehicle control confound these data. Approximately 27% of the cells exposed to DMSO were induced for CYP1A1. Upon later treatment with new DMSO, CYP1A1 induction returned to near zero. However, these experiments were not repeated with the new DMSO, partly because of the subtle increase in CYP1A1 induction upon treatment with U0126 with PCB.

Arylhydrocarbon Receptor and Flow Cytometry: Flow cytometry was employed to determine the distribution of the AhR in H4IIE cells after DMSO and PCB 126 treatment. After 16 h treatment with DMSO or 2.5 x 10^{-8} M PCB 126, approximately 95 % and 87% of the cells expressed the AhR, respectively (Figure 3.5). The histogram overlay shows the distribution of cells containing the AhR after DMSO or PCB 126 treatment in region 2, and the cells within region 1 represent background fluorescence of the cells and any nonspecific binding of the rabbit IgG antibody used for gating purposes (Figure 3.5). The distinct separation of these curves signifies the presence of the AhR in the majority of the cell population after PCB 126 treatment.

Custom Protein Array: Cells were treated with 2.5 x 10^{-7} M PCB 126 or DMSO for 30 min and 6 h. At 30 min, the antibody against CREB/CREM (46/26 kDa) detected an increase of 1.25-1.9 fold of the smaller 26 kDa band. This band represents an alternatively spliced product of the gene CREM known as the cAMP-inducible repressor isoform or ICER (**I**nducible **c**AMP **E**arly **R**epressor). At 6 h, two unknown proteins (109 kDa, 233 kDa) showed an increase in phosphoserine/phosphoserine/threonine residues by

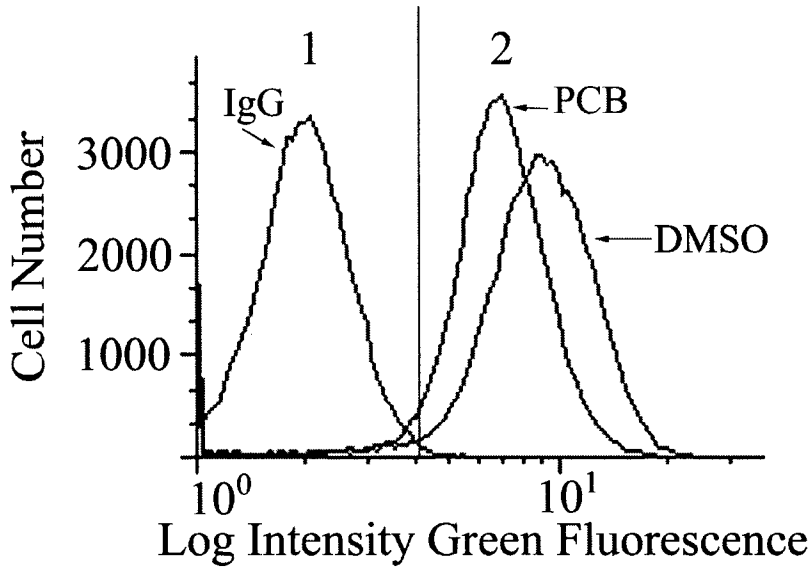

Figure 3.5. Flow Cytometry for AhR. Histogram overlay showing curves for rabbit IgG and the AhR. Cells within region 1 represent background fluorescence. Cells within region 2 contain the AhR. After 16 h treatment with DMSO or 2.5 x 10^{-8} M PCB 126, approximately 95% and 87% of the cells expressed the AhR, respectively. Figure represents three independent treatments.

1.25-1.9 fold. Protein kinase A regulatory subunit IIb (PKARIIb, pS114), phospho-specific was decreased by more than 2 fold at 6 h. Jun was increased by more than 1.5 fold at 6 h. These data are summarized in Table 3.1. Table 3.2 lists the PKC isoforms detected. A representative western blot for the 6 h PCB treatment can be seen in Figure 3.6. The list of proteins on the protein array can be seen in Table 3.3.

Western Blot Analysis of P-ERK, ERK, P-JNK, JNK: Cells were treated with 40 or 120 nM PMA for 30 min, 2.5 x 10^{-7} M PCB 126 or DMSO for 5 min, 15 min, 30 min, and 60 min. Only PMA stimulated P-ERK and P-JNK at 30 min as seen by the P-ERK bands at 44/42 kDa and P-JNK bands at 54/46 kDa (Figure 3.7 a, b). The positive control PC12 cell extracts for P-ERK (stimulated with NGF) and P-JNK (stimulated with sorbitol) both displayed bands at 44/42 kDa and 54/46 kDa respectively, allowing for confirmation of band sizes. Both extracts also stained for ERK and JNK. Treatments had no effect on levels of ERK and JNK (Figure 3.7 a, b).

PCB 126 Tx	Protein	Fold Change	Sign of Change	Observed MW	Lane
30 min	CREB/CREM/ ICER	1.25-1.9	+	27 kDa	6
6 hours	Phosphoserine/Phosphoserine/threonine	1.25-1.5	+	109 kDa	24
6 hours	Phosphoserine/Phosphoserine/threonine	1.25-1.9	+	233 kDa	24
6 hours	PKARIIb (pS114), Phospho-Specific	> 2	-	62 kDa	19
6 hours	Jun	>1.5	+	43 kDa	26

Table 3.1. Custom 40 Antibody Protein Array. Cells were treated for 30 min or 6 h with 2.5 x 10^{-7} M PCB 126 or DMSO. Fold change indicates changes in treatment (PCB 126) as compared to control (DMSO).

PKC Isoforms on Protein Array	Detected
Alpha - α	yes
Beta - β	no
Delta - δ	yes
Epsilon - ε	yes
Gamma - γ	no
Iota - ι	yes
Lambda - λ	yes
Theta - θ	no

Table 3.2. List of PKC Isoforms Measured and Detected on the Custom 40 Antibody Protein Array.

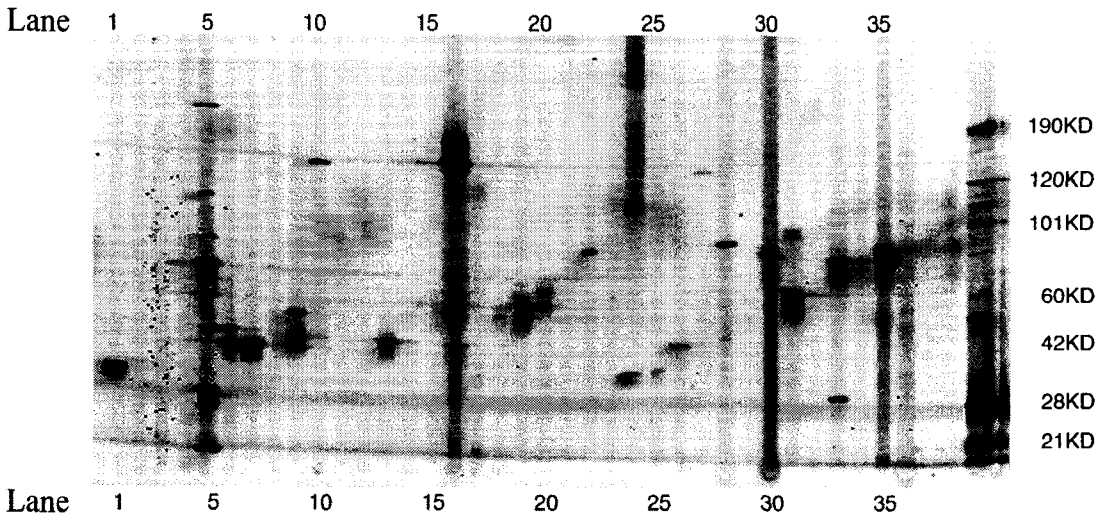

Figure 3.6. Custom Protein Array. Representative Western blot for PCB 126 6 h treatment. Blots were performed in triplicate.

30 m Protein Array	6 h Protein Array
Caveolin 1	Cdk1/Cdc2
Caveolin (pY14), Phospho-Specific	Cdc2 (pY15), Phospho-Specific
Cdk1/Cdc2	CREB/CREM
Cdc2 (pY15), Phospho-Specific	CREB (aa 123-136) Phospho-Specific
Exportin-1/CRM1	Phosphotyrosine
MCM	Exportin-1/CRM1
Nucleoporin p62	MCM
alpha-Tubulin	Nucleoporin p62
Actin (Neomarkers)	alpha-Tubulin
KNP-1/HES1	Actin (Neomarkers)
NTF2	KNP-1/HES1
CREB	NTF2
Phospho-CREB	ERK1
eNOS/NOS Type III	ERK2
eNOS (pS1177), Phospho-Specific	ERK1/2 (pT202/pY204) Phospho-Specific
eNOS (pT495), Phospho-Specific	pan-JNK/SAPK1
ERK1	JNK (pT183/pY185) Phospho-Specific
ERK2	Phospholipase Cg (pY783), Phospho-Specific
ERK1/2 (pT202/pY204) Phospho-Specific	lck
FAK	Lck (pY505), Phospho-Specific
FAK (pY397), Phospho-Specific	p38a/SAPK2a
Integrin b3 (pY759), Phospho-Specific	p38 (pT180/pY182) Phospho-Specific
pan-JNK/SAPK1	p53 (pS392) Phospho-Specific
JNK (pT183/pY185) Phospho-Specific	Phospholipase Cg1
lck	Phosphotyrosine
Lck (pY505), Phospho-Specific	PKARIIb
p120 Catenin/pp120 (src substrate)	PKARIIb (pS114), Phospho-Specific
p120 Catenin (pY280), Phospho-Specific	PKBa/Akt
p120 Catenin (pY228), Phospho-Specific	Src (pY418) Phospho-Specific
p120 Catenin (pY96), Phospho-Specific	ZAP70 Kinase
p38a/SAPK2a	ZAP70 (pY319), Phospho-Specific
p38 (pT180/pY182) Phospho-Specific	Phosphoserine
Phospho-p53	Phosphoserine/threonine
Phospholipase Cg1	DGKq
Phospholipase Cg (pY783), Phospho-Specific	Jun
Phosphotyrosine	p62 lck ligand
Phosphotyrosine	PKCa
PKARIIb	PKCb
PKARIIb (pS114), Phospho-Specific	PKCd
PKBa/Akt	PKCe
Phospho-PKBa/AKT	Yes
Phospho-PKBa/AKT	PKCg
Phospho-SRC	PKCi
ZAP70 Kinase	PKCl
ZAP70 (pY319), Phospho-Specific	Rsk
p190	phospho-AKT

30 m Protein Array cont'd	6 h Protein Array cont'd
Hip1R	PKC theta
Transportin	PKC alpha (pT638)
Calreticulin	p190
Arp3	Hip1R
eIF-6	Transportin
Rap2	Calreticulin
Phosphoserine	Arp3
Phosphoserine/threonine	eIF-6
	Rap2

Table 3.3. List of Proteins on the 30 min and 6 h Custom Protein Array. Housekeeping genes used for controls are also listed.

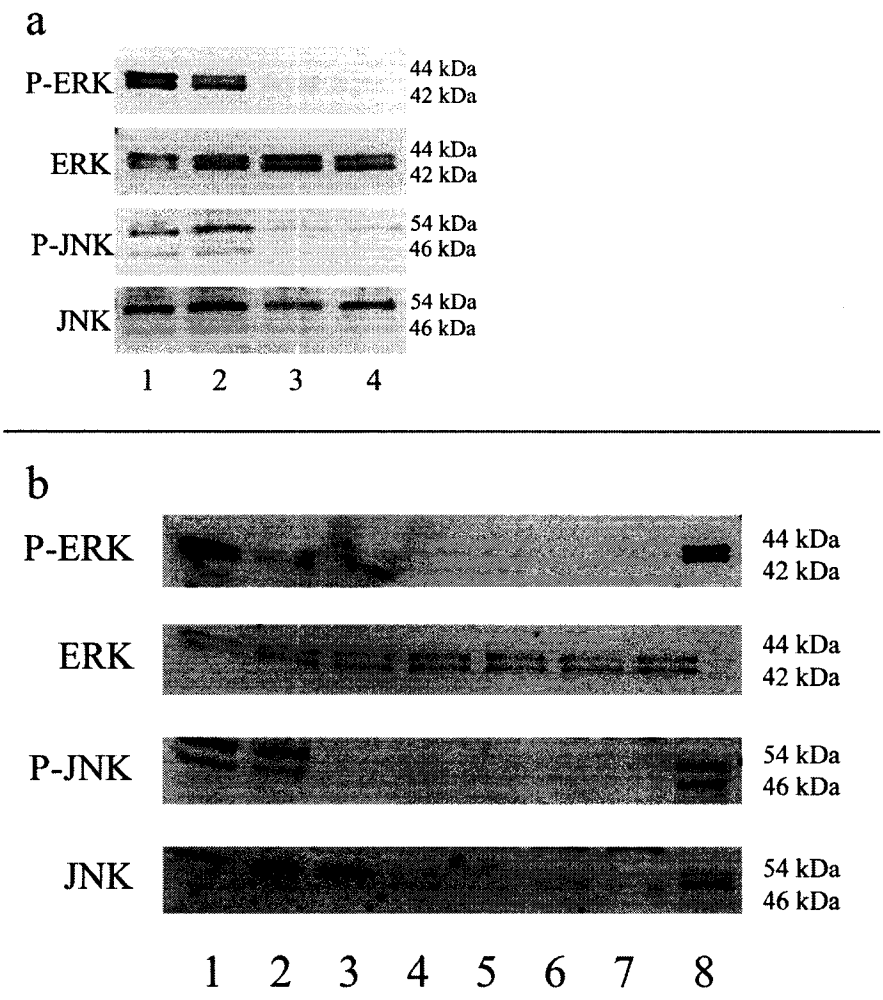

Figure 3.7. Western blots for P-ERK, ERK, P-JNK, JNK. (a) Lane 1: PC12 positive control cells used for band localization. **Lane 2:** H4IIE cells, 120 nM PMA 30 min; positive control **Lane 3:** H4IIE cells, 2.5 x 10^{-7} M PCB 126 30 min. **Lane 4:** H4IIE cells, DMSO vehicle control 30 min. Representative of 4 Western blots.

(b) Lane 1: H4IIE cells, 120 nM PMA 30 min; positive control. **Lane 2:** H4IIE cells, 40 nM PMA 30 min; positive control. **Lane 3:** H4IIE cells, DMSO 30 min. **Lane 4:** H4IIE cells, 2.5 x 10^{-7} M PCB 60 min. **Lane 5:** H4IIE cells, 2.5 x 10^{-7} M PCB 30 min. **Lane 6:** H4IIE cells, 2.5 x 10^{-7} M PCB 15 min. **Lane 7:** H4IIE cells, 2.5 x 10^{-7} M PCB 5 min. **Lane 8:** PC12 positive control cells used for band localization.

Western Blot Analysis of PKC α, δ, ε, and λ: Cells were treated with 2.5 x 10^{-8} M PCB 126 or DMSO for 10 min, 30 min, 2 h, 6 h, or 16 h (Figure 3.8a, b, c, d). 120 nM PMA was applied for 10 minutes as a positive control. The α, δ, and ε PKC isoforms responded to PMA treatment, displaying translocation from the cytosol to the membrane. PKC λ, an atypical PKC, is not capable of responding to PMA. The purpose of these experiments was to determine if PCB 126 treatment was capable of activating PKC translocation from the cytosolic to the membrane fraction. Figure 3.8a shows a typical response at the 10 minute time point. There were no striking differences between PCB 126 treatment and DMSO control at any of the time points measured; PCB 126 did not induce membrane translocation of any of the 4 isoforms tested. PKC α remained primarily in the cytosolic fraction at all times tested. PKC δ, ε and λ did not redistribute to the membrane fraction in response to PCB 126, and were present in both the cytosolic and membrane fractions at all times measured. The media only control showed that, constitutively, PKC α remains mostly in the cytosolic fraction. In contrast, the δ, ε and λ isoforms display constitutive localization to both the cytoplasmic and membrane fractions.

PKC Kinase Activity: H4IIE cells were treated with media only, DMSO or 2.5 x 10^{-8} M PCB 126 for 5 min, 10 min, 30 min, and 1h. No significant difference between the PCB treatment and the DMSO vehicle control at any time point was found as determined by ANOVA (Table 3.4). The media only samples had similar absorbances to all treatments. Despite the lack of increased PKC kinase activity at any time point measured, there was a trend of increased kinase activity at the 1 h time point.

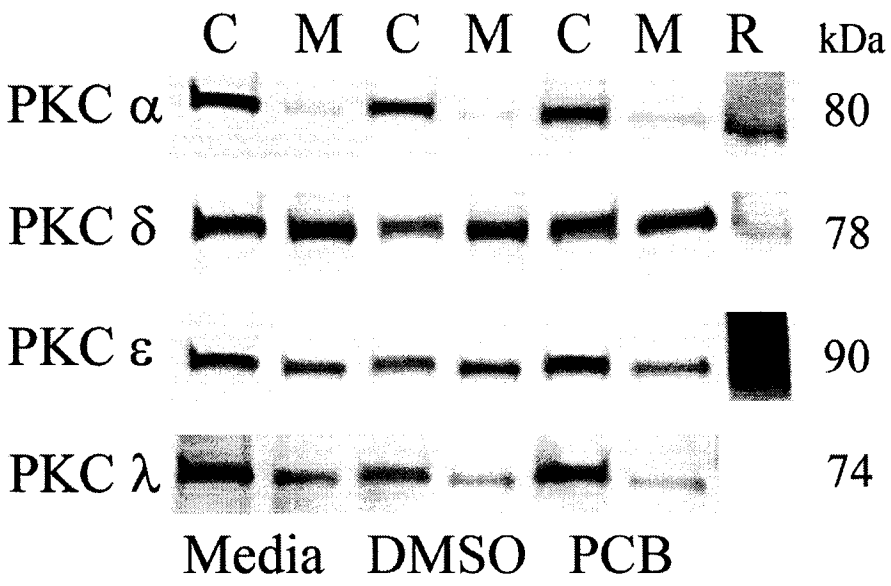

Figure 3.8a. PKC α, δ, ε, λ Western Blots. C= cytosol, M=membrane. Representative western blots after 10 min DMSO and 2.5 x 10^{-8} M PCB 126 treatments. Representative of 3 Western blots. The R is rat cerebrum lysate, a positive control used for band localization.

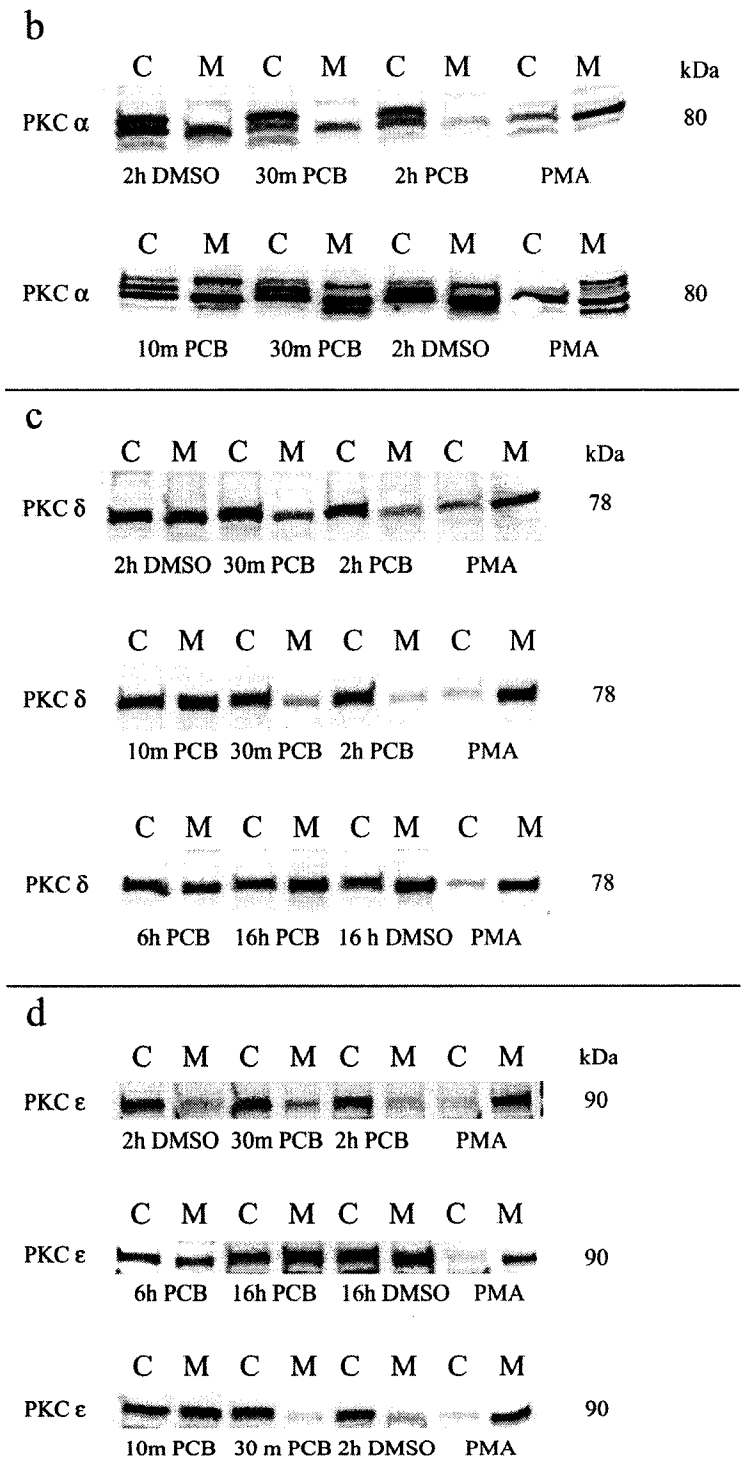

Figure 3.8b, c, d. PKC α, δ, and ε Western Blots. C= cytosol, M=membrane. Western blots after DMSO and 2.5 x 10^{-8} M PCB 126 treatments at the listed time points. **b)** PKC α. **c)** PKC δ. **d)** PKC ε.

Treatment	CREB phosphoryation (% of Respective DMSO Control)
5 m PCB	98
10 m PCB	91
30 m PCB	101
1 h PCB	110

Table 3.4. PKC Kinase Activity Assay. H4IIE cells were treated with DMSO or 2.5 x 10^{-8} M PCB 126 for the indicated time points. Each treatment was run in triplicate wells, and these data were averaged, the background fluorescence of the blank well was subtracted, and the PCB treatment value was divided by the respective control value to determine a relative percent kinase CREB phosphorylation. ANOVA analysis was used to determine significant difference between the PCB treatment at each time point and the DMSO control at each time point. No significant difference was found between PCB treatment and DMSO control at any time point measured.

Discussion

This research stems from previous studies documenting a switch-like response to CYP1A1 induction both in vivo and in vitro (Bars and Elcombe 1991; Bars *et al.* 1989; Broccardo *et al.* 2004; French *et al.* 2004). Biologically, this behavior represents a hybrid switch model, and is comparable to a dimmer on a light switch where a switch works in concert with a rheostat. Experimentally, such a hybrid switch model on the single cell level represents an initial induction threshold then a graded response thereafter (Broccardo *et al.* 2004; French *et al.* 2004).

Full activation of the AhR pathway may involve/require phosphorylation of: 1) the AhR, 2) cofactors that bind to the AhR, or may be required for 3) translocation of the liganded AhR into the nucleus, 4) dimerization of AhR to ARNT, 5) DRE binding, 6) chromatin remodeling, or 7) phosphorylation of a basal transcription factor necessary for AhR mediated transcription, or some other unidentified role.

PKC is a family of protein kinases that have been shown to be intimately involved in AhR mediated CYP1A1 induction. The PKC family includes at least 12 isozymes, with the regulatory region containing one or two zinc finger-membrane motifs (C1 and C2 domains). The C1 domain is activated by 1,2 diacylglycerol (DAG), phorbol esters, and phosphatidylserine (PS). The C2 domain contains a calcium binding motif. The conventional PKCs (α, βI, βII, γ) contain functional C1 and C2 domains. Novel/ nonconventional PKCs (δ, ε, η, μ, θ) contain a functional C1 domain, but lack a functional C2 domain. The atypical PKCs (ζ, ι, λ) contain a non-ligand-binding C1 domain and no C2 domain (Ventura and Maioli 2001). PKC localization is tightly regulated and subcellular targeting plays a major role in isoform activation (Newton

2003; Ohmori *et al.* 2000; Ohmori *et al.* 1998; Rybin *et al.* 2004; Shirai and Saito 2002; Ventura and Maioli 2001).

TCDD has been shown to activate PKC α, perhaps by an increase in intracellular calcium (Hanneman *et al.* 1996). Recently, it has been shown that a mixture of conventional PKC isoforms (α, β, γ) are capable of phosphorylating serine/threonine residues on the full length AhR and that further, tyrosine 9 of the AhR greatly facilitates this phosphorylation (Minsavage *et al.* 2004).

The co-treatment of cells with PCB 126 and the PKC inhibitor, H-7 resulted in a dramatic decrease in CYP1A1 induction, indicating a major role for PKC. It would also appear that PKA plays only a minor role in this response, as determined with the HA-1004 PKA inhibitor experiments. Further, treatment with PMA, which can decrease CYP1A1 induction by irreversibly binding PKC, did appear to decrease the % cells expressing CYP1A1 at the 4 h time point. It appeared that induction had returned to the same levels as with PCB treatment alone at 8 and 16 h PMA + PCB treatment. It is possible that synthesis of new PKC allowed to cells to recover and respond to PCB treatment at later timepoints. However, at the time points we tested (10 min, 30 min, 2 h, 6 h, 16 h), PCB 126 did not induce membrane translocation of PKC distinct from DMSO controls. It is possible that the translocation is so transient that the time points studied were not sufficient to observe the response. For example, ATP induces membrane translocation of PKC δ within 30 s, and a subsequent retranslocation to the cytosol within 3 minutes (Ohmori *et al.* 1998). Alternatively, PCB 126 may activate PKC kinase activity without membrane translocation. Hydrogen peroxide has been shown to increase tyrosine phosphorylation on PKC δ and concomitantly increase its enzymatic activity

without inducing membrane translocation (Konishi *et al.* 2001). However, this does not appear to be the case, as no increase in PKC kinase activity was detected at the time points measured. As such, the behaviors of PKCs in response to an activator are not as clear cut as simply observing membrane translocation or even increased kinase activity.

It is important to understand the mechanism of the PKC inhibitor, H-7, since we obtained such a significant decline in CYP1A1 levels with H-7. This isoquinolinesulonamide compound competes with ATP at the active center of PKC, and does not have an effect on the membrane translocation of PKC (Hidaka *et al.* 1984). As such, this compound would not affect any PCB induced translocation, but would inhibit phosphorylation of the PKC substrate. It is possible that the inhibition of basal PKC activity is sufficient to decrease CYP1A1 induction.

It has been shown that the MAPKs ERK (extracellular regulated kinase) and JNK (c-Jun N-terminal kinase) are activated independently of the AhR (i.e. AhR is not required for their activation) (Tan *et al.* 2002). However, hepatic CYP1A1 induction is still high in ERK1 (-/-) knockout mice transfected with siERK2 (90% ERK2 knockdown) (Andrieux *et al.* 2004). In vivo, the role of MAPKs in AhR activity appear to be highly tissue specific, as JNK2 knockout mice demonstrated opposite roles of JNK2 in the liver versus the thymus and testes (Tan *et al.* 2004). Other studies suggest that the AhR interacts with a protein/s that are a substrate of serine/threonine protein kinases, such as p42/p44 MAPK or PKC (Yim *et al.* 2004). This would imply the existence of a regulatory protein associated with the AhR modulating the activity of the AhR. No role for p38 in the AhR pathway appears to be likely at this point (Tan *et al.* 2004).

Given the clear involvement of phosphorylation in the AhR pathway, we decided to have two high throughput (40 antibody) custom protein arrays performed after 30 min and 6 h PCB 126 treatments. These time points were designed to observe the typically fast response of phosphorylation, and also to observe any changes in immediate early genes. At the 30 min time point there was an increase in the transcriptional repressor ICER (**I**nducible **c**AMP **E**arly **R**epressor). ICER is involved in autoregulatory feedback loops that regulate the transcription of immediate early genes such as Jun and all genes that contain a **c**AMP **r**esponse **e**lement (CRE) (Servillo *et al.* 2002). ICER is induced in H35 hepatoma cells by cAMP as early as 30 min and peaks by 2 h; ICER is also induced by 2 h after a partial hepatectomy (Servillo *et al.* 1997). At 6 h, there were two proteins containing increased phosphoserine/phosphoserine/threonine residues with an observed molecular weight of 233 and 109 kDa. This is an interesting observation given the likelihood that the AhR is associated with numerous phosphoproteins. The downregulation of the phosphorylated form of PKA regulatory subunit IIb represents potential modulation of the PKA pathway by PCB 126. AhR ligands are known to activate the PKA pathway and our research does show a minor role of PKA in PCB 126 mediated CYP1A1 induction (Vogel *et al.* 2004). The increased levels of the protooncogene Jun at 6 h is consistent with the literature and TCDD and PCB 126 has been shown to affect this pathway (Hoffer *et al.* 1996; Puga *et al.* 1992; Tanno and Aoki 1996). TCDD has been shown to induce Jun and increase AP-1 transcription factor activity, and this response may be PKC dependent (Puga *et al.* 1992). In addition to AhR independent pathways, Jun contains DRE sequences in its promoter region, lending this gene to direct regulation by the AhR pathway (Hoffer *et al.* 1996). PCB 126 has also

been shown to lead to increased phosphorylation of c-Jun (Tanno and Aoki 1996). These results represent a dynamic cellular response to PCB 126 involving cAMP, PKA, and Jun. It is plausible that PCB 126 increases cAMP thus activating PKA. ICER is then induced in an autoregulatory feedback loop downregulating the cAMP mediated transcriptional responses, including Jun.

Given the established role of the MAPK pathways ERK and JNK to AhR ligands, it was interesting that increased levels of P-ERK or P-JNK were not identified in the custom protein array, especially at the 30 minute time point. In order to confirm this response, we measured P-ERK and P-JNK after 5 min, 15 min, 30 min, and 60 min PCB 126 treatment and performed a Western blot analysis. The PMA positive control did increase levels of P-ERK and P-JNK, however none of the PCB 126 treatments caused increased levels of P-ERK and P-JNK. These data indicate that these pathways are not activated in response to PCB 126 in H4IIE cells. Given the highly cell-specific responses to MAPK activation, this result is not without precedence (Tan *et al.* 2004). Additionally, activation of this pathway has been observed primarily with TCDD, not a coplanar PCB. The U0126 MEK inhibitor data do not provide a clear conclusion regarding the role of the ERK pathway; it would appear that U0126 may be a ligand for the AhR at the concentration used. DMSO vehicle control contamination issues further confound the interpretation of these data; however, given the lack of PCB 126 induced activation of the ERK or JNK pathways, further study with U0126 may not be warranted.

An underlying question that must be answered is the distribution of the AhR on a single cell basis. If many cells have lost the AhR, this could potentially explain the lack of PCB 126 mediated CYP1A1 induction in the non-responding population of cells.

After 16 h treatment with DMSO or 2.5 x 10^{-8} M PCB 126, approximately 95 % and 87% of the cells expressed the AhR, respectively. The histogram overlay for the rabbit IgG isotype control and AhR show two distinct sets of curves, indicating that a majority of the cell population does, in fact, contain the AhR. Further, it is likely that the amount of AhR present is not a limiting factor in the H4IIE cells, as the Hepa 1c1c7 cells contain 100 times as much AhR (Holmes and Pollenz 1997), but display about 20 times less CYP1A1 induction (Broccardo *et al.* 2004). A similar argument holds true for ARNT: Hepa 1c1c7 cells contain twice as much ARNT as the H4IIE cells (Holmes and Pollenz 1997). Therefore, it is not likely that AhR or ARNT are limiting factors in this pathway given the lack of a relationship between their levels and CYP1A1 induction.

The purpose of these experiments was to begin to uncover the mechanism for the switch-like response to PCB 126 mediated CYP1A1 induction. These results indicate a potential role for PKC in the PCB 126 mediated switch-like response to CYP1A1 induction. Focused experiments would help to reveal the role of PKC in this system, as the traditional membrane translocation of PKC did not occur at the time points measured and there was no increased kinase activity after PCB 126 treatment. It is possible that the PKC response is highly transient and was not observed at the time points measured. However, it is also plausible that basal, constitutive activity of PKC is required in the functioning of the AhR pathway, and that PKC translocation or kinase activity does not increase due to PCB 126 treatment. This hypothesis would be consistent with the dramatic decrease in CYP1A1 induction observed after the use of the PKC inhibitor H-7. In conclusion, the AhR pathway is highly complex and undergoes cell-specific modulation, possibly by PKC, resulting in a multitude of potential cellular responses.

CHAPTER 4

Discussion

The AhR Pathway: A Receptor Based Model for Biological Switching

Transcriptional Regulation: To Switch or Not to Switch?

Theoretically, there are two distinct modes of gene regulation. A cell may respond to a stimulus as a stable on/off switch, behaving in a threshold manner and displaying a sigmoid concentration-response curve (Fiering *et al.* 1990; Ko *et al.* 1990; Newlands *et al.* 1998; Ross *et al.* 1994; White *et al.* 1995). This may also be described as a binary, quantal, digital, threshold, or switch response. Conversely, a cell may respond by initiating quantitative gene regulation, resulting in continuously variable gene expression (Hazzalin and Mahadevan 2002). This type of regulation would allow the cell to control how many copies of a gene to transcribe based on the strength of the signal. This is also known as an analog, rheostat, graded, or linear response. There are biological advantages to both modes of gene expression, and one type may be more suitable to specialized scenarios such as development (Ferrell and Machleder 1998), long term potentiation in the hippocampus (Bhalla and Iyengar 1999), or the activation of immediate early genes (Hazzalin and Mahadevan 2002).

Regulation at the level of signal transduction or at the level of chromatin remodeling is known to play a role in both types of transcriptional responses. Often, phosphorylation events in the cytosol are translated into phosphorylation or acetylation at

the level of the chromatin, mediated by a series of transcription factors. As such, the complex activation and interaction of signal transduction cascades and transcription factors may affect a unique transcriptional response. It is accepted that there is a certain level of redundancy within the cell, and that the interplay between multiple pathways and transcription factors determine the ultimate outcome. Therefore, it is likely that there may be some variability in the strength of each pathway activated on a cell by cell basis, based on the stochastic nature of molecular interactions. Specifically, this could be explained by the simultaneous use of several transcription factors, associated proteins, cofactors, or regulatory elements, depending on which MAPKs (or other kinases) are activated by a particular stimulus and which transcription factors are phosphorylated/ activated. It is possible that the rate of transcription is directly dependent on which combination of elements is used (Hazzalin and Mahadevan 2002). Therefore, it is possible that there are multiple "activation modules" that one stimulus may activate given the stochastic nature of molecular interactions. It is plausible that once one module is activated, not all of the potential modules will be co-activated, giving rise to some of the observed cell specific response. This may be based on the simple amounts of members of each pathway present in a given cell or cell type. The dynamic nature of the cell, other stimuli utilizing the pathway members, and the continuous turnover of proteins may all be factors in this process. Such behavior would not negate the typical stimuli specific responses, it would simply modulate it. Similar concepts have been discussed by several groups (Hume 2000; Rossi *et al.* 2000).

As clearly pointed out in Hazzalin *et al.*, (Hazzalin and Mahadevan 2002), the switch and the graded responses are not mutually exclusive events, it is possible that

there may be some mechanistic overlap in these two concepts. For example, once a gene is technically "switched" on, other factors may modulate its rate of transcription leading to an initial switch-like response with a continuously variable response thereafter. Such an event may be termed a hybrid switch, representing a functional switch-rheostat mechanism.

Benefits of a switching mechanism to the cell include: filtering of noise or fleeting signals (noise caused by the stochastic nature of molecular interactions) and the potential to generate distinct populations of cells whereby expression can either be turned on or off (Berg *et al.* 2000; Biggar and Crabtree 2001). In contrast, graded mechanisms allow a greater sense of fine-tuning for the cell in responding proportionately to stimuli. All cells within the population would remain homogeneous (Biggar and Crabtree 2001). A mixed response or a so-called hybrid switch would allow the cell to filter out background noise via the switch mechanism, and then precisely control the rate of gene transcription thereafter. Additionally, it is also possible that some systems may be so complex in their activation processes that a stimulus threshold must be achieved before there is sufficient flux through a signal transduction pathway/s for the system to respond. This would be in contrast to a system/response that is sensitive to even the smallest stimuli. This clearly represents two different types of systems, and biologically there are needs for both.

How to Switch: Posttranslational Modifications

Mechanistically, how is a switch turned on? A common theme throughout the literature on the topic of switching is phosphorylation. There are numerous examples of

signal transduction pathways mediating phosphorylation of transcription factors and other regulatory proteins turning on transcription in a switch-like fashion, or phosphorylation cascades inducing an ultimate cell fate event (Bhalla *et al.* 2002; Ferrell 1996; Ferrell and Machleder 1998; Ferrell and Xiong 2001; Hazzalin and Mahadevan 2002).

Cell Fate Switch: Induction by Phosphorylation

An elegant example whereby a continuously variable stimulus can be converted into an all-or-none biological response is found in the study of Ferrell and Machleder on progesterone-induced maturation in *Xenopus* oocytes (Ferrell and Machleder 1998). Upon exposure to progesterone, the oocyte switches from a G2-like arrest state to a maturation state that subsequently results in meiosis (I) and (II) metaphase arrest. The progesterone mediated activation of a mitogen activated protein kinase (MAPK) cascade (and subsequent phosphorylation of the Cdc2-cyclin B complex) was shown to give rise to the ultimate, irreversible, maturation response.

Within a potentially heterogeneous group of intact oocytes, the response of MAPK activation following progesterone exposure was more typical of a Michaelis-Menton relationship (i.e. hyperbolic response with increasing stimulus). However, upon examining the response at the level of the individual oocyte, the response to an intermediate progesterone concentration was all-or-none, yielding a sigmoid dose response curve. Further studies would reveal that the switch-like behavior was based on ultrasensitivity of the enzymes creating an activation threshold, and via positive feedback. Both ultrasensitivity and positive feedback are several key features of an all-or-none, switch response (Louis and Becskei 2002).

Another key feature frequently observed in a system exhibiting switching is hysteresis. A bistable system is one that toggles between two discrete, alternative stable steady states, in contrast to a monostable system which slides along a continuum of steady states (Ferrell and Xiong 2001). It has been hypothesized that bistability is crucial to cellular processes such as differentiation and cell cycle progression (Ferrell and Machleder 1998; Laurent and Kellershohn 1999; Thron 1997). Bistable systems are though to be involved in the generation of switch-like biochemical responses. Bistability can arise in signaling systems that contain a positive-feedback loop or a mutually inhibitory, double-negative feedback loop. These factors are not always sufficient to term a system bistable, however, and one must also analyze for other features, such as hysteresis. Hysteresis can be defined in several ways: 1) an irreversible change, 2) distinct splitting of the stimulus-response relationship, or 3) the ability to remember a stimulus long after it has been withdrawn (Ferrell and Xiong 2001). A clear biological example of hysteresis can be found in the maturation of *Xenopus* oocytes as discussed above (Ferrell and Machleder 1998). When progesterone levels reach a certain threshold concentration, a MAPK cascade triggers a true cellular switch: the oocytes are permanently matured. Further, the cells may not exist in some in between level of maturity, they are either mature or not. Removal of the progesterone does not induce subsequent "de-maturing," the cells are irreversibly fated.

A bistable system can be described in many ways, including digital, switch-like, binary, or stochastic and may exhibit hysteresis or threshold behavior. The advantage to the cell of such a response could be to filter out noise or fleeting signals, allowing the cell to remain in a stable state. Bistable cell signaling systems appear to be responsible

for the digital, all-or-none character of the action potential, various cell fate induction processes, and progression from one discrete phase of the cell cycle to another. Bistable cell signaling systems also offer the possibility of providing a sort of biochemical memory, which may contribute to the irreversibility of some cell differentiation processes (Ferrell and Xiong 2001). Graphical depictions of hysteresis and a bistable response are seen in figures 4.1 and 4.2. (Ferrell and Xiong 2001; Pomerening *et al.* 2003). With hysteresis, the on-state is permanent, whereas it is reversible in a bistable system.

As can be seen by the shape of the response in the bistable and hysteresis figures, they are characterized by a very steep stimulus-response curve. A mathematical way of characterizing the steepness of the response and evaluating if it displays switch- like nature is the Hill Equation. In the example below, the equation is tailored towards a concentration-response for gene induction.

$$\text{Induction}=\text{Induction}_{max} * \text{Concentration}^n/(\text{Concentration}^n + K_d^n)$$

Where n is the Hill coefficient and K_d is ligand receptor binding affinity.

The transformed form of this relationship is:

$$R(d,t)=R_0 + (R_{max,t} - R_0)/(1+10\text{^}(\text{LogEC}_{50}\text{-LogDose})*n^H))$$

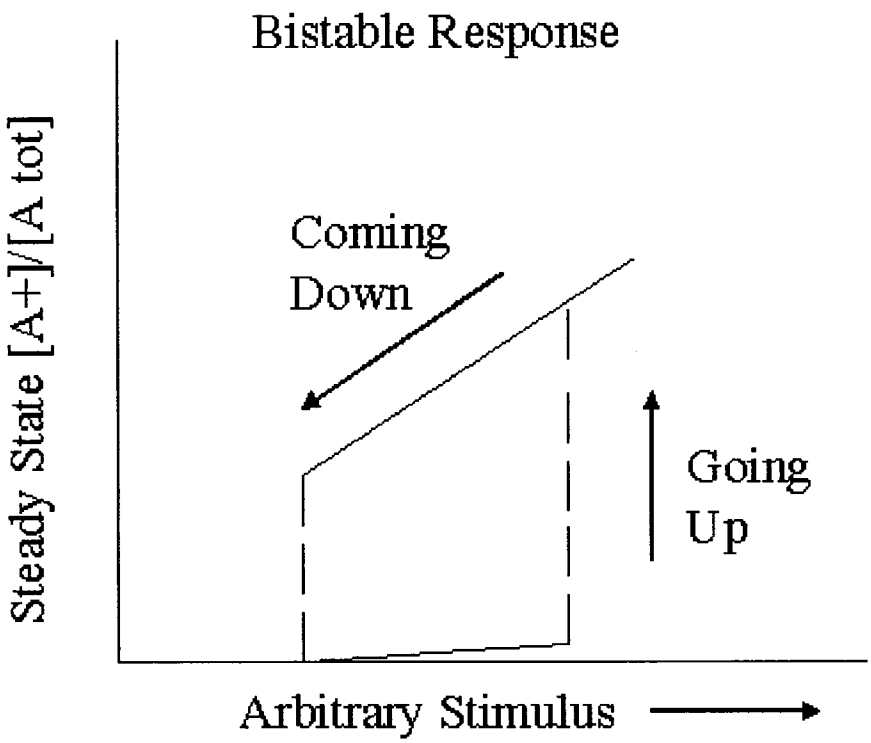

Figure 4.1. Stimulus-response curve for a bistable response. When the stimulus is increased, the system can switch from the off-state to the on-state. When the stimulus is decreased back to zero, the system returns to the off-state.

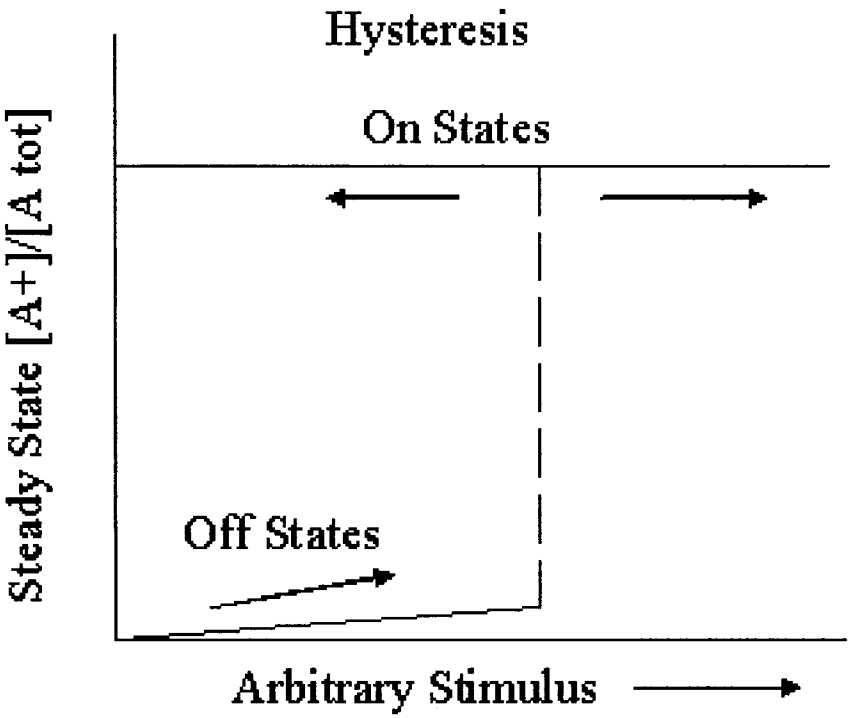

Figure 4.2. Stimulus-response curve for hysteresis. When the stimulus is increased, the system can switch from the off-state to the on-state. However, when the stimulus is decreased back to zero, the system remains stuck in the on-state.

Where R(d,t)=response at a given time t after dosing; R_0=initial response; $R_{max,t}$=maximal response at a given time t after dosing; $LogEC_{50}$= log dose at 50 percent maximal response; n^H = Hill slope.

This is a sigmoid dose-response (variable slope) equation that generates a n^H (Hill slope), EC_{50} and r^2 for the concentration-response studies. The Hill slope for a Michaelian response is n^H =1. If the Hill slope is calculated to be greater than 1, the system displays characteristics of a switch, displaying a sharp rise in response over a small range in concentration. In the oocyte example above, the Hill slope for MAPK phosphorylation was n^H=35 for each individual oocyte. This is thus a very sharp response and represents a clear example of a switch response.

Transcriptional Switch: Phosphorylation of Transcription Factors

Hazzalin *et al.*, (Hazzalin and Mahadevan 2002) offer a hypothetical, generally applicable, model of how phosphorylation events may provide for either a graded or switch response at the level of gene transcription. First, the model for a graded (continuously variable) response will be discussed. The key characteristic of this model is that addition of phosphate groups on the transcription factor are regarded not as a stable modification, but as one that can be dynamically turned over by the continuous and opposing action of kinases and phosphatases. Therefore, if each cycle of transcriptional initiation is linked to a single event of phosphorylation and dephosphorylation, then transcription is not regarded as a stable, but a dynamic event dependent on the rate of phosphorylation and dephosphorylation. This would produce tight quantitative coupling between the balance of kinase and phosphatase activities at the transcription factor and

the rate of transcriptional initiation, providing for exquisite quantitative control. This is a very demanding process in terms of ATP, but allows the cell to precisely control transcription. They also propose that a similar response could be obtained from any event which is reversible and controlled by signal-transduction cascades, for example protein-protein or protein-DNA interactions at the promoter, given that the event is supported by a single cycle of transcription.

In contrast to the cycling of phosphorylation events to produce a graded response, a stable on/off switch is linked to stable phosphorylation events. Consider a gene whose transcriptional switch is dependent on kinase mediated phosphorylation of a transcription factor. Upon arrival of the activated transcription factor at the promoter region, a stable chromatin conformation is established, and transcription will proceed at a preset rate dependent on the nature of the interaction of the transcription factor and the promoter. At the end of the preset rate of transcription, the transcription factor will be dephosphorylated, leave the promoter region, and the gene will revert to its stable off state (Hazzalin and Mahadevan 2002). They further propose that different combinations of factors may produce different rates of transcription for a particular gene, and this will be termed "activation modules," and will serve as a model for further discussion.

Structural Switching: Chromatin Remodeling

Chromatin integrates a variety of endogenous and exogenous signals and functions as a biological relay station and signaling platform (Cheung *et al.* 2000a). The N-terminal histone tails participate in the modulation of chromatin architecture via several potential mechanisms. Firstly, they are targets for ATP-dependent chromatin

remodeling factors such as Swi/Snf and NURF (Georgel *et al.* 1997; Lee *et al.* 1999). Secondly, the histone tails undergo a multitude of posttranslational modifications, such as acetylation and phosphorylation which may modulate the contacts between histones and DNA. Because these modifications are reversible, they can act as chromatin-based on/off switches that regulate a multitude of DNA-related processes. Further, the structural accessibility of the histone tails makes them prime targets for signal-activated enzymes, and they may function as important links between signal transduction and gene expression.

The MAPK signaling cascades have been shown to directly phosphorylate histone tails. Specifically, the ERK-activated Rsk-2, and Msk-1 (activated by ERK and p38) kinases have been shown to phosphorylate histone H3 (Sassone-Corsi *et al.* 1999; Thomson *et al.* 1999). Phosphorylation of histone tails does not always occur independent of other modifications. In fact, several histone acetyl transferases (HATs) have shown preference for previously phoshorylated histone tails, resulting in a dual-modification (Cheung *et al.* 2000b). In fact, such a dual modification on H3 has been associated with EGF (epidermal growth factor) activated genes. The mechanisms whereby these modifications are able to elicit ultimate gene transcription are still under study. However, it is likely that these modifications play a role in attracting transcription factors to the chromatin. For example, $TAF_{II}250$ (a member of TFIID basal transcription factor complex) contains HAT activity and is attracted to multiply acetylated regions of chromatin. It may be that the initial modifications attract the transcription factor complex and this complex may further modify the chromatin, readying it for transcription (Cheung *et al.* 2000a). Protein kinase C (PKC) has also been shown to phosphorylate the family

of H1 histones, and this appears to play a major role in cell cycle-related decisions (Ventura and Maioli 2001). The dynamic and varied modifications on histone tails no doubt play a pivotal role in gene expression, and the precise role they play requires much further study. The question is how might such modifications provide for the observed on/off nature of transcription for many genes?

If a promoter is tightly bound into chromatin it is inaccessible to transcription factors that would initiate transcription. The dynamic shift between states of accessibility may provide for a switch between transcriptionally incompetent and competent states. This switch could impart a binary character to transcriptional response involving alterations in chromatin structure (Biggar and Crabtree 2001; Fischle *et al.* 2003; Hazzalin and Mahadevan 2002). Other factors that may serve to impart a binary nature to transcription at the level of chromatin are silencers, enhancers, and locus control regions which are always in a state of competition (Kamakaka 1997).

A Receptor Based Switch Model: The Arylhydrocarbon Receptor Pathway

What is The Switch in the AhR Pathway?

The AhR pathway is one of the most well studied receptor pathways in the cell. Much is known about the regulation of this pathway and the variety of components that are critical to its success. These include chaperone proteins, coactivators, and a variety of signal mediators including the MAPKs, PKC, and possible receptor and non-receptor tyrosine kinases. What are less clear are the precise phosphorylation events that are crucial to this pathway. There appear to be a variety of constitutively phosphorylated residues (serine/threonine and/or tyrosine), and others that are inducible. Which kinases

mediate the multitude of modifications at each site is still under study, and it is possible that more than one kinase could mediate some of the events or may be involved in a cell specific fashion. The upstream activators in this process are not precisely known either. In order to begin to focus in on where the switch in the AhR pathway may be, we performed a variety of experiments, mostly focusing on phosphorylation events, in the H4IIE rat hepatoma cells. Since this cell line has faithfully modeled the in vivo switch response, and that of primary rat hepatocytes, they serve as a convenient model for mechanistic studies. The following section will outline the initial results of our mechanistic studies. A more complete description of the role of each pathway or modulating factor in general will be discussed thereafter.

Given the clear involvement of phosphorylation in the AhR pathway, we decided to have two high throughput (40 antibody) custom protein arrays performed after 30 min and 6 h PCB 126 treatments. At the 30 min time point there was an increase in the transcriptional repressor ICER (**I**nducible **c**AMP **E**arly **R**epressor). ICER is involved in autoregulatory feedback loops that regulate the transcription of immediate early genes such as jun and all genes that contain a **c**AMP **r**esponse **e**lement (CRE) (Servillo *et al.* 2002). At 6 h, there were two proteins containing increased phosphoserine/ phosphoserine/threonine residues with an observed molecular weight of 233 and 109 kDa. This is an interesting observation given the likelihood that the AhR is associated with numerous phosphoproteins. The observed downregulation of the phosphorylated form of PKA regulatory subunit IIb represents potential modulation of the PKA pathway by PCB 126. AhR ligands are known to activate the PKA pathway and our research does show a minor role of PKA in PCB 126 mediated CYP1A1 induction (Vogel *et al.* 2004).

The increased levels of the protooncogene Jun at 6 h is consistent with the literature and TCDD and PCB 126 has been shown to affect this pathway (Hoffer *et al.* 1996; Puga *et al.* 1992; Tanno and Aoki 1996). TCDD has been shown to induce Jun and increase AP-1 transcription factor activity, and this response may be PKC dependent (Puga *et al.* 1992). In addition to AhR independent pathways, Jun contains DRE sequences in its promoter region, lending this gene to direct regulation by the AhR pathway (Hoffer *et al.* 1996). PCB 126 has also been shown to lead to increased phosphorylation of c-Jun (Tanno and Aoki 1996). These results represent a dynamic cellular response to PCB 126 involving cAMP, PKA, and Jun. It is plausible that PCB 126 increases cAMP thus activating PKA. ICER is then induced in an autoregulatory feedback loop downregulating the cAMP mediated transcriptional responses, including Jun. Unfortunately, none of these results give much insight as to where the AhR mediated switch may be, but do fit in with the literature. However, we were able to measure precisely which PKC isoforms were present and at what relative levels. This allowed us to perform further studies revolving around PKC.

Protein kinase C or PKC is a family of protein kinases that have been shown to be intimately involved in AhR mediated CYP1A1 induction. The co-treatment of cells with PCB 126 and the PKC inhibitor, H-7 resulted in a dramatic decrease in CYP1A1 induction, indicating a major role for PKC. However, at the time points we tested, PCB 126 did not induce membrane translocation of PKC α, δ, ε or λ distinct from DMSO controls. There are several explanations for this response. It is possible that the translocation is so transient that the time points studied were not sufficient to observe the response. For example, ATP induces membrane translocation of PKC δ within 30 s, and

a subsequent retranslocation to the cytosol within 3 minutes (Ohmori *et al.* 1998). Alternatively, PCB 126 may activate PKC kinase activity without membrane translocation. H_2O_2 has been shown to increase tyrosine phosphorylation on PKC δ and concomitantly increase its enzymatic activity without inducing membrane translocation (Konishi *et al.* 2001). However, this does not appear to be the case; we did not detect PCB 126 induced increased kinase activity at any of the time points we measured. Further, the inhibitor H-7 may also inhibit PKA in our dose range. In fact, we did identify minimal CYP1A1 inhibition (from 57% to 43% of the cells) using the PKA inhibitor HA-1004. As such, the behaviors of PKCs in response to an activator are not as clear cut as simply observing membrane translocation or increased kinase activity. It is possible that the inhibition of basal PKC activity by H-7 is sufficient to decrease CYP1A1 induction independent of PCB 126 mediated increases of PKC translocation or activity.

Given the established role of the MAPK pathways ERK and JNK in this system, it was interesting that increased levels of P-ERK or P-JNK were not identified in the custom protein array, especially at the 30 minute timepoint. In order to confirm this response, we measured P-ERK and P-JNK after 5 min, 15 min, 30 min, and 60 minutes PCB 126 treatment and performed a Western blot analysis. The TPA positive control did increase levels of P-ERK and P-JNK, however none of the PCB 126 treatments caused increased levels of P-ERK and P-JNK. These data indicate that these pathways are not activated in response to PCB 126 in H4IIE cells. Given the highly cell-specific responses to MAPK activation, this result is not without precedence. Additionally, activation of this pathway has been observed primarily with TCDD, not a coplanar PCB.

The sum of this research indicates a likely role for PKC in the switching response. It is likely that basal PKC activity is crucial to the full activation of the AhR pathway in H4IIE cells. The lack of MAPK activation is quite revealing, and may represent a cell specific response or a unique response to PCB 126 vs TCDD.

Posttranslational Modifications within AhR Pathway

There are many identified posttranslational modifications that appear to be important in the AhR pathway. It is possible that without these modifications, the key players in the AhR pathway will not be fully activated. As such, it is essential to begin to assemble a potential model of all of the activated pathways and the key proteins within the AhR pathway. Visualizing all of these complex factors at once may help in our understanding in the switch like nature of this unique receptor based model. For ease, the cytosolic vs nuclear posttranslational modification events will be separated for discussion sake, acknowledging that they are truly a fluid process.

Cytosolic Posttranslational Events

In addition to the prototypical AhR mediated gene induction, AhR ligands may activate pathways independent of the AhR. For example, it is known that the MAPKs (mitogen activated protein kinases) ERK (extracellular regulated kinase) and JNK (c-Jun N-terminal kinase) are activated independently of the AhR (i.e. AhR is not required for their activation) (Tan *et al.* 2002). There are at least 3 MAPK modules, including ERK, JNK, and p38 (English *et al.* 1999). Both the JNK and p38 modules are often referred to as the stress-activated protein kinases. MAPKs are important intracellular signaling

mediators, controlling gene expression through phosphorylation of transcription factors and modulation of the function of these factors. These enzymes may be activated by numerous events, including stress, UV, cytokines, growth factors, and exogenous chemicals. Each of the described modules constitutes a series of sequentially phosphorylated MAPKs that transmit a signal ultimately to the nucleus to influence cellular events such as differentiation, apoptosis, and stress responses. Unfortunately, two commercially available MEK inhibitors, PD98059 and U0126, are also AhR ligands and as such must be used with great caution when studying the role of MAPK activation and CYP1A1 induction (Andrieux *et al.* 2004; Reiners *et al.* 1998). Interestingly, hepatic CYP1A1 induction is still high in ERK1 (-/-) knockout mice transfected with siERK2 (90% ERK2 knockdown) (Andrieux *et al.* 2004). In vivo, the role of MAPKs in AhR activity appears to be highly tissue specific. A recent paper studying the roles of ERK, JNK, and p38 MAPKs in AhR activation demonstrated distinct tissue and cell line specific responses (Tan *et al.* 2004). JNK2 knockout mice demonstrated opposite roles of JNK2 in the liver versus the thymus and testes; induction of CYP1A1 by TCDD was significantly reduced in the thymus and testis while it was actually significantly increased in the liver. Overexpression of a mutant MEK1, which activates ERK, in African Green Monkey kidney CV-1 cells (which lack the AhR) caused increased activity of AhR/ARNT-dependent luciferase activities in cells transfected with AhR/ARNT reporter constructs (Tan *et al.* 2004). As such, it would appear that activation of the ERK pathway increases the activity of AhR/ARNT luciferase activity. However, TPA (12-O-tetradecanoylphorbol-13-acetate; also called PMA), a potent activator of PKC and activator of ERK failed to exert an effect on AhR-dependent luciferase expression

whereas epidermal growth factor and serum did. One must conclude that there is a potential role for ERK and JNK in this pathway, but that it is, again, tissue/cell line specific. This group further identified ARNT as a potential target over AhR for the MAPKs and suggest that MAPK-mediated ARNT phosphorylation can lead to the transcriptional activation of either ARNT-ARNT homodimers or ARNT-AhR heterodimers (Tan *et al.* 2004). No role for p38 in the AhR pathway appears to be likely at this point (Tan *et al.* 2004).

A recent paper probed even further the role of the ERK pathway in AhR activation (Yim *et al.* 2004). The continued use of the MEK inhibitor PD98059 by this group introduces a level of ambiguity to some of their experiments; however they reveal some very interesting results. In Hepa 1c1c7 cells, two hours of TCDD treatment increased the phosphorylation of p44/p42 MAPK and p42 MAPK, in particular, was the primary player in dioxin-dependent transcription. Cotransfection of Hepa 1c1c7 cells with the DRE-driven reporter plasmid pGud luc 1.1, together with plasmids that encode dominant negative forms of p44 and p42 revealed that the loss of p42 dramatically reduced dioxin-dependent expression of the DRE-driven reporter gene. In order to determine if the ERK pathway may, in fact, be phosphorylating the AhR itself, they performed a series of immunoprecipitations using AhR and anti-phosphoserine and phosphothreonine antibodies. Hepa 1c1c7 cells treated with TCDD were immunprecipitated first with the anti-phosphoserine and anti-phosphothreonine antibodies then co-precipitated AhR was detected by Western blotting. The results revealed that the AhR is a component of a protein complex containing phosphoserine or phosphothreonine residues and the amount of co-precipitated AhR was increased due to

TCDD treatment. Then, to determine if the AhR itself was directly phosphorylated they first immunoprecipitated using an anti-AhR antibody then measured any phosphoserine or phosphothreonine residues via Western blotting. No phosphoserine or phosphothreonine residues were detected on the immunoprecipitated AhR complexes, indicating that TCDD did not induce serine or threonine residue phosphorylation on the AhR. Instead, TCDD treatment increased the interaction between the AhR and other unidentified phosphoproteins suggesting that the AhR interacts with a protein/s that are a substrate of serine/threonine protein kinases, such as p42/p44 MAPK or PKC. This would imply the existence of a regulatory protein associated with the AhR modulating the activity of the AhR. Of note, it appears that the total levels of AhR phosphorylation may not change upon treatment (Mahon and Gasiewicz 1995).

Clearly, the role of MAPKs in AhR mediated CYP1A1 induction is still under study. Although it does not appear that MAPKs directly phosphorylate the AhR, they may directly phosphorylate ARNT, some associated modulatory protein/s to the AhR, or chromatin. Further, all of the proteins in the AhR core complex are phosphoproteins, and the phosphorylation status of AhR, Hsp90, and XAP2 are likely to play a role in AhR transactivation. Could these proteins be the substrate for MAPKs or PKCs? Why would TCDD treatment increase their association with the AhR? Or does the AhR bind inducibly to some other unknown phosphoprotein? These questions remain unanswered.

Protein kinase C (PKC) is another family of protein kinases that has been shown to be intimately involved in AhR mediated CYP1A1 induction. TCDD has been shown to activate PKC in primary rat hippocampal neurons, perhaps by an increase in intracellular calcium (Hanneman *et al.* 1996). The PKC family consists of at least 12

isozymes, which can be further classified based on their structure and cofactor regulation (Ventura and Maioli 2001). All PKC isoforms consist of a single polypeptide chain containing an N-terminal regulatory domain and a C-terminal kinase domain. The regulatory region of PKCs contains an autoinhibitory domain, the pseudosubstrate, and one or two zinc finger membrane motifs (C1 and C2 domains). The C1 and C2 domains may come in two forms: one that is capable of ligand binding or one that lacks determinants that allow for ligand binding and is, as such, nonfunctional. The C1 domain is activated by 1,2 diacylglycerol (DAG), phorbol esters, and phosphatidylserine (PS). The C2 domain contains a Ca^{2+} binding motif. The conventional PKCs (α, βI, βII, γ) contain functional C1 and C2 domains, thus responding to DAG and Ca^{2+} signals. Novel/nonconventional PKCs (δ, ε, η, μ, θ) contain a functional C1 domain, but lack a functional C2 domain. The atypical PKCs (ζ, ι/ λ) contain a non-ligand-binding C1 domain and no C2 domain, and as a consequence, respond to neither DAG nor Ca^{2+}, but respond to PS, phosphatidylinositides, or unsaturated fatty acids.

Well over a dozen papers since the 1980's have confirmed the relationship between PKC activity and AhR activity. Despite the use of in vivo experiments and a myriad of complex molecular in vitro systems, the exact role of PKC in the functionality of the AhR pathway remains elusive. The use of potato acid phosphatase with ligand activated receptor has revealed that phosphorylation (in general) is required for AhR complex DNA binding (Mahon and Gasiewicz 1995; Pongratz *et al.* 1991). To more closely link PKC action with the AhR TPA has been extensively utilized, despite its time and cell-line dependent actions. In the short term, TPA activates PKC and thus results in a synergistic induction of CYP1A1 when administered in conjunction with an AhR ligand

(Long and Perdew 1999; Long *et al.* 1998). In converse, extended treatment with TPA results in down-regulation of PKC thus inhibiting CYP1A1 induction (Berghard *et al.* 1993; Okino *et al.* 1992; Reiners *et al.* 1993). Results of experiments with TPA must not be over-extended to different cell types or to different time points, given the extreme variability in the effect of TPA on CYP1A1 induction. General and specific inhibitors of PKC have been extensively used. However, caution is advised in the use of such inhibitors, as they may be ligands of the AhR, as in the case of staurosporine (but not H-7 or Calphostin c) (Schafer *et al.* 1993). Unfortunately, the use of staurosporine to study PKCs action on the AhR pathway persists and conclusions from such studies must be interpreted carefully (Chen and Tukey 1996).

Mechanistic studies on the exact role of PKC in AhR activity have provided many insights, but frequently the systems required to study such detail are not biologically representative and must be verified, if possible, in a whole cell system. Conceptually, there are many possible roles PKC may play in this pathway. 1) PKC may directly phosphorylate the AhR, 2) PKC may phosphorylate some known/unknown cofactor that binds to the AhR, 3) PKC may be required for ligand binding, 4) PKC activity may be required for translocation of the liganded AhR into the nucleus, 5) PKC may be required for dimerization of AhR to ARNT, 6) PKC may be crucial to the binding of the AhR/ARNT complex to the DRE region of responsive genes, 7) PKC may directly phosphorylate chromatin thus transforming it into an accessible conformation, 8) PKC may phosphorylate a basal transcription factor necessary for AhR mediated transcription, or PKC may play some other role not described herein. The complex nature of this

question is evident, and these possibilities do not take into account potential interplay from other pathways/actions (MAPKs, tyrosine phosphorylation, etc.).

Recent experiments probed an obvious potential action of PKC: direct phosphorylation of the AhR (Minsavage *et al.* 2004). They have shown that a mixture of conventional PKC isoforms (α, β, γ) are capable of phosphorylating serine/threonine residues on the full length AhR and that further, tyrosine 9 of the AhR greatly facilitates this phosphorylation. Mechanistically, they propose that PKC activity is required for the recruitment of coactivators that interact with the N-terminus of the AhR and/or ARNT or that PKC directly phosphorylates the N-terminus of the AhR and/or ARNT. Further, phosphorylation of the AhR may result in a changed affinity for one or multiple associated proteins in the cytoplasm and/or the nucleus resulting in increased DNA binding affinity and transcriptional activation (Minsavage *et al.* 2004). Additionally, the DNA binding domain of the AhR consists of two basic clusters separated by about 20 amino acids. These two clusters must come into proximity in order to bind the 4-5 nucleotide long DRE. It is proposed that PKC mediated phosphorylation of the AhR may confirm some conformational change maintaining an optimal three-dimensional structure for AhR:DRE binding (Minsavage *et al.* 2004).

Phosphorylation, PKC dependent or not, does not appear to be necessary for ligand binding to the AhR. Pongratz *et. al.* have shown that a dephosphorylated AhR exhibited control levels of ligand binding (Pongratz *et al.* 1991). The addition of several PKC inhibitors (H-7 and Calphostin c) prior to TCDD addition had no significant effect on TCDD binding to guinea pig, rat, or mouse hepatic cytosolic AhR (Schafer *et al.*

1993). Further, it appears that the total levels of AhR phosphorylation may not change upon treatment (Mahon and Gasiewicz 1995).

The binding of the ligand:AhR complex to the DRE is most commonly measured using the EMSA (elecrophoretic mobility shift assay), whereby radiolabeled DRE sequences are added to the ligand:AhR complex and binding is measured. Such an assay is informative, but not necessarily representative of the DRE in its native state when it is surrounded by chromatin. General phosphorylation of the AhR has been shown to be necessary for AhR:DRE binding, as seen after phosphatase treatment and measured via EMSA (Mahon and Gasiewicz 1995; Pongratz *et al.* 1991). TPA treatment has been shown to decrease DNA binding as well via EMSA (Berghard *et al.* 1993; Okino *et al.* 1992). In contrast, Schafer *et. al.* showed DNA binding even when there was no measurable PKC activity in cytosol or after PKC inhibitor pretreatment as measured via EMSA (Schafer *et al.* 1993). The results of the DNA binding assay performed by Chen and Tukey are confounded by their use of staurosporine, the PKC inhibitor which is also an AhR ligand (Chen and Tukey 1996). The variable actions of TPA make interpretation of these data difficult. As such, the precise role of PKC in the AhR pathway is still under study.

There are numerous types of protein tyrosine kinases in the cell but they can be categorized into two major groups: receptor tyrosine kinases and non-receptor tyrosine kinases. Many growth factor receptors have intrinsic protein tyrosine kinase activity and are the prototypical model for this group. Ligand binding to most such receptors induces a conformational change leading to phosphorylation of several residues in its own cytosolic domain or on certain substrate proteins (Lowes *et al.* 2002). The

phosphorylated tyrosine residues are then recognized by intracellular signaling molecules to propagate the signal. General pathways that may be triggered include the MAPK pathway. Non-receptor protein tyrosine kinases are intermediate conductors of diverse intracellular signaling pathways. Many are associated with transmembrane receptors, such as hormone receptors or growth factor receptors, and they may be activated by such receptors. The Src protein is a classic example of the non-receptor tyrosine kinases (Tatosyan and Mizenina 2000). The members of the Src family are divided into two classes: tyrosine kinases with a broad expression range (Fyn, Yes) and those with limited expression (Fgr, Lyn, Hck, Lck, Blk, Yrc). The proteins of this group, ranging in molecular mass from 52 to 62 kD, contain six distinct functional domains: Src homology domain 4 (SH4), a unique domain, SH3 domain, SH2 domain, a catalytic domain (SH1), and a C-terminal regulatory region.

The relationship between tyrosine phosphorylation and the AhR pathway has been under study since at least 1994. Src kinase has been shown to be physically associated with the AhR in cytosol from guinea pig and mice adipocytes (Enan and Matsumura 1996) as well as in isolated cytosol under cell-free conditions or with the Hsp 90 (Hutchison *et al.* 1992; Whitelaw *et al.* 1991). In vivo, a single dose of TCDD in Macaques increased the activity of c-Src and protein tyrosine kinases in endocervical epithelium and increased the DNA binding activity of AP-1 (Enan *et al.* 1998b). In vitro, TCDD has been shown to increase levels of membrane c-Src and this translocation was abolished with the application of geldanamycin, which disrupts cytosolic heat shock protein association/s with AhR and Src (Kohle *et al.* 1999). However, Enan et al. found that the TCDD-mediated induction of CYP1A1 is independent of the c-Src mediated

pathway in c-Src (-/-) mice (Enan *et al.* 1998a). As such, the necessity of c-Src in this process is not clear and may not be obligatory.

There is also a body of evidence supporting a role of general tyrosine phosphorylation in the AhR pathway/constituents (Backlund *et al.* 1997; Carlson and Perdew 2002; Dieter *et al.* 2001; Gradin *et al.* 1994; Lemaire *et al.* 2004; Park *et al.* 2000). However the precise mechanism these phosphorylations may play is still under study. Two recent papers by Minsavage et al. reveal a very interesting role for tyrosine residues (Minsavage *et al.* 2004; Minsavage *et al.* 2003). It now appears that tyrosine residues are required for AhR activity, but in a different mechanism than initially suspected. The conserved AhR tyrosine 9 is not itself a phosphorylated residue, but is required for DRE binding (Minsavage *et al.* 2004). Mutation of this residue prevents necessary serine/threonine phosphorylation, possibly by PKC, on the AhR. As such, this tyrosine residue maintains proper conformation of the AhR thus allowing for critical phosphorylation events elsewhere. How this relates to the confirmed tyrosine phosphoresidues on the AhR is still unclear, and what direct role those phosphoresidues play remains to be determined. It is possible that the tyrosine phosphorylation is constitutive and as such primarily helps in maintaining proper posttranslational conformation of the AhR. This would explain why inhibiting tyrosine phosphorylation on the AhR has been shown to reduce CYP1A1 induction (Gradin *et al.* 1994).

Nuclear Posttranslational Events

In addition to the constitutive and/or inducible posttranslational events occurring in the cytosol, there are a multitude of modifications within the nuclear compartment to

proteins involved in the AhR pathway. Some may be important for maintaining proper conformation of the proteins, but some may also be in response to ligand. Additionally, chromatin modification in response to ligand is crucial to the transcriptional process.

Chromatin remodeling is crucial for the transcription of many genes. In the eukaryotic nucleus, DNA is tightly compacted into a nucleoprotein complex referred to as chromatin. Chromatin consists of repeated units called nucleosomes. Nucleosomes are an octameric core of the histone proteins H2A, H2B, H3, and H4. DNA is wrapped around the nucleosome twice (approximately 80 bp/turn) in a left-handed superhelix. The nucleosomes are then tightly coiled around each other in an ordered fashion. This organization is not just structural, but allows for the precise control of gene transcription. Genes wrapped tightly in chromatin are not accessible to transcription factors and are thus repressed. In order for transcription to take place, certain enzymes, transcription factors, activators, coactivators, etc. must somehow alter the structure of the chromatin, transforming it into an open conformation allowing for full access of the transcriptional machinery. The structure of the CYP1A1 gene is no exception to this process: the enhancer and promoter region are tightly bound in a nucleosomal configuration constitutively, and a series of not fully understood events must take place in order for transcription to occur.

One of the first papers to study the role of chromatin in CYP1A1 gene transcription used ligation-mediated PCR to analyze dioxin-induced changes in protein-DNA interactions and chromatin structure of the CYP1A1 enhancer-promoter region (Okino and Whitlock 1995). Upon binding of the AhR/ARNT complex to the DRE in the

enhancer region, there was a localized (~200 bp) alteration in chromatin structure resulting in increased accessibility of the DNA. Interestingly, these changes in the enhancer region must somehow be transmitted to the distant promoter region by a distinct mechanism other than AhR/ARNT binding.

Frequently, transcription is accompanied by the addition of acetyl (CH_3CO) to histone tails. Such additions may neutralize the positively charged tails, which could disrupt the interaction of tails with negatively charged DNA and free TATA boxes from nucleosomes thus initiating transcription (Xu *et al.* 1997). This process is mediated by histone acetyltransferase and deacetylase. Trichostatin A (TSA) is a specific inhibitor of histone deacetylase, thus allowing for hyperacetylation of chromatin, maintaining it in an open conformation. The addition of TSA to TCDD treated primary rat hepatocyte cultures has been shown to result in superinduction of CYP1A1 (Xu *et al.* 1997). A similar response has been found in our laboratory with the addition of TSA to H4IIE cells. H4IIE cells were treated with DMSO, 2.5 x 10^{-8} M PCB 126, PCB + 0.5, 1, or 2 μM TSA for 16 h and CYP1A1 protein was measured via flow cytometry as described in previous chapters. The addition of TSA to the PCB treatment increased the % of cells expressing CYP1A1 by around 13% (Figures 4.3a, b) As such, it would appear that histone acetylation must play some role in CYP1A1 induction and that the AhR/ARNT complex may recruit some molecule with acetyltransferase activity. In fact, several coactivators with such activity have now been shown to be recruited (Kumar and Perdew 1999). Beischlag et al. have shown a role for the SRC family of coactivators in TCDD-dependent gene regulation (Beischlag *et al.* 2002). The nuclear receptor coactivator/steroid receptor coactivator (NCoA/SRC/p160) family of proteins has been

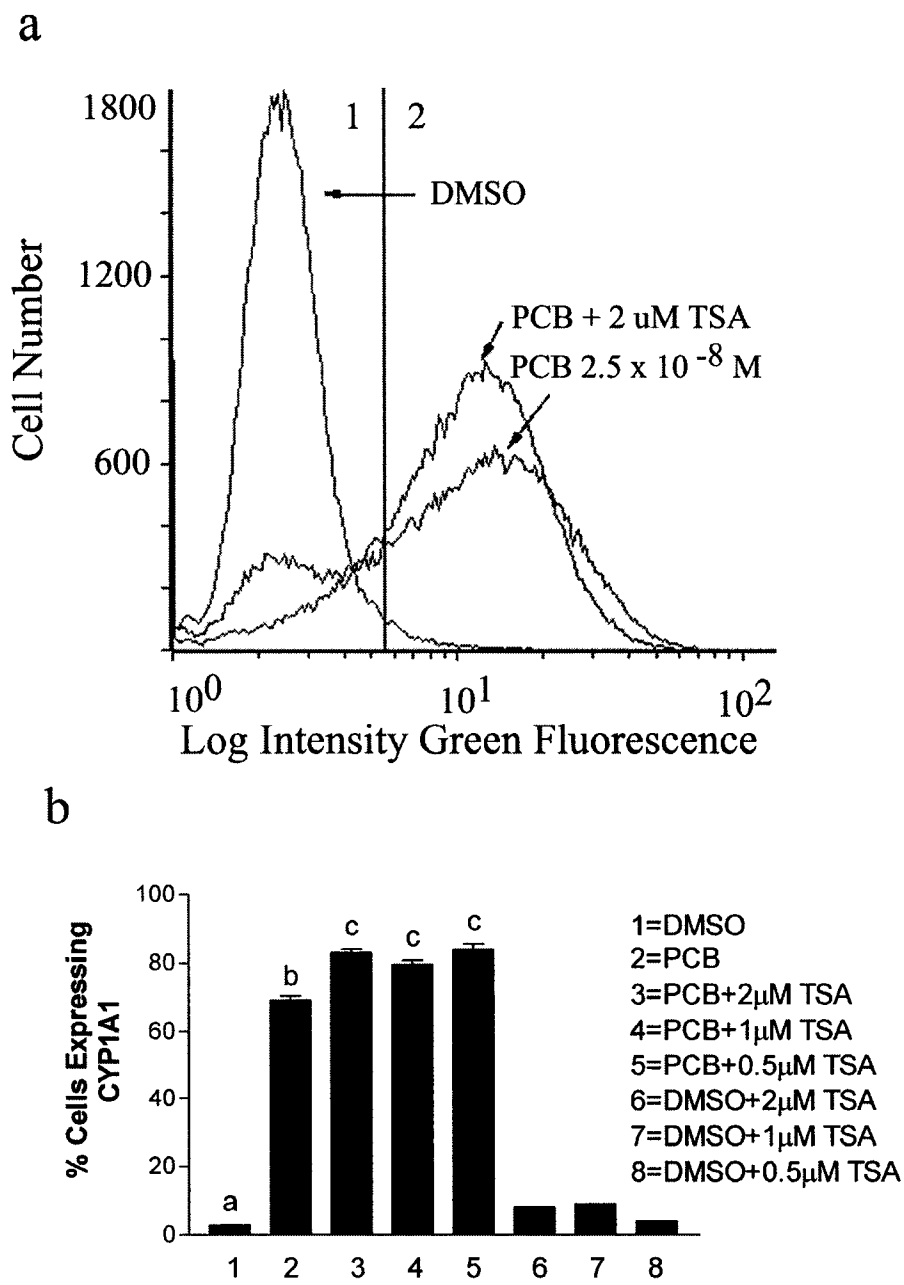

Figure 4.3a, b. TSA Treatment and CYP1A1 Flow Cytometry. H4IIE cells were treated with DMSO, 2.5 x 10^{-8} M PCB 126, PCB + 0.5, 1, or 2 μM TSA for 16 h and CYP1A1 protein was measured via flow cytometry as described in previous chapters. **a)** Histogram overlay showing the distribution of CYP1A1. Cells within region 1 do not express CYP1A1 and cells within region 2 are positive for CYP1A1. TSA treatment increased the number of cells positive for CYP1A1. **b)** % cells expressing CYP1A1 after indicated treatments. Bars with different letters are significantly different ($p<.001$).

shown to play a dual role by forming a "bridge" between several classes of transcription factors and the core transcription initiation complex as well as facilitating a more open chromatin conformation via their intrinsic histone acetyltransferase activities. It was shown that ARNT is capable of interacting with SRC-1 and NCoA-2, while the AhR interacts with all three coactivator proteins, the third being p/CIP. These proteins enhance AhR/ARNT mediated transactivation and associate with an AhR/ARNT regulated enhancer region in a dioxin dependent fashion. There are several other coactivators that have been implicated in dioxin mediated chromatin remodeling, including TRAP/DRIP/ARC/human Mediator (Wang *et al.* 2004) and Brahma/SWI2-related Gene 1 protein (Wang and Hankinson 2002) which all contain ATPase activity, in addition to a number of other basal transcription factors (Swanson 2002).

Much research is still being done in the field of chromatin remodeling and the role it plays in CYP1A1 induction, and a key technique being employed is the chromatin immunoprecipitation assay or ChIP assay. Following treatment under conditions in which the gene of interest is transcriptionally affected, nuclear protein:DNA complexes are cross-linked with one percent formaldehyde. Nuclei are then isolated and the DNA is sheared. After DNA fragmentation, chromatin immunoprecipitation is achieved using the appropriate modification-specific histone antibody. The crosslinking is then reversed and the DNA is purified and quantified. Finally, the enriched DNA sequences are examined for regions of interest, generally by PCR. This powerful technique allows one to test for specific chromatin modifications in specific regions of the DNA.

There are many types of chromatin modifications (acetylation, phosphorylation, methylation, ribosylation, ubiquitination, glycosylation) and a multitude of mediators in this process. However, one intriguing possibility is the capability of PKC to phosphorylate histones (Bauer *et al.* 2001). Alternatively, inhibition of histone acetyltransferase function of p300 by PKC delta has been shown, and may represent a signal transduction pathway by which PKC delta may inhibit cell growth and promote cellular differentiation (Yuan *et al.* 2002). The role of PKC in this process needs further study.

In addition to chromatin modification, other nuclear proteins involved in the AhR pathway also undergo crucial changes during the activation process. ARNT, the nuclear binding partner for the AhR, is also a phosphoprotein. Treatment of ARNT with nonspecific acid phosphatase has been shown to eliminate AhR/ARNT heterodimerization (Berghard *et al.* 1993). The pattern of charge heterogeneity of ARNT is further changed upon binding with the AhR, indicating some further modifications (Tsai and Perdew 1997). Further, MAPK-mediated ARNT phosphorylation can lead to the transcriptional activation of either ARNT-ARNT homodimers or ARNT-AhR heterodimers (Tan *et al.* 2004), linking serine/threonine phosphorylation of ARNT to its activity. There is no direct evidence showing tyrosine phosphorylation on ARNT at this point.

In addition to the AhR pathway being affected by a variety of signal transduction pathways, there are also a variety of coregulators that further modulate this pathway. The term "coregulator" encompasses transcriptional coactivators and corepressors. Some of these coregulators include universal basal transcription factors, coactivators that also

regulate the activity of other receptor mediated pathways, and AhR pathway specific repressor proteins. It is clear that some of these coregulators are necessary for successful AhR mediated transcription, and some simply increase the level of transcription. The mode of activation for these coregulators is not entirely known, and the full mechanistic role that they play is still under study. Many of these coregulators play a major role in chromatin remodeling. In general, there are two types of chromatin remodeling factors/complexes: those that have histone acetyltransferase (HAT) activity (acetylators), and those that utilize ATP to disrupt histone-DNA intereactions (phosphorylators). Table 4.1 outlines most of the known coregulators involved in the AhR pathway and is adapted from a review (Carlson and Perdew 2002). Some of the coregulators directly bind to AhR, ARNT, or possibly both.

Not all of these coregulators have been identified or studied in all tissues, and it is likely that not all of them play a role in AhR mediated transcription in all tissues. It is possible that the differential activation of a particular set of coregulators may play a role in modulating transcription in a cell/tissue specific basis. These factors, in addition to differential activation of signal transduction pathways, may further contribute to the hybrid switch response of the AhR pathway. As such, it is possible that there are multiple "activation modules" that may be turned on within a cell. The stochastic nature of molecular interactions within the cell may contribute to the subtle variability in response, depending on which factors (signal transduction pathways or coregulators) are activated. An overall schematic of the AhR pathway, signal transduction pathways activated, and the nuclear interactions between these events and coregulators can be seen in figure 4.4.

Table 4.1. Coregulators Involved in the AhR Pathway

BRG-1 coactivator	(Wang and Hankinson 2002)
RIP 140 coactivator	(Kumar *et al.* 1999)
p300/CBP coactivator	(Kobayashi *et al.* 1997)
SRC-1, NCoA-2, pCIP coactivator	(Beischlag *et al.* 2002; Kumar and Perdew 1999)
ERAP 140 coactivator	(Nguyen *et al.* 1999)
Mediator Complex (Med 220) adaptor	(Wang *et al.* 2004)
P-TEFb basal transcriptional activator	(Tian *et al.* 2003)
Sp1 basal transcription factor (TF)	(Wang *et al.* 1999)
TFIIB, TFIIE, TBP basal TFs	(Rowlands *et al.* 1996; Swanson and Yang 1998)
SMRT corepressor	(Nguyen *et al.* 1999)
SHP corepressor	(Klinge *et al.* 2001)
AhR repressor	(Mimura *et al.* 1999)
ARNT repressor	(Gradin *et al.* 1999)

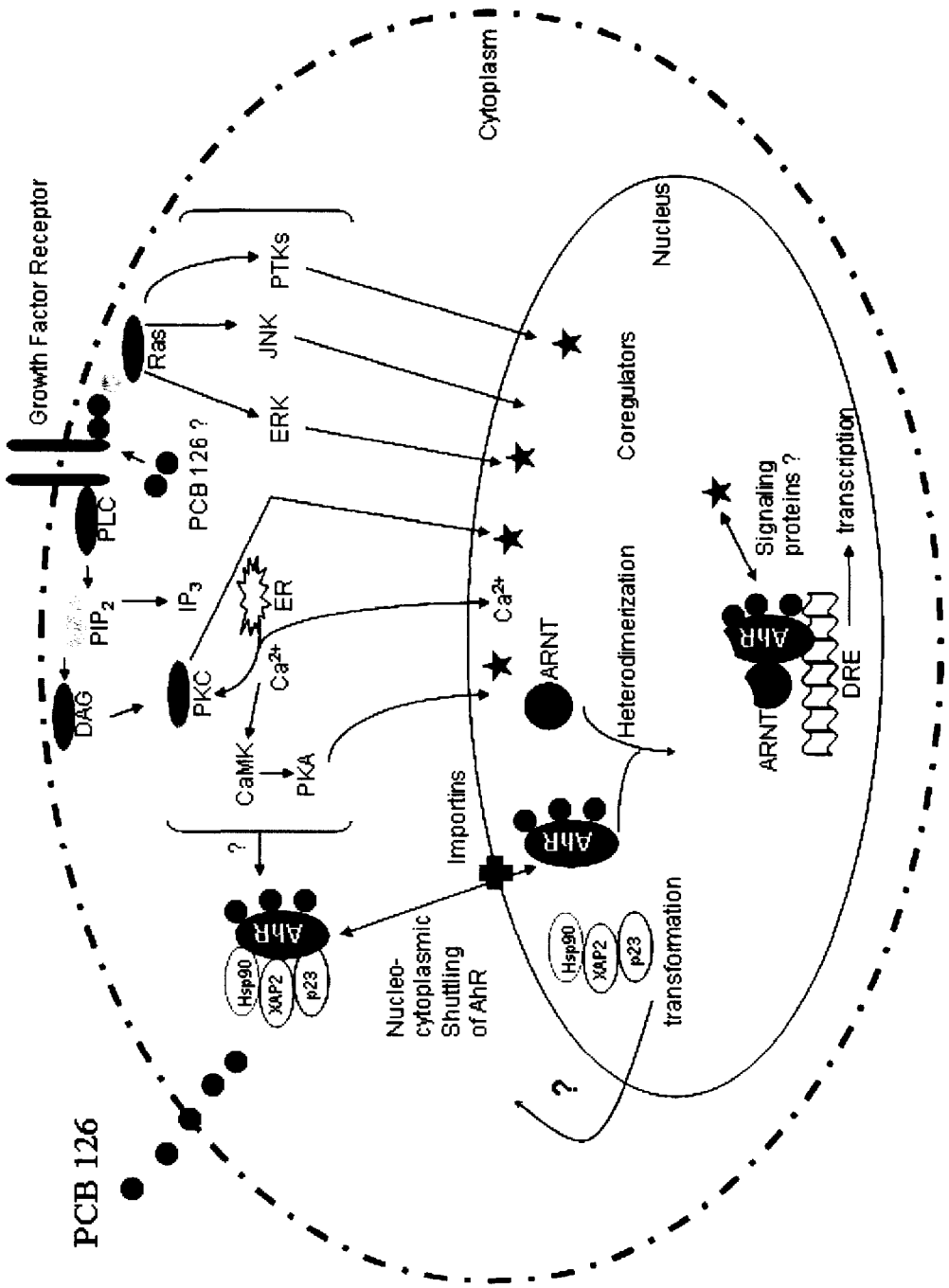

Figure 4.4 Model of AhR Pathway

The following is a hypothetical description of the details of the AhR pathway. PCB 126 enters the cell and binds to the AhR. Simultaneously, PCB 126 activates the intracellular surface of the growth factor receptor. The downstream effects include activation of multiple pathways, including PKC, PKA, ERK, JNK, and protein tyrosine kinases. These cascades may directly affect the cytosolic AhR complex, or the signal may be propagated to the nucleus where it may activate other signaling proteins, coregulators, transcription factors or may directly affect ARNT. Upon entry of ligand bound AhR into the nucleus, it dissociates from its partner proteins and heterodimerizes with ARNT. Upon binding to multiple coregulators, this complex binds to the dioxin response element (DRE), and further basal transcription factors and coregulators are recruited. The chromatin is fully transformed into its open conformation. At this point all factors required for transcription have been assembled and transcription may begin. Depending on which "activation module" is activated, transcription will proceed at a preset rate. For example, in the H4IIE cells it does not appear that the ERK or JNK pathways are activated in response to PCB 126, but inhibition of PKC greatly reduces transcription. One could hypothesize, that in this system, the primary activation module is PKC, not ERK or JNK. Therefore, only coregulators activated by PKC (or its downstream effects) will be turned on in this scenario and transcription will proceed at a rate determined by these particular coregulators. Other scenarios might include activation of the ERK and/or JNK cascade, PKA, and/or protein tysosine kinases. Differential activation of these signaling cascades would recruit a unique assembly of coregulators. This modulation of the AhR pathway may, in part, account for some of the tissue specific effects observed throughout the literature.

Mechanism for the Hybrid Switch

How might these proposed activation modules play a part in the hybrid switch response? What constitutes the switch and what mechanism allows for a graded response thereafter? First, there are a few assumptions that must be made clear to the reader. It is likely that the amount of AhR present is not a limiting factor in the H4IIE cells, as the Hepa 1c1c7 cells contain 100 times as much AhR (Holmes and Pollenz 1997), but display about 20 times less CYP1A1 induction (Broccardo *et al.* 2004). A similar argument holds true for ARNT: Hepa 1c1c7 cells contain twice as much ARNT as the H4IIE cells (Holmes and Pollenz 1997). Therefore, it is not likely that AhR or ARNT are limiting factors in this pathway given the lack of a relationship between their levels and CYP1A1 induction.

It is often assumed that the level of binding to a receptor is directly related to the level of gene induction. Such a relationship assumes a linear relationship between receptor occupancy and biological response (Poland 1996). However, it was noted that not all systems responded in this clear, hypothetical manner. It was proposed that there may, in fact, be a threshold response that reflects biological inertia of the response. Below this threshold, there is no response to the ligand-receptor interactions and not all relationships between fractional receptor occupancy and biological response are linear (Ariens 1954; Ariens and Beld 1977).

Now several assumptions have been established: that the AhR and ARNT are probably not limiting in this system, and that the relationship between receptor occupancy and response is not always linear. Several mechanistic models for the hybrid switch response will now be discussed. The first model is reliant on the fact that, 1) a

certain number of receptors must be occupied before the pathway is activated and 2) that the crucial signaling cascade/s has been initiated. These events constitute the initial switch. Once these events have occurred, the sufficiently activated AhR-ligand complex will then enter the nucleus. Depending on which signaling pathways were activated in the cytosol, there will be differential recruitment of nuclear coregulators, which will result in a preset rate of transcription. Each cell may respond slightly differently, generating a graded response at the population level. Some coregulators are not inherently necessary, but greatly increase the rate of transcription and, as such, make this scenario plausible (Carlson and Perdew 2002; Kumar and Perdew 1999; Swanson 2002; Swanson and Yang 1998).

Another scenario would place the switch at the level of the chromatin. Until the chromatin has been remodeled into its open conformation, transcription cannot take place. The graded response could then be explained by receptor occupancy: the more AhR-ligand complex bound to the DREs, the more transcription. This is also a quite plausible explanation, and relies on signal transduction cascades and the nuclear AhR complex itself to remodel the chromatin. Notably, it has been shown that once the chromatin is transformed to its open conformation, it remains open throughout transcription, and is not continuously cycling between an open and closed state (Morgan and Whitlock 1992).

It is also possible that the switch may be a single obligatory event. This event could be a signaling cascade mediated event, a binding/dissociation event, or some other unidentified event. Whatever it may be, until this takes place the cell is in the off state.

When the cell is switched on, the graded response could result from the mechanisms described above or simply due to biological variation and stochasticity.

Future Directions

Finding the exact location of the switch is not an easy scientific task. The approach we have taken is to first identify pathways that are important to PCB 126 mediated CYP1A1 induction. Using an inhibitor, we identified that the PKC pathway appears to play a major role in this system. It appears that basal PKC activity may be crucial to the full activation of the AhR pathway, as PCB 126 did not induce membrane translocation or increase PKC kinase activity. Further experiments could be planned to further study the precise role of PKC in this system.

On a larger scale, what experiments could be performed to further identify the switch and/or important modulating factors? A key technique to solving this problem would be to sort the on and off cells for CYP1A1 induction, and further observe what is different between the two populations. Unfortunately, we have attempted and been unsuccessful at this approach. If we could transfect the H4IIE cells with a green fluorescent protein (GFP) construct attached to a DRE sequence we could directly measure activation of the AhR pathway and use the GFP as a surrogate for CYP1A1 expression. The primary problems with this approach are that 1) existing constructs are for mouse (not rat) and 2) even if the construct were to enter the nucleus, it is unknown whether chromatin would be incorporated into an artificial construct and thus be biologically representative. If a rat construct were to be generated, and it would enter the

nucleus and incorporate chromatin, then it would be an excellent model and could be extensively utilized.

In order to identify specific modifications (like phosphorylation or acetylation) on particular stretches of chromatin, the ChIP assay may be performed. There are several modifications that have been linked to TCDD, and provide as an excellent starting point for research. Both TCDD and TSA (Trichostatin A) have been shown to increase acetylated H4 in the TATA box and DRE of CYP1A1 in Hepa 1c1c7 cells (Ke *et al.* 2001; Shibazaki *et al.* 2004). PKC and TPA have been shown to phosphorylate histone H1. This effect is likely via a novel or atypical PKC, not a conventional PKC (Ventura and Maioli 2001). It has been shown that TCDD preferentially increases the protein expression, kinase activity and induces the sub-cellular redistribution of PKC delta, a novel PKC activated by DAG (Williams *et al.* 2004) and this isoform has been shown to be present in H4IIE cells (Chapter 3). As such, both of these modifications would be worth considering in the ChIP assay. Ideally, one would be able to perform this assay on live cells sorted for CYP1A1 expression, as this would allow for identification of any histone modification differences.

In conclusion, this research has further verified the hybrid switch response in the H4IIE rat hepatoma cell line, and identified PKC as an important player in this response. This is a unique example of biological switching in the field of toxicology. As toxicologists, it is imperative that we continue to integrate our field with mainstream biological theories and techniques. In doing so, toxicologists could provide a unique, applied outlook to the basic sciences.

REFERENCES

Adachi, J., Mori, Y., Matsui, S., Takigami, H., Fujino, J., Kitagawa, H., Miller, C. A., 3rd, Kato, T., Saeki, K., and Matsuda, T. (2001). Indirubin and indigo are potent aryl hydrocarbon receptor ligands present in human urine. *J Biol Chem* **276**, 31475-8.

Andersen, M. E., Mills, J. J., Jirtle, R. L., and Greenlee, W. F. (1995). Negative selection in hepatic tumor promotion in relation to cancer risk assessment. *Toxicology* **102**, 223-37.

Andrieux, L., Langouet, S., Fautrel, A., Ezan, F., Krauser, J. A., Savouret, J. F., Guengerich, F. P., Baffet, G., and Guillouzo, A. (2004). Aryl Hydrocarbon Receptor Activation and Cytochrome P450 1A Induction by the Mitogen-Activated Protein Kinase Inhibitor U0126 in Hepatocytes. *Mol Pharmacol* **65**, 934-43.

Ariens, E. J. (1954). Affinity and intrinsic activity in the theory of competitive inhibition. Part 1. Problems and theory. *Arch. Int. Pharmacol.* **99**, 32-49.

Ariens, E. J., and Beld, A. J. (1977). Commentary: The receptor concept in evolution. *Biochem Pharmacol* **26**, 913-8.

Backlund, M., Johansson, I., Mkrtchian, S., and Ingelman-Sundberg, M. (1997). Signal transduction-mediated activation of the aryl hydrocarbon receptor in rat hepatoma H4IIE cells. *J Biol Chem* **272**, 31755-63.

Bager, Y., Kato, Y., Kenne, K., and Warngard, L. (1997). The ability to alter the gap junction protein expression outside GST-P positive foci in liver of rats was associated to the tumour promotion potency of different polychlorinated biphenyls. *Chem Biol Interact* **103**, 199-212.

Bars, R. G., and Elcombe, C. R. (1991). Dose-dependent acinar induction of cytochromes P450 in rat liver. Evidence for a differential mechanism of induction of P450IA1 by beta-naphthoflavone and dioxin. *Biochem J* **277**, 577-80.

Bars, R. G., Mitchell, A. M., Wolf, C. R., and Elcombe, C. R. (1989). Induction of cytochrome P-450 in cultured rat hepatocytes. The heterogeneous localization of specific isoenzymes using immunocytochemistry. *Biochem J* **262**, 151-8.

Bauer, P. I., Buki, K. G., and Kun, E. (2001). Selective augmentation of histone H1 phosphorylation sites by interaction of poly(ADP-ribose) polymerase and cdc2-kinase: comparison with protein kinase C. *Int J Mol Med* **8**, 691-3.

Beischlag, T. V., Wang, S., Rose, D. W., Torchia, J., Reisz-Porszasz, S., Muhammad, K., Nelson, W. E., Probst, M. R., Rosenfeld, M. G., and Hankinson, O. (2002). Recruitment of the NCoA/SRC-1/p160 family of transcriptional coactivators by the aryl hydrocarbon receptor/aryl hydrocarbon receptor nuclear translocator complex. *Mol Cell Biol* **22**, 4319-33.

Berg, O. G., Paulsson, J., and Ehrenberg, M. (2000). Fluctuations in repressor control: thermodynamic constraints on stochastic focusing. *Biophys J* **79**, 2944-53.

Berghard, A., Gradin, K., Pongratz, I., Whitelaw, M., and Poellinger, L. (1993). Cross-coupling of signal transduction pathways: the dioxin receptor mediates induction of cytochrome P-450IA1 expression via a protein kinase C-dependent mechanism. *Mol Cell Biol* **13**, 677-89.

Bhalla, U. S., and Iyengar, R. (1999). Emergent properties of networks of biological signaling pathways. *Science* **283**, 381-7.

Bhalla, U. S., Ram, P. T., and Iyengar, R. (2002). MAP kinase phosphatase as a locus of flexibility in a mitogen-activated protein kinase signaling network. *Science* **297**, 1018-23.

Biggar, S. R., and Crabtree, G. R. (2001). Cell signaling can direct either binary or graded transcriptional responses. *Embo J* **20**, 3167-76.

Blankenship, A., and Matsumura, F. (1997). 2,3,7,8-Tetrachlorodibenzo-p-dioxin-induced activation of a protein tyrosine kinase, pp60src, in murine hepatic cytosol using a cell-free system. *Mol Pharmacol* **52**, 667-75.

Britten, R. J., and Davidson, E. H. (1969). Gene regulation for higher cells: a theory. *Science* **165**, 349-57.

Broccardo, C. J., Billings, R. E., Chubb, L. S., Andersen, M. E., and Hanneman, W. H. (2004). Single Cell Analysis of Switch-Like Induction of CYP1A1 in Liver Cell Lines. *Toxicol Sci* **78**, 287-94.

Carey, M. (1998). The enhanceosome and transcriptional synergy. *Cell* **92**, 5-8.

Carlson, D. B., and Perdew, G. H. (2002). A dynamic role for the Ah receptor in cell signaling? Insights from a diverse group of Ah receptor interacting proteins. *J Biochem Mol Toxicol* **16**, 317-25.

Chen, Y. H., Riby, J., Srivastava, P., Bartholomew, J., Denison, M., and Bjeldanes, L. (1995). Regulation of CYP1A1 by indolo[3,2-b]carbazole in murine hepatoma cells. *J Biol Chem* **270**, 22548-55.

Chen, Y. H., and Tukey, R. H. (1996). Protein kinase C modulates regulation of the CYP1A1 gene by the aryl hydrocarbon receptor. *J Biol Chem* **271**, 26261-6.

Cheung, P., Allis, C. D., and Sassone-Corsi, P. (2000a). Signaling to chromatin through histone modifications. *Cell* **103**, 263-71.

Cheung, P., Tanner, K. G., Cheung, W. L., Sassone-Corsi, P., Denu, J. M., and Allis, C. D. (2000b). Synergistic coupling of histone H3 phosphorylation and acetylation in response to epidermal growth factor stimulation. *Mol Cell* **5**, 905-15.

Cogliano, V. J. (1998). Assessing the cancer risk from environmental PCBs. *Environ Health Perspect* **106**, 317-23.

Dieter, M. Z., Freshwater, S. L., Solis, W. A., Nebert, D. W., and Dalton, T. P. (2001). Tryphostin AG879, a tyrosine kinase inhibitor: prevention of transcriptional activation of the electrophile and the aromatic hydrocarbon response elements. *Biochem Pharmacol* **61**, 215-25.

Enan, E., Dunlap, D. Y., and Matsumura, F. (1998a). Use of c-Src and c-Fos knockout mice for the studies on the role of c-Src kinase signaling in the expression of toxicity of TCDD. *J Biochem Mol Toxicol* **12**, 263-74.

Enan, E., El-Sabeawy, F., Scott, M., Overstreet, J., and Lasley, B. (1998b). Alterations in the growth factor signal transduction pathways and modulators of the cell cycle in

endocervical cells from macaques exposed to TCDD. *Toxicol Appl Pharmacol* **151**, 283-93.

Enan, E., and Matsumura, F. (1996). Identification of c-Src as the integral component of the cytosolic Ah receptor complex, transducing the signal of 2,3,7,8-tetrachlorodibenzo-p-dioxin (TCDD) through the protein phosphorylation pathway. *Biochem Pharmacol* **52**, 1599-612.

English, J., Pearson, G., Wilsbacher, J., Swantek, J., Karandikar, M., Xu, S., and Cobb, M. H. (1999). New insights into the control of MAP kinase pathways. *Exp Cell Res* **253**, 255-70.

Estabrook, R. W. (1996). The remarkable P450s: a historical overview of these versatile hemeprotein catalysts. *Faseb J* **10**, 202-4.

Ferrell, J. E., Jr. (1996). Tripping the switch fantastic: how a protein kinase cascade can convert graded inputs into switch-like outputs. *Trends Biochem Sci* **21**, 460-6.

Ferrell, J. E., Jr., and Machleder, E. M. (1998). The biochemical basis of an all-or-none cell fate switch in Xenopus oocytes. *Science* **280**, 895-8.

Ferrell, J. E., and Xiong, W. (2001). Bistability in cell signaling: How to make continuous processes discontinuous, and reversible processes irreversible. *Chaos* **11**, 227-236.

Fiering, S., Northrop, J. P., Nolan, G. P., Mattila, P. S., Crabtree, G. R., and Herzenberg, L. A. (1990). Single cell assay of a transcription factor reveals a threshold in transcription activated by signals emanating from the T-cell antigen receptor. *Genes Dev* **4**, 1823-34.

Fiering, S., Whitelaw, E., and Martin, D. I. (2000). To be or not to be active: the stochastic nature of enhancer action. *Bioessays* **22**, 381-7.

Fischle, W., Wang, Y., and Allis, C. D. (2003). Binary switches and modification cassettes in histone biology and beyond. *Nature* **425**, 475-9.

French, C. T., Hanneman, W. H., Chubb, L. S., Billings, R. E., and Andersen, M. E. (2004). Induction of CYP1A1 in Primary Rat Hepatocytes by 3,3',4,4',5-Pentachlorobiphenyl: Evidence for a Switch Circuit Element. *Toxicol Sci* **78**, 276-86.

Frueh, F. W., Hayashibara, K. C., Brown, P. O., and Whitlock, J. P., Jr. (2001). Use of cDNA microarrays to analyze dioxin-induced changes in human liver gene expression. *Toxicol Lett* **122**, 189-203.

Fujisawa-Sehara, A., Sogawa, K., Yamane, M., and Fujii-Kuriyama, Y. (1987). Characterization of xenobiotic responsive elements upstream from the drug-metabolizing cytochrome P-450c gene: a similarity to glucocorticoid regulatory elements. *Nucleic Acids Res* **15**, 4179-91.

Georgel, P. T., Tsukiyama, T., and Wu, C. (1997). Role of histone tails in nucleosome remodeling by Drosophila NURF. *Embo J* **16**, 4717-26.

Goldbeter, A., and Koshland, D. E., Jr. (1984). Ultrasensitivity in biochemical systems controlled by covalent modification. Interplay between zero-order and multistep effects. *J Biol Chem* **259**, 14441-7.

Gradin, K., Toftgard, R., Poellinger, L., and Berghard, A. (1999). Repression of dioxin signal transduction in fibroblasts. Identification Of a putative repressor associated with Arnt. *J Biol Chem* **274**, 13511-8.

Gradin, K., Whitelaw, M. L., Toftgard, R., Poellinger, L., and Berghard, A. (1994). A tyrosine kinase-dependent pathway regulates ligand-dependent activation of the dioxin receptor in human keratinocytes. *J Biol Chem* **269**, 23800-7.

Hanneman, W. H., Legare, M. E., Barhoumi, R., Burghardt, R. C., Safe, S., and Tiffany-Castiglioni, E. (1996). Stimulation of calcium uptake in cultured rat hippocampal neurons by 2,3,7,8-tetrachlorodibenzo-p-dioxin. *Toxicology* **112**, 19-28.

Hazzalin, C. A., and Mahadevan, L. C. (2002). MAPK-regulated transcription: a continuously variable gene switch? *Nat Rev Mol Cell Biol* **3**, 30-40.

Hestermann, E. V., Stegeman, J. J., and Hahn, M. E. (2000). Relative contributions of affinity and intrinsic efficacy to aryl hydrocarbon receptor ligand potency. *Toxicol Appl Pharmacol* **168**, 160-72.

Hidaka, H., Inagaki, M., Kawamoto, S., and Sasaki, Y. (1984). Isoquinolinesulfonamides, novel and potent inhibitors of cyclic nucleotide dependent protein kinase and protein kinase C. *Biochemistry* **23**, 5036-41.

Hoffer, A., Chang, C. Y., and Puga, A. (1996). Dioxin induces transcription of fos and jun genes by Ah receptor-dependent and -independent pathways. *Toxicol Appl Pharmacol* **141**, 238-47.

Holmes, J. L., and Pollenz, R. S. (1997). Determination of aryl hydrocarbon receptor nuclear translocator protein concentration and subcellular localization in hepatic and nonhepatic cell culture lines: development of quantitative Western blotting protocols for calculation of aryl hydrocarbon receptor and aryl hydrocarbon receptor nuclear translocator protein in total cell lysates. *Mol Pharmacol* **52**, 202-11.

Huang, C. Y., and Ferrell, J. E., Jr. (1996). Ultrasensitivity in the mitogen-activated protein kinase cascade. *Proc Natl Acad Sci U S A* **93**, 10078-83.

Hume, D. A. (2000). Probability in transcriptional regulation and its implications for leukocyte differentiation and inducible gene expression. *Blood* **96**, 2323-8.

Hutchison, K. A., Brott, B. K., De Leon, J. H., Perdew, G. H., Jove, R., and Pratt, W. B. (1992). Reconstitution of the multiprotein complex of pp60src, hsp90, and p50 in a cell-free system. *J Biol Chem* **267**, 2902-8.

Kamakaka, R. T. (1997). Silencers and locus control regions: opposite sides of the same coin. *Trends Biochem Sci* **22**, 124-8.

Ke, S., Rabson, A. B., Germino, J. F., Gallo, M. A., and Tian, Y. (2001). Mechanism of suppression of cytochrome P-450 1A1 expression by tumor necrosis factor-alpha and lipopolysaccharide. *J Biol Chem* **276**, 39638-44.

Klinge, C. M., Jernigan, S. C., Risinger, K. E., Lee, J. E., Tyulmenkov, V. V., Falkner, K. C., and Prough, R. A. (2001). Short heterodimer partner (SHP) orphan nuclear receptor inhibits the transcriptional activity of aryl hydrocarbon receptor (AHR)/AHR nuclear translocator (ARNT). *Arch Biochem Biophys* **390**, 64-70.

Ko, M. S., Nakauchi, H., and Takahashi, N. (1990). The dose dependence of glucocorticoid-inducible gene expression results from changes in the number of transcriptionally active templates. *Embo J* **9**, 2835-42.

Kobayashi, A., Numayama-Tsuruta, K., Sogawa, K., and Fujii-Kuriyama, Y. (1997). CBP/p300 functions as a possible transcriptional coactivator of Ah receptor nuclear translocator (Arnt). *J Biochem (Tokyo)* **122**, 703-10.

Kohle, C., Gschaidmeier, H., Lauth, D., Topell, S., Zitzer, H., and Bock, K. W. (1999). 2,3,7,8-Tetrachlorodibenzo-p-dioxin (TCDD)-mediated membrane translocation of c-Src protein kinase in liver WB-F344 cells. *Arch Toxicol* **73**, 152-8.

Konishi, H., Yamauchi, E., Taniguchi, H., Yamamoto, T., Matsuzaki, H., Takemura, Y., Ohmae, K., Kikkawa, U., and Nishizuka, Y. (2001). Phosphorylation sites of protein kinase C delta in H2O2-treated cells and its activation by tyrosine kinase in vitro. *Proc Natl Acad Sci U S A* **98**, 6587-92.

Kumar, M. B., and Perdew, G. H. (1999). Nuclear receptor coactivator SRC-1 interacts with the Q-rich subdomain of the AhR and modulates its transactivation potential. *Gene Expr* **8**, 273-86.

Kumar, M. B., Tarpey, R. W., and Perdew, G. H. (1999). Differential recruitment of coactivator RIP140 by Ah and estrogen receptors. Absence of a role for LXXLL motifs. *J Biol Chem* **274**, 22155-64.

Laurent, M., and Kellershohn, N. (1999). Multistability: a major means of differentiation and evolution in biological systems. *Trends Biochem Sci* **24**, 418-22.

Lee, K. M., Sif, S., Kingston, R. E., and Hayes, J. J. (1999). hSWI/SNF disrupts interactions between the H2A N-terminal tail and nucleosomal DNA. *Biochemistry* **38**, 8423-9.

Lemaire, G., Delescluse, C., Pralavorio, M., Ledirac, N., Lesca, P., and Rahmani, R. (2004). The role of protein tyrosine kinases in CYP1A1 induction by omeprazole and thiabendazole in rat hepatocytes. *Life Sci* **74**, 2265-78.

Livak, K. J., and Schmittgen, T. D. (2001). Analysis of relative gene expression data using real-time quantitative PCR and the 2(-Delta Delta C(T)) Method. *Methods* **25**, 402-8.

Long, W. P., Chen, X., and Perdew, G. H. (1999). Protein kinase C modulates aryl hydrocarbon receptor nuclear translocator protein-mediated transactivation potential in a dimer context. *J Biol Chem* **274**, 12391-400.

Long, W. P., and Perdew, G. H. (1999). Lack of an absolute requirement for the native aryl hydrocarbon receptor (AhR) and AhR nuclear translocator transactivation domains in protein kinase C-mediated modulation of the AhR pathway. *Arch Biochem Biophys* **371**, 246-59.

Long, W. P., Pray-Grant, M., Tsai, J. C., and Perdew, G. H. (1998). Protein kinase C activity is required for aryl hydrocarbon receptor pathway-mediated signal transduction. *Mol Pharmacol* **53**, 691-700.

Louis, M., and Becskei, A. (2002). Binary and graded responses in gene networks. *Sci STKE* **2002**, PE33.

Lowes, V. L., Ip, N. Y., and Wong, Y. H. (2002). Integration of signals from receptor tyrosine kinases and g protein-coupled receptors. *Neurosignals* **11**, 5-19.

Ma, Q. (2001). Induction of CYP1A1. The AhR/DRE paradigm: transcription, receptor regulation, and expanding biological roles. *Curr Drug Metab* **2**, 149-64.

Mahon, M. J., and Gasiewicz, T. A. (1995). Ah receptor phosphorylation: localization of phosphorylation sites to the C-terminal half of the protein. *Arch Biochem Biophys* **318**, 166-74.

McGuire, J., Whitelaw, M. L., Pongratz, I., Gustafsson, J. A., and Poellinger, L. (1994). A cellular factor stimulates ligand-dependent release of hsp90 from the basic helix-loop-helix dioxin receptor. *Mol Cell Biol* **14**, 2438-46.

McKnight, S., and Tjian, R. (1986). Transcriptional selectivity of viral genes in mammalian cells. *Cell* **46**, 795-805.

Miller, C. A., 3rd (1997). Expression of the human aryl hydrocarbon receptor complex in yeast. Activation of transcription by indole compounds. *J Biol Chem* **272**, 32824-9.

Mimura, J., Ema, M., Sogawa, K., and Fujii-Kuriyama, Y. (1999). Identification of a novel mechanism of regulation of Ah (dioxin) receptor function. *Genes Dev* **13**, 20-5.

Minsavage, G. D., Park, S. K., and Gasiewicz, T. A. (2004). The Aryl hydrocarbon receptor (AhR) tyrosine 9, a residue that Is essential for AhR DNA binding activity, is not a phosphoresidue but augments AhR phosphorylation. *J Biol Chem.*

Minsavage, G. D., Vorojeikina, D. P., and Gasiewicz, T. A. (2003). Mutational analysis of the mouse aryl hydrocarbon receptor tyrosine residues necessary for recognition of dioxin response elements. *Arch Biochem Biophys* **412**, 95-105.

Morgan, J. E., and Whitlock, J. P., Jr. (1992). Transcription-dependent and transcription-independent nucleosome disruption induced by dioxin. *Proc Natl Acad Sci U S A* **89**, 11622-6.

Nebert, D. W., Roe, A. L., Dieter, M. Z., Solis, W. A., Yang, Y., and Dalton, T. P. (2000). Role of the aromatic hydrocarbon receptor and [Ah] gene battery in the oxidative stress response, cell cycle control, and apoptosis. *Biochem Pharmacol* **59**, 65-85.

Newlands, S., Levitt, L. K., Robinson, C. S., Karpf, A. B., Hodgson, V. R., Wade, R. P., and Hardeman, E. C. (1998). Transcription occurs in pulses in muscle fibers. *Genes Dev* **12**, 2748-58.

Newton, A. C. (2003). Regulation of the ABC kinases by phosphorylation: protein kinase C as a paradigm. *Biochem J* **370**, 361-71.

Nguyen, T. A., Hoivik, D., Lee, J. E., and Safe, S. (1999). Interactions of nuclear receptor coactivator/corepressor proteins with the aryl hydrocarbon receptor complex. *Arch Biochem Biophys* **367**, 250-7.

Ohmori, S., Sakai, N., Shirai, Y., Yamamoto, H., Miyamoto, E., Shimizu, N., and Saito, N. (2000). Importance of protein kinase C targeting for the phosphorylation of its substrate, myristoylated alanine-rich C-kinase substrate. *J Biol Chem* **275**, 26449-57.

Ohmori, S., Shirai, Y., Sakai, N., Fujii, M., Konishi, H., Kikkawa, U., and Saito, N. (1998). Three distinct mechanisms for translocation and activation of the delta subspecies of protein kinase C. *Mol Cell Biol* **18**, 5263-71.

Okino, S. T., Pendurthi, U. R., and Tukey, R. H. (1992). Phorbol esters inhibit the dioxin receptor-mediated transcriptional activation of the mouse Cyp1a-1 and Cyp1a-2 genes by 2,3,7,8-tetrachlorodibenzo-p-dioxin. *J Biol Chem* **267**, 6991-8.

Okino, S. T., and Whitlock, J. P., Jr. (1995). Dioxin induces localized, graded changes in chromatin structure: implications for Cyp1A1 gene transcription. *Mol Cell Biol* **15**, 3714-21.

Park, S., Henry, E. C., and Gasiewicz, T. A. (2000). Regulation of DNA binding activity of the ligand-activated aryl hydrocarbon receptor by tyrosine phosphorylation. *Arch Biochem Biophys* **381**, 302-12.

Peter Guengerich, F., Martin, M. V., McCormick, W. A., Nguyen, L. P., Glover, E., and Bradfield, C. A. (2004). Aryl hydrocarbon receptor response to indigoids in vitro and in vivo. *Arch Biochem Biophys* **423**, 309-16.

Petrulis, J. R., Kusnadi, A., Ramadoss, P., Hollingshead, B., and Perdew, G. H. (2003). The hsp90 Co-chaperone XAP2 alters importin beta recognition of the bipartite nuclear localization signal of the Ah receptor and represses transcriptional activity. *J Biol Chem* **278**, 2677-85.

Petrulis, J. R., and Perdew, G. H. (2002). The role of chaperone proteins in the aryl hydrocarbon receptor core complex. *Chem Biol Interact* **141**, 25-40.

Poland, A., and Knutson, J. C. (1982). 2,3,7,8-tetrachlorodibenzo-p-dioxin and related halogenated aromatic hydrocarbons: examination of the mechanism of toxicity. *Annu Rev Pharmacol Toxicol* **22**, 517-54.

Poland, A. D. (1996). Meeting report: receptor-acting xenobiotics and their risk assessment. *Drug Metab Dispos* **24**, 1385-8.

Pomerening, J. R., Sontag, E. D., and Ferrell, J. E., Jr. (2003). Building a cell cycle oscillator: hysteresis and bistability in the activation of Cdc2. *Nat Cell Biol* **5**, 346-51.

Pongratz, I., Stromstedt, P. E., Mason, G. G., and Poellinger, L. (1991). Inhibition of the specific DNA binding activity of the dioxin receptor by phosphatase treatment. *J Biol Chem* **266**, 16813-7.

Puga, A., Hoffer, A., Zhou, S., Bohm, J. M., Leikauf, G. D., and Shertzer, H. G. (1997). Sustained increase in intracellular free calcium and activation of cyclooxygenase-2 expression in mouse hepatoma cells treated with dioxin. *Biochem Pharmacol* **54**, 1287-96.

Puga, A., Nebert, D. W., and Carrier, F. (1992). Dioxin induces expression of c-fos and c-jun proto-oncogenes and a large increase in transcription factor AP-1. *DNA Cell Biol* **11**, 269-81.

Puga, A., Xia, Y., and Elferink, C. (2002). Role of the aryl hydrocarbon receptor in cell cycle regulation. *Chem Biol Interact* **141**, 117-30.

Reiners, J. J., Jr., Clift, R., and Mathieu, P. (1999). Suppression of cell cycle progression by flavonoids: dependence on the aryl hydrocarbon receptor. *Carcinogenesis* **20**, 1561-6.

Reiners, J. J., Jr., Lee, J. Y., Clift, R. E., Dudley, D. T., and Myrand, S. P. (1998). PD98059 is an equipotent antagonist of the aryl hydrocarbon receptor and inhibitor of mitogen-activated protein kinase kinase. *Mol Pharmacol* **53**, 438-45.

Reiners, J. J., Jr., Scholler, A., Bischer, P., Cantu, A. R., and Pavone, A. (1993). Suppression of cytochrome P450 Cyp1a-1 induction in murine hepatoma 1c1c7 cells by 12-O-tetradecanoylphorbol-13-acetate and inhibitors of protein kinase C. *Arch Biochem Biophys* **301**, 449-54.

Robertson, L. W., Espandiari, P., Lehmler, H. J., Pereg, D., Srinivasan, A., Tampal, N., Twaroski, T., Ludewig, G., Glauert, H. P., Arif, J., and Gupta, R. (2000). Metabolism and activation of polychlorinated biphenyls (PCBs). *Cent Eur J Public Health* **8 Suppl**, 14-5.

Ross, I. L., Browne, C. M., and Hume, D. A. (1994). Transcription of individual genes in eukaryotic cells occurs randomly and infrequently. *Immunol Cell Biol* **72**, 177-85.

Rossi, F. M., Kringstein, A. M., Spicher, A., Guicherit, O. M., and Blau, H. M. (2000). Transcriptional control: rheostat converted to on/off switch. *Mol Cell* **6**, 723-8.

Rowlands, J. C., McEwan, I. J., and Gustafsson, J. A. (1996). Trans-activation by the human aryl hydrocarbon receptor and aryl hydrocarbon receptor nuclear translocator proteins: direct interactions with basal transcription factors. *Mol Pharmacol* **50**, 538-48.

Rybin, V. O., Guo, J., Sabri, A., Elouardighi, H., Schaefer, E., and Steinberg, S. F. (2004). Stimulus-specific differences in protein kinase C delta localization and activation mechanisms in cardiomyocytes. *J Biol Chem* **279**, 19350-61.

Safe, S. (1984). Polychlorinated biphenyls (PCBs) and polybrominated biphenyls (PBBs): biochemistry, toxicology, and mechanism of action. *Crit Rev Toxicol* **13**, 319-95.

Safe, S. (1989). Polychlorinated biphenyls (PCBs): mutagenicity and carcinogenicity. *Mutat Res* **220**, 31-47.

Safe, S. (1990). Polychlorinated biphenyls (PCBs), dibenzo-p-dioxins (PCDDs), dibenzofurans (PCDFs), and related compounds: environmental and mechanistic

considerations which support the development of toxic equivalency factors (TEFs). *Crit Rev Toxicol* **21**, 51-88.

Safe, S. H. (1994). Polychlorinated biphenyls (PCBs): environmental impact, biochemical and toxic responses, and implications for risk assessment. *Crit Rev Toxicol* **24**, 87-149.

Santiago-Josefat, B., and Fernandez-Salguero, P. M. (2003). Proteasome inhibition induces nuclear translocation of the dioxin receptor through an Sp1 and protein kinase C-dependent pathway. *J Mol Biol* **333**, 249-60.

Santini, R. P., Myrand, S., Elferink, C., and Reiners, J. J., Jr. (2001). Regulation of Cyp1a1 induction by dioxin as a function of cell cycle phase. *J Pharmacol Exp Ther* **299**, 718-28.

Sassone-Corsi, P., Mizzen, C. A., Cheung, P., Crosio, C., Monaco, L., Jacquot, S., Hanauer, A., and Allis, C. D. (1999). Requirement of Rsk-2 for epidermal growth factor-activated phosphorylation of histone H3. *Science* **285**, 886-91.

Savouret, J. F., Antenos, M., Quesne, M., Xu, J., Milgrom, E., and Casper, R. F. (2001). 7-ketocholesterol is an endogenous modulator for the arylhydrocarbon receptor. *J Biol Chem* **276**, 3054-9.

Schafer, M. W., Madhukar, B. V., Swanson, H. I., Tullis, K., and Denison, M. S. (1993). Protein kinase C is not involved in Ah receptor transformation and DNA binding. *Arch Biochem Biophys* **307**, 267-71.

Schaldach, C. M., Riby, J., and Bjeldanes, L. F. (1999). Lipoxin A4: a new class of ligand for the Ah receptor. *Biochemistry* **38**, 7594-600.

Servillo, G., Della Fazia, M. A., and Sassone-Corsi, P. (2002). Coupling cAMP signaling to transcription in the liver: pivotal role of CREB and CREM. *Exp Cell Res* **275**, 143-54.

Servillo, G., Penna, L., Foulkes, N. S., Magni, M. V., Della Fazia, M. A., and Sassone-Corsi, P. (1997). Cyclic AMP signalling pathway and cellular proliferation: induction of CREM during liver regeneration. *Oncogene* **14**, 1601-6.

Shibazaki, M., Takeuchi, T., Ahmed, S., and Kikuchi, H. (2004). Suppression by p38 MAP kinase inhibitors (pyridinyl imidazole compounds) of Ah receptor target gene

activation by 2,3,7,8-tetrachlorodibenzo-p-dioxin and the possible mechanism. *J Biol Chem* **279**, 3869-76.

Shirai, Y., and Saito, N. (2002). Activation mechanisms of protein kinase C: maturation, catalytic activation, and targeting. *J Biochem (Tokyo)* **132**, 663-8.

Silberhorn, E. M., Glauert, H. P., and Robertson, L. W. (1990). Carcinogenicity of polyhalogenated biphenyls: PCBs and PBBs. *Crit Rev Toxicol* **20**, 440-96.

Sinal, C. J., and Bend, J. R. (1997). Aryl hydrocarbon receptor-dependent induction of cyp1a1 by bilirubin in mouse hepatoma hepa 1c1c7 cells. *Mol Pharmacol* **52**, 590-9.

Stauber, K. L., Laskin, J. D., Yurkow, E. J., Thomas, P. E., Laskin, D. L., and Conney, A. H. (1995). Flow cytometry reveals subpopulations of murine epidermal cells that are refractory to induction of cytochrome P-4501A1 by beta-naphthoflavone. *J Pharmacol Exp Ther* **273**, 967-76.

Swanson, H. I. (2002). DNA binding and protein interactions of the AHR/ARNT heterodimer that facilitate gene activation. *Chem Biol Interact* **141**, 63-76.

Swanson, H. I., and Yang, J. H. (1998). The aryl hydrocarbon receptor interacts with transcription factor IIB. *Mol Pharmacol* **54**, 671-7.

Tan, Z., Chang, X., Puga, A., and Xia, Y. (2002). Activation of mitogen-activated protein kinases (MAPKs) by aromatic hydrocarbons: role in the regulation of aryl hydrocarbon receptor (AHR) function. *Biochem Pharmacol* **64**, 771.

Tan, Z., Huang, M., Puga, A., and Xia, Y. (2004). A Critical Role for MAP Kinases in the Control of Ah Receptor Complex Activity. *Toxicol Sci.*

Tanno, K., and Aoki, Y. (1996). Phosphorylation of c-Jun stimulated in primary cultured rat liver parenchymal cells by a coplanar polychlorinated biphenyl. *Biochem J* **313 (Pt 3)**, 863-6.

Tatosyan, A. G., and Mizenina, O. A. (2000). Kinases of the Src family: structure and functions. *Biochemistry (Mosc)* **65**, 49-58.

Thomson, S., Clayton, A. L., Hazzalin, C. A., Rose, S., Barratt, M. J., and Mahadevan, L. C. (1999). The nucleosomal response associated with immediate-early gene induction is mediated via alternative MAP kinase cascades: MSK1 as a potential histone H3/HMG-14 kinase. *Embo J* **18**, 4779-93.

Thron, C. D. (1997). Bistable biochemical switching and the control of the events of the cell cycle. *Oncogene* **15**, 317-25.

Tian, Y., Ke, S., Chen, M., and Sheng, T. (2003). Interactions between the aryl hydrocarbon receptor and P-TEFb. Sequential recruitment of transcription factors and differential phosphorylation of C-terminal domain of RNA polymerase II at cyp1a1 promoter. *J Biol Chem* **278**, 44041-8.

Torchia, J., Glass, C., and Rosenfeld, M. G. (1998). Co-activators and co-repressors in the integration of transcriptional responses. *Curr Opin Cell Biol* **10**, 373-83.

Tritscher, A. M., Goldstein, J. A., Portier, C. J., McCoy, Z., Clark, G. C., and Lucier, G. W. (1992). Dose-response relationships for chronic exposure to 2,3,7,8-tetrachlorodibenzo-p-dioxin in a rat tumor promotion model: quantification and immunolocalization of CYP1A1 and CYP1A2 in the liver. *Cancer Res* **52**, 3436-42.

Tsai, J. C., and Perdew, G. H. (1997). Ah receptor nuclear translocator protein heterogeneity is altered after heterodimerization with the Ah receptor. *Biochemistry* **36**, 9066-72.

Ventura, C., and Maioli, M. (2001). Protein kinase C control of gene expression. *Crit Rev Eukaryot Gene Expr* **11**, 243-67.

Vogel, C. F., Sciullo, E., Park, S., Liedtke, C., Trautwein, C., and Matsumura, F. (2004). Dioxin increases C/EBPbeta transcription by activating cAMP/protein kinase A. *J Biol Chem* **279**, 8886-94.

Wang, F., Wang, W., and Safe, S. (1999). Regulation of constitutive gene expression through interactions of Sp1 protein with the nuclear aryl hydrocarbon receptor complex. *Biochemistry* **38**, 11490-500.

Wang, S., Ge, K., Roeder, R. G., and Hankinson, O. (2004). Role of mediator in transcriptional activation by the aryl hydrocarbon receptor. *J Biol Chem* **279**, 13593-600.

Wang, S., and Hankinson, O. (2002). Functional involvement of the Brahma/SWI2-related gene 1 protein in cytochrome P4501A1 transcription mediated by the aryl hydrocarbon receptor complex. *J Biol Chem* **277**, 11821-7.

Wei, Y. D., Helleberg, H., Rannug, U., and Rannug, A. (1998). Rapid and transient induction of CYP1A1 gene expression in human cells by the tryptophan photoproduct 6-formylindolo[3,2-b]carbazole. *Chem Biol Interact* **110**, 39-55.

White, M. R., Masuko, M., Amet, L., Elliott, G., Braddock, M., Kingsman, A. J., and Kingsman, S. M. (1995). Real-time analysis of the transcriptional regulation of HIV and hCMV promoters in single mammalian cells. *J Cell Sci* **108**, 441-55.

Whitelaw, M. L., Hutchison, K., and Perdew, G. H. (1991). A 50-kDa cytosolic protein complexed with the 90-kDa heat shock protein (hsp90) is the same protein complexed with pp60v-src hsp90 in cells transformed by the Rous sarcoma virus. *J Biol Chem* **266**, 16436-40.

Whitlock, J. P., Jr. (1999). Induction of cytochrome P4501A1. *Annu Rev Pharmacol Toxicol* **39**, 103-25.

Williams, S. R., Son, D. S., and Terranova, P. F. (2004). Protein kinase C delta is activated in mouse ovarian surface epithelial cancer cells by 2,3,7,8-tetrachlorodibenzo-p-dioxin (TCDD). *Toxicology* **195**, 1-17.

Xu, L., Ruh, T. S., and Ruh, M. F. (1997). Effect of the histone deacetylase inhibitor trichostatin A on the responsiveness of rat hepatocytes to dioxin. *Biochem Pharmacol* **53**, 951-7.

Yim, S., Oh, M., Choi, S. M., and Park, H. (2004). Inhibition of the MEK-1/p42 MAP kinase reduces aryl hydrocarbon receptor-DNA interactions. *Biochem Biophys Res Commun* **322**, 9-16.

Yuan, L. W., Soh, J. W., and Weinstein, I. B. (2002). Inhibition of histone acetyltransferase function of p300 by PKCdelta. *Biochim Biophys Acta* **1592**, 205-11.

Zeytun, A., McKallip, R. J., Fisher, M., Camacho, I., Nagarkatti, M., and Nagarkatti, P. S. (2002). Analysis of 2,3,7,8-tetrachlorodibenzo-p-dioxin-induced gene expression profile in vivo using pathway-specific cDNA arrays. *Toxicology* **178**, 241-60.